January 2020

The Role Of Bca2 In Regulation Of Warburg-Like Glucose And Lactate Metabolism In Breast Cancer Cell Lines

Richard T. Arkwright Iii
Wayne State University, rarkwrig@me.com

THE ROLE OF BCA2 IN REGULATION OF WARBURG-LIKE GLUCOSE AND LACTATE METABOLISM IN BREAST CANCER CELL LINES

by

RICHARD T. ARKWRIGHT III

DISSERTATION

Submitted to the Graduate School

of Wayne State University,

Detroit, Michigan

in partial fulfillment of the requirements

for the degree of

DOCTOR OF PHILOSOPHY

2020

MAJOR: CANCER BIOLOGY

Approved By:

_____

Advisor Date

_____

_____

_____

_____

DEDICATION

I dedicate this dissertation to my family. My family has been steadfast and has stood by me through all the many challenges I have faced. My family has helped me become a more rigorous scientist by teaching me how to turn challenges into lessons and find creative solutions to any obstacle in front of me while being thorough and precise in my work. Their guidance through these challenges has made me stronger personally and professionally.

To my parents, Tom and Judy Arkwright, who fostered and molded my love and interest in science and math starting at a young age. They advocated for my intelligence and abilities even when some doubted me. They encouraged all investigations into nature, teaching me to always be curious about the world around me, and encouraged me to dedicate my intelligence and skills to help the betterment of society through innovation. My parents taught me to ask the eternal question of why and how in everything I did. For years, I thought I wanted to become a medical doctor to treat patients. In 2006, my grandfather was diagnosed with bladder cancer resulting in my fascination with the medical sciences. As a result, I began researching cancer medicine. This was when I realized I wanted to become a research scientist. I dedicate this dissertation to my parents and to my Rumpa (my grandfather and my namesake), who died of bladder cancer in 2010. I also dedicate it to my wife and children who have sacrificed greatly in order to allow me to accomplish my endeavors.

To my beautiful and brilliant wife Paige Arkwright and to our two amazing sons, you are my world, and I could not have done this without you. Despite my health issues and the multitude of hurdles we have had to overcome to get here, you have been my heart and soul and the driving force in my life to finish what I have started. My children are motivation and inspiration and drive me to contribute to the creation of a better world. Paige, you are my rock, my support, and my life

partner whom I love beyond words. I dedicate this dissertation to you and both our sons, Richard T. Arkwright IV and Maximus A. Arkwright, as well as my parents who have stood by me throughout my life through the good times and the bad.

I sincerely believe that the culmination of my knowledge will afford me the tools necessary to make a valuable and significant contribution towards the betterment of medical science. I hope to either directly or indirectly inspire others in research and medicine. I am dedicated to working toward finding potential cures to cancer, uncovering innovations in cancer diagnostics, and improving targeted cancer treatments for the betterment of society and with the hopes of contributing knowledge to other forms of human disease.

ACKNOWLEDGMENTS

Many brilliant and talented researchers and scientists contributed to the research presented within this dissertation. They have played key roles in the planning, implementing, guidance, and completion of this work as well as providing the motivation and guidance necessary to persevere. Further, this project was only possible because of the fellowship I received through the Cancer Biology Program at Wayne State University (WSU). Dr. Waltz, the Associate Dean for Research and Graduate Programs, thank you for your personal, academic, and financial support. Dr. Matherly was instrumental in choosing which lab and mentor would be the best fit. Thank you for your academic and personal guidance throughout my tenure in the program. I must also acknowledge and express my appreciation to Nadia Daniels, Dr. Matherly's Administrative Assistant. You were invaluable in guiding me through countless bureaucratic and operational challenges and assisting me in streamlining this process so that I could earn my PhD. I truly appreciate your support and guidance, especially when I needed it most.

I will forever be grateful to Dr. Q. Ping Dou, my principal investigator, as well as my scientific and research mentor. Thank you for taking me in as a third year PhD student with only a fundamental understanding of the techniques and procedures of scientific investigation. Dr. Dou's approach to teaching truly enabled me to "come into my own" as he provided me multiple opportunities to conduct and compose my own research. Dr. Dou's tutelage guided me to overcome numerous challenges and supported my efforts to publish on my own. Due to Dr. Dou's mentoring, I am prepared and able to make a significant contribution to any research team I have the privilege of joining.

I also want to acknowledge all the past and present Dou lab members for their assistance, academic discussions, and comic relief. Especially Yasmine, Kush, Claire, and Rohini, all of who were extraordinary students with brilliant minds and fantastic work ethics. Thank you. I especially would like to thank Dr. Dou's Administrative Assistant Jean Guerin. I am not sure there are proper words to express my appreciation for your support. Truly, your guidance and supportive words throughout my research were invaluable to me and helped me to continue moving forward toward my goal.

I would also like to acknowledge the other members of my dissertation committee. Dr. Brush, the Assistant Director of the Cancer Biology program, has guided my research and helped me to maneuver through the processes of the department. Dr. Maik Hüttemann, a Professor at the Center for Molecular Medicine and Genetics and a member of the Department of Biochemistry and Molecular Biology and the Karmanos Cancer Institute, took time out of his extremely busy schedule to help me understand the complexities of metabolism, as well as supporting me personally as I became a husband and father twice over. Dr. Hüttemann helped me to understand how to prioritize and work efficiently instead of just working hard. Finally, Dr. Jian Wang contributed significantly to my research design and assisted in the identification of key genes/enzymes. Further, Dr. Wang actively guided me in my research design as well as aided in the processing of samples and teaching me how to understand the calculations necessary for the correct interpretation of the data I was querying. Finally, Dr. Wang guided me in assessing the levels of lactate and glucose in the media of the samples evaluated. Without these critical data, and his valuable insights, this project may not have reached completion.

I would like to give special acknowledgement to the work of Dr. Daniella Buac-Ventro whose research provided the background and preliminary data that led to this investigation.

Fortunately, Dr. Buac-Ventro took meticulous notes allowing me to closely follow her work and techniques in order to maintain continuity between our two investigations, although they eventually diverged. However, the overall findings and the significance of breast cancer associated gene 2 to cancer cell metabolism paralleled her initial insights. In connection with Dr. Buac-Ventro, I want to thank Dr. Paul Stemmer, Dr. Carruthers, and Dr. Caruso from the Proteomics Core for their assistance with the technical aspects of the phospho-enriched mass-spec analysis of the titanium dioxide (TiO2) phospho-array of diBCA2 relative to non-targeting siRNA (siNT), and for assistance in interpreting the data to identify the key upregulated phosphoproteins associated between the two variables.

I would like to thank Dr. Seongho Kim for assisting with the statistical analysis, and for advising me on the best way to present the data. Dr. Kim graciously gave his time, helped me to better understand the statistical analysis that I was using, what the significance of the different types of analysis were, and also reviewed my work to ensure that I did not make any errors in my analysis.

Finally, there are seven individuals in my personal life I would like to acknowledge. I have been plagued with health issues over the last year and a half and they have helped me through extremely difficult and hospital-ridden times. Truly, this dissertation would not have reached completion without their persistent and steadfast support. I acknowledge and thank you for your unending support: My wife Paige Arkwright, my parents Tom and Judy Arkwright, colleague and friend Nicole Dragoi, mentor Dr. Thomas Cappas, and lifelong family friends and mentors Dr. Michael Reeber and Dr. Terry Bradford. To all of you, thank you for your never-ending guidance and support.

PREFACE

The aim of this dissertation is to determine the relationship between the E3-ubiquitin ligase, Breast Cancer Associated Gene 2 (BCA2), and Nicotinamide Mono-transferase Adenly-transferase-1 (NMNAT1) and their potential roles in the regulation of breast cancer cellular metabolism. The inverse correlation between BCA2 and NMNAT1 was originally identified by Dr. Jian Wang via his expert evaluation of the phospho-proteomic mass-spec-analysis performed by Dr. Buac-Ventro in Dr. Dou's laboratory and the proteomics core facility. The analysis compared the mass spectroscopy (MS) phospho-proteomic profiles of MDA-MB-231 triple negative breast cancer (TNBC) cell lines of siBCA2 relative to a siNT control utilizing siRNA knockdown (KD) to modulate the expression of BCA2. This experiment was performed by Dr. Buac-Ventro. The analysis was performed in triplicate, in collaboration with the Wayne State University proteomics core facility, by Dr. Paul Stemmer. Dr. Jian Wang identified NMNAT1 as one of the upregulated phospho-peptides, which had not been previously reported. NMNAT1 is the master regulator of nuclear Nicotinamide Adenine Dinucleotide (NAD^+) levels and in concert with NAD-dependent deacetylase sirtuin-1 (SIRT1) has been shown to regulate the expression of several key metabolic enzymes specific to whole cell glycolytic and Warburg metabolism (Chiarugi, Dolle, Felici, & Ziegler, 2012).

Previous findings by Dr. Daniella Buac-Ventro identified BCA2 as a significant regulator of adenosine monophosphate activated protein kinase (AMPK) phosphorylation/activation. Since AMPK is the master regulator of cellular energy homeostasis, it seemed logical to investigate other potential mechanisms wherein BCA2 might have affected cancer cell metabolism. Preliminary research findings suggested inhibition of AMPK signaling associated with increased BCA2

expression is associated with an intermediate. Hence, NMNAT1 could be a potential target of BCA2 either directly or indirectly. Dr. Buac-Ventro's investigation began to prove the potential role of BCA2 in the regulation of cancer cell metabolism. Hence, prior works and analyses conducted by Dr. Wang, Dr. Stemmer, Dr. Carruthers, Dr. Caruso, Dr. Buac-Ventro and Dr. Dou suggested BCA2 could be a potent potential target for cancer therapeutics because cancer cell metabolism is one of the most critical and distinct markers of all cancers, and BCA2 is primarily overexpressed in breast cancer cells.

To generate a more stable model system for investigating the role of BCA2 in the regulation of cancer cell metabolism, I employed a shRNA-KD model system to generate stable shRNA-KD of BCA2 in two TNBC cell lines: MDA-MB-468, and MDA-MB-231. Dr. Buac-Ventro's model system provided the basis for both investigating how BCA2 might regulate the metabolic system and the potential efficacy of targeting BCA2 for cancer cell treatment. The preliminary experiments were intended to establish the optimum glucose concentration in the media for the subsequent experiments.

My hope is that the discoveries made within this body of work will provide the basis for the development of BCA2 inhibitors for the clinical treatment of TNBC. Warburg-like metabolism is indicative of rapidly proliferating cells within the body. Cancers exhibit unique and characteristic metabolic activity known as Warburg metabolism. Experimental evidence supports the inhibition of Warburg metabolism as a therapeutic target in cancer treatment. NMNAT1 has been shown to regulate cellular metabolism in association with SIRT1 (Zhang et al., 2009). These studies support the case for further investigation into BCA2's involvement in Warburg-like metabolism as it relates to cancer cells.

FUNDING

This work is original, except where references are made to previously published or unpublished works and was funded in part by the National Cancer Institute – R21 CA184788-0 (PQA1), Office of the Vice President for Research (OVPR), DeRoy Testamentary Foundation and the Thomas C. Rumble pre-doctoral fellowships.

TABLE OF CONTENTS

LIST OF FIGURES

LIST OF ABBREVIATIONS

ACS	American Cancer society
AICAR	5-Aminoimidazole-4-carboxamide ribonucleotide
AKT	Protein Kinase B
AMP	Adenosine Monophosphate
AMPK	Adenosine Mono-Phosphate Activated Protein Kinase
ARG	Arginine
ATP	Adenosine Triphosphate
BCA2	Breast Cancer Associated Gene 2
BSA	Bovine Serum Albumin
dKd	Double Knockdown
DMEM	Dulbecco's Modified Eagle *Medium*
DNA	Deoxyribonucleic Acid
DUB	Deubiquitinating
ECM	Extracellular Matrix
EGCG	Epigallocatechin Gallate
FBS	Fetal Bovine Serum
GFP	Green Fluorescent Protein
GLUT1	Glucose Transporter 1
HECT	Homologous to the E6-AP Carboxyl Terminus
HER2	Human Epidermal Growth Factor Receptor 2
HK/G6PDH	Hexokinase/Glucose-6-Phosphate Dehydrogenase
HIF1	Hypoxia Inducible Factor 1

HIS	Histidine
HRP	Horseradish Peroxidase
ILE	Isoleucine
KD	Knockdown
LDHA	Lactate Dehydrogenase Isoform A
LDHB	Lactate Dehydrogenase Isoform B
LDH	Lactate Dehydrogenase
LEU	Leucine
LYS	Lysine
MDA-MB-231	Human Breast Carcinoma Cell Line
MDA-MB-468	Human Breast Carcinoma Cell Line
MDM2	Murine Double Minute 2
MMDB	Molecular Modeling Database
mRNA	Messenger Ribonucleic Acid
MS	Mass Spectrum Phospho-proteomic
NAD^+	Nicotinamide Adenine Dinucleotide
NADH	Reduced Nicotinamide Adenine Dinucleotide
NADPH	Reduced Nicotinamide Adenine Dinucleotide Phosphate
NCBI	National Center for Biotechnology Information
NMNAT1	Nicotinamide Mono-transferase Adenly-transferease-1
NMN	Nicotinamide Mononucleotide
pAMPK	Phosphorylation of AMPK
PARP1	Poly (ADP Ribose) Polymerase

PCR	Polymerase Chain Reaction
PGPH	Post-Glutamyl Peptide Hydrolase-Like
PHD	Plant Homeodomain
PHE	Phenylalanine
PI	Proteasome Inhibitor
pNMNAT	Phosphorylated NMNAT1
Pr	Parental
PUR	Puromycin
R5P	Ribose-5-Phosphate
RING	Really Interesting New Gene
RLU	Relative Luciferase Units
RNF115	Ring Finger Protein 115
SCF	Skp1-Cullin-F-box
SDS	Sodium Dodecyl Sulfate
SIRT1	NAD-Dependent Deacetylase Sirtuin-1
shBCA2	Small Hairpin Breast Cancer Associated Gene 2
shNMNAT1	Small Hairpin NMNAT1
shRNA	Small Hairpin Ribonucleic Acid
shRNAi	Small Hairpin Ribonucleic Acid Interference
siNT	Non-Targeting siRNA
± SEM	(Standard Error Mean +/-)
TBST	Tris-Buffered Saline, 0.1% Tween ® 20 Detergent
TCA	Tricarboxylic Acid Cycle

TE Buffer	Tris EDTA Buffer
Ti02	Titanium Dioxide
TNBC	Triple-Negative Breast Cancer
TRP	Tryptophan
TYR	Tyrosine
UBR1	Ubiquitin Protein Ligase E3 Component N-Recognin 1
UBR2	Ubiquitin Protein Ligase E3 Component N-Recognin 2
UPS	Ubiquitin Proteasome System
Ub	Ubiquitin
WSU	Wayne State University
WT	Wild Type
XIAP	X-linked IAP
Zn^{2+}	Zinc

CHAPTER 1: INTRODUCTION

1.1 Breast cancer

According to the American Cancer Society (ACS), 13% of women in the United States (U.S.) will be diagnosed with invasive breast cancer over the course of their lifetime (ACS, 2019). That means one in every eight women will be diagnosed with invasive breast cancer. Further, the ACS projects an estimated 268,600 total new cases of breast cancer annually (ACS, 2019). In addition, the ACS predicts that another 62,930 of women will be diagnosed with a non-invasive breast cancer (breast cancer *in-situ*) (ACS, 2019). Intriguingly, from 1989 to 2015 breast cancer mortality rates significantly decreased, presumably due to early detection (mammograms), improvements in chemotherapy and targeted treatments, as well as massive and popular campaigns to increase breast cancer awareness and the importance of self-exams. Current statistics project that an estimated 41,760 women will die from breast cancer this year alone (ACS, 2019). Therefore, the frequency of breast cancer mortality is only second to lung cancer as the leading cause of cancer deaths for women in the United States. This high incidence of mortality emphasizes the importance of continued research into potential targets and the underlying mechanisms responsible for the development and progression of breast cancer, and the need for novel therapeutics for treatments to specifically target the disease.

Stage, grade, size, and phenotype are key factors that are considered when determining the treatment and prognosis of breast cancer. Current treatment options include surgical resection, radiation therapy, chemotherapy, endocrine (hormone) therapy, and targeted therapies (Nounou et al., 2015), which includes the highly effective clonal antibody-based targeting technologies. However, these antibody-based therapies are extremely expensive and specific to only a few thoroughly delineated forms of cancer.

Many breast cancer cases are hormone-receptor (estrogen and progesterone) or HER2 (Human Epidermal Growth Factor Receptor 2) positive and therefore are responsive to hormone therapies in conjunction with other chemotherapeutic treatments. A smaller subset of breast cancers is triple-negative breast cancer (TNBC), lacking estrogen, progesterone and HER2 receptors. As a result of the lack of these targetable receptor-specific endocrine therapeutics, TNBCs are extremely aggressive. TNBCs are associated with a poorer prognosis and are frequently found primarily in younger patients.

The TNBC phenotype constitutes 10-20% of breast cancer cases overall (Lehmann et al., 2011). Although the culmination of early screening, advanced diagnostics, and better/targeted treatment options have reduced mortality rates of breast cancer patients, patients expressing the triple negative phenotype have fewer treatment options outside of chemotherapy because they lack "well defined molecular targets" (Lehmann et al., 2011). One such chemotherapeutic strategy that has proven effective in multiple cancer types targets the ubiquitin proteasome system (UPS) via inhibition of the 26S proteasome. Inhibition of the UPS has proven effective and selective in the targeting of rapidly proliferating cancers.

1.2 The structure and function of the 26s proteasome

The 26S proteasome structure (depicted in Figure 1.1) consists of two alpha and two beta rings. The two beta rings are found in the middle of the proteasome and form its barrel-like structure, while the two alpha rings are found on the periphery sandwiching the beta rings together between them (Matyskiela & Martin, 2013). The alpha rings and beta rings each contain 7-α and 7-β subunits. This structure makes the 20S catalytic core structure with a heptagon pore through the center of the barrel, which is where the proteolytic activity occurs (Matyskiela & Martin, 2013). In addition to the alpha and beta rings, the proteasome has two 19S regulatory complexes or caps

that binds to the alpha rings. The 19S caps are the “gate keepers” to the catalytic 20S proteasome core. The 19S caps both perform deubiquitylation and impart selectivity of targeted proteins to the proteasome according to the specific ubiquitin (Ub)-branching patterns of the ubiquitinated-proteins (Matyskiela & Martin, 2013).

The catalytic activity of the 20S core is primarily carried out by three proteolytic sites (Figure 1.1) (Matyskiela & Martin, 2013). The proteolytic sites include: 1.) β-1 or PGPH (post-glutamyl peptide hydrolase-like) or caspase-like activity; 2.) β-2 (Trypsin-like); and 3.) β-5 (Chymotrypsin-like (CT)) activity (Shen, Schmitt, Buac, & Dou, 2013). In the UPS, targeted proteins are tagged with ubiquitin (Ub) moieties in variable lysine linked branching patterns (Matyskiela & Martin, 2013). The Ub-targeted proteins are recognized by the 19S cap, which binds the polyubiquitin chains. The rest of the protein is then linearized and guided into the proteasome where it is degraded by 20S proteasomes into small peptides (Matyskiela & Martin, 2013). The Ub chains are cleaved by deubiquitinating enzymes (DUBs), and the small peptide chains and the Ub moieties are recycled (Tanaka, 2009). Recycling by DUBs allows Ub to be reused and the small peptide sequences to be used for rapid protein synthesis (Matyskiela & Martin, 2013).

1.3 Discovery and functions of the UPS

Over the course of about 60 years, the details about the UPS were slowly discovered through the collaboration of multiple works and researchers (De Duve, Pressman, Gianetto, Wattiaux, & Appelmans, 1955; Etlinger & Goldberg, 1977; Hershko, Eytan, Ciechanover, & Haas, 1982; Rabinovitz & Fisher, 1964). Christian de Duve accidentally discovered lysosomes while examining rat liver enzymes in 1955 (De Duve et al., 1955). Proteins were thought to be relatively stable prior to this discovery. Rabinovitz and Fisher (1964) determined that another proteolytic system must exist outside of lysosomal activity when they witnessed the rapid degradation of an

abortive protein in rabbit reticulocytes in 1964. It was concluded that another system existed for proteolysis since reticulocytes do not contain lysosomes (Rabinovitz & Fisher, 1964). In two separate studies conducted in 1977 and 1978 by Etlinger, Hershko, and colleagues, it was concluded that the proteolytic system within reticulocytes was both cell-free and energy-dependent (Etlinger & Goldberg, 1977; Hershko et al., 1982). These findings triggered investigations into alternative mechanisms/pathways for protein degradation.

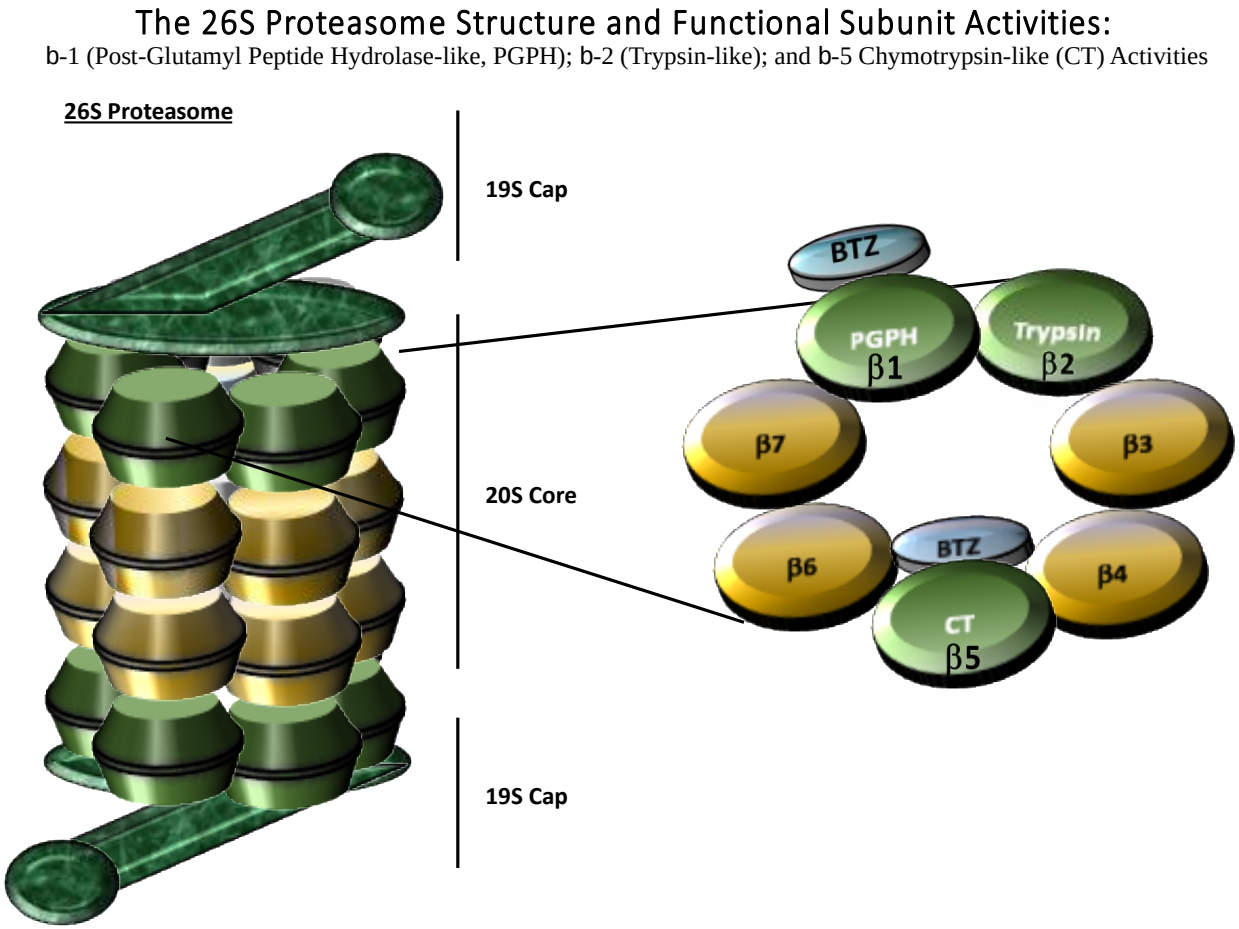

Figure 1.1 26S Proteasome Structure and Functional Subunit Activities.

The 26S proteasome consists of a 20S core and one or two 19S regulatory cap or Ub binding caps. The core consists of 2 alpha and 2 beta rings. The two beta rings are stacked together in the middle of the core and have alpha rings on either side. Each ring consists of either 7-α or 7-β rings. Beta ring enzymatic subunits consist of 3 proteolytic sites: β-1 (Post-glutamyl peptide hydrolase-like, PGPH, also known as caspase-like activity); β-2 (Trypsin-like); and β-5 (Chymotrypsin-like (CT) activity).

1.4 The discovery of the UPS and the significance in cancer and disease

Hershko and colleagues characterized the polypeptide associated with the unknown proteolytic system from 1980-1983. The group characterized the requirement of adenosine triphosphate (ATP) in protein breakdown. They then identified that ATP breakdown to ADP + PPi provides the energy necessary for the activation of the proteolytic enzymes that constitute the UPS. It was identified that ATP was essential for the tagging of proteins to be degraded, and they were the first to demonstrate how proteins were tagged by Ubiquitin (Ub) and targeted for proteolytic degradation.

Hershko and colleagues also identified other components of the UPS and investigated the proteasome and the role of UPS in proteolysis. Aaron Ciechanover, Avran Hershko, and Irwin Rose were awarded the Nobel Prize in Chemistry in 2004 as a result of their discovery and research into the UPS and the regulatory mechanisms associated with this ATP dependent and cell free protein degradation pathway (Ciechanover, Elias, Heller, Ferber, & Hershko, 1980; Haas, Warms, Hershko, & Rose, 1982; Hershko, Ciechanover, Heller, Haas, & Rose, 1980; Hershko et al., 1982; Hershko, Heller, Elias, & Ciechanover, 1983).

The discovery of the UPS established the foundation for researchers to determine the etiology for multiple diseases from cancer to neurodegenerative diseases such as Alzheimer's disease. Further, the UPS has become a chemotherapeutic target in the treatment of multiple diseases and especially liquid (blood) cancers. Proteasome inhibitors (PIs) disrupt cells' abilities to cycle proteins associated with cell cycle and survival pathways, thus resulting in cell death in rapidly and actively dividing cells (Paul, 2008).

1.4.1 The UPS pathway and ubiquitin ligases

The main function of the UPS is the catabolism of specific regulatory and deleterious intracellular proteins (Matyskiela & Martin, 2013). The UPS is responsible for the degradation, activation, deactivation, as well as localization of Ub-targeted proteins. As a result of the UPS's specific and specialized regulatory machinery, the UPS is responsible for the regulation of cell cycle progression, deoxyribonucleic acid (DNA)-damage repair, transcriptional regulation, and signal transduction pathways (Morreale & Walden, 2016). The UPS can control the localization of proteins to specific cellular compartments and cytoplasmic regions within the cell (Matyskiela & Martin, 2013). The UPS is also essential in removing deleterious and misfolded proteins from within the cell to maintain the normal cellular activities (Morreale & Walden, 2016).

The UPS plays a critical role in the regulation of cellular functions by switching on and off various signaling pathways within the cell. This is done through ubiquitination and subsequent proteolytic catabolism of key regulators of those pathways (Matyskiela & Martin, 2013). Alternatively, the UPS can regulate the activity of a targeted protein by ligating Ub moieties to critical regions of the targeted proteins, changing the accessibility of specific binding and activity domains, and changing the conformation of the proteins (Matyskiela & Martin, 2013). Most cancer cells fully utilize the 26S-proteasome activities to ensure the proliferation and survival, which led to the development and discovery of specific proteasome inhibitors (Nounou et al., 2015).

A protein must first be ubiquitinated to be targeted and degraded by the UPS (McClellan, Laugesen, & Ellgaard, 2019). Ubiquitination is a post-translational modification process whereby a lysine on the target protein is covalently linked to a Ub-moiety by a thioester bond. The formation of the Ub-thioester bond is catalyzed by a series of three ubiquitinating enzymes (E1-, E2-, and E3-ligases) (McClellan, Laugesen, & Ellgaard, 2019). The first enzyme in this series is the Ub

activating enzyme (E1-ligase), which links lysine with the carboxyl end of Ub in an ATP-dependent reaction. Secondary enzymes in the series include the Ub-conjugating enzymes (E2-ligases), which receive the Ub from E1-ligases via a cytosine residue on the E2-ligase (McClellan et al., 2019). E2-ligases possess enhanced target specificity for the third class of UPS enzymes, the E3-ligases. E3-ligases bring specifically targeted proteins together with their corresponding E2-ligase, conjugating the Ub transfer from the E2-ligase to a lysine residue on the targeted protein, thus forming an iso-peptide bond (McClellan et al., 2019). E3-ligases have protein and polypeptide motif specific targeting, allowing for targeted regulation of specific protein, thereby determining its fate. The targeted proteins are frequently ubiquitinated several times, creating a polyubiquitin chain with distinctive branching patterns (McClellan et al., 2019). The polyubiquitinated proteins are then transferred to the 26S proteasome for degradation and recycling of the Ub moieties and the cleaved peptide fragments (Figure 1.2) (McClellan et al., 2019).

1.4.2 Classes, structure, binding-domains and activities of E3-ligases

E3-ligases are the most heterogeneous class of the three Ub-enzymes in the UPS pathway. The different classes of E3-ligases are represented by their characteristic structural and binding domains. The specific binding domains that characterize the different E3-ligases include N-end Rule Ub-ligases, HECT (Homologous to the E6-AP Carboxyl Terminus), and Really Interesting New Gene (RING) domain ligases. Their unique structural domains and binding sequences determine their protein-target specificity (An, 2008). They have been stratified into three classifications based on their characteristic structures: 1.) HECT; 2.) Adaptor/ (N-end rule Ub ligases); and 3.) RING. These are further divided into monomeric and multi-subunits (An, 2008; Burger, Amemiya, Kitching, & Seth, 2006b; Chen et al., 2006; Ohta & Fukuda, 2004).

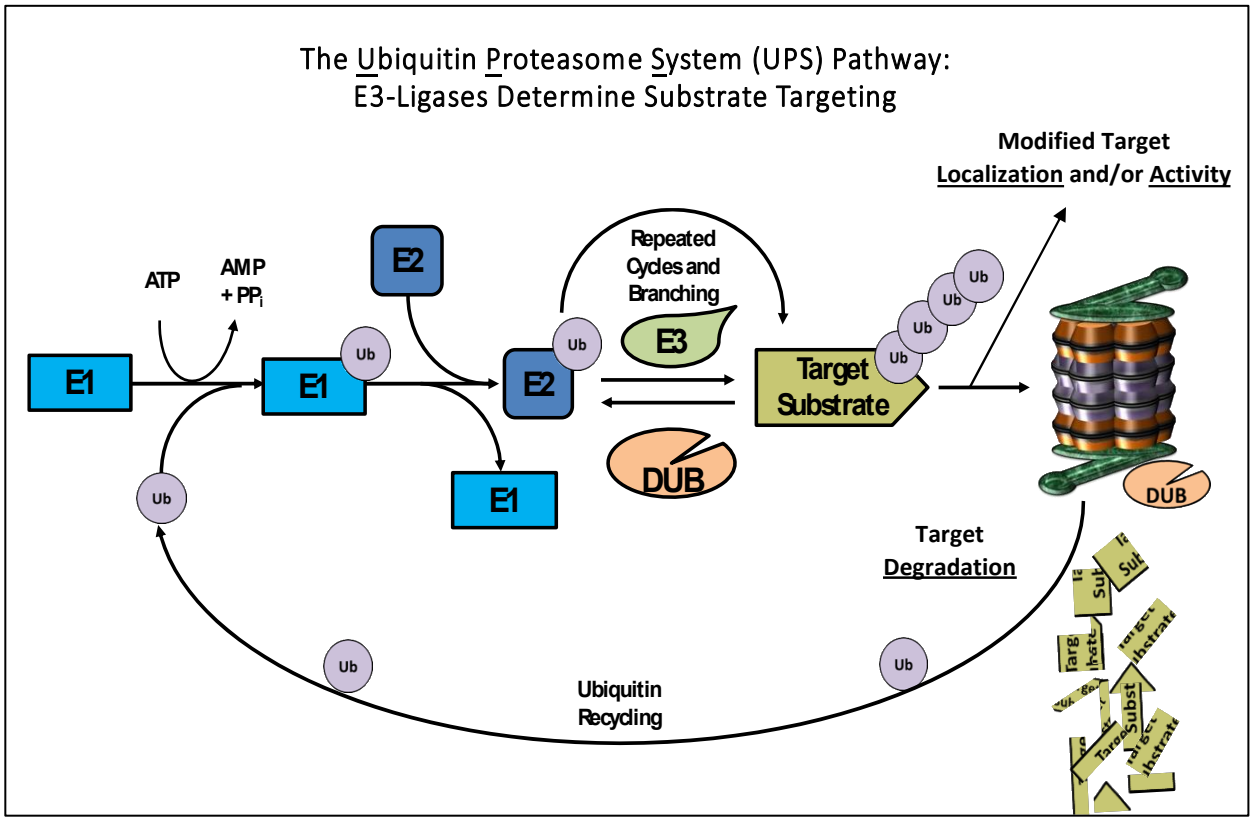

Figure 1.2 The UPS regulates the degradation, activation and localization of target proteins
The UPS differentially regulates the degradation, activation, localization, and complex formations of protein structures in a dynamic and specific manner in response to differential Ub patterns. The patterns of Ub polymerization and branching are in response to the expression profile of the E3-Ligases expressed in the cells shown above. It is dynamically regulated by the differential expression of the E3-ligases. The extensive variety (600+) of different E3s has different tissue and cell type expression profiles. This allows for the dynamic, spatial, and selective regulation of protein expression and activity. Therefore, E3-ligases could be potential candidates for the development of targeted therapies that specifically inhibit key cellular pathways in cancer.

The first class of E3-ligases is the HECT domain-containing ligases. HECT domain-containing E3-ligases consist of about 30 members, including the E6-associated protein (E6-AP), which serves as the prototypical HECT domain ligase, as well as the prototype of the HECT domain containing class of E3-ligases. E6-AP, together with the oncoprotein E6 promotes p53 ubiquitination and subsequent degradation (Chua, Liew, Guo, & Lane, 2015; DeHart, Perlman, & Flint, 2015; Ooga, Suzuki, & Aoki, 2015). HECT E3-ligases consist of approximately 350 amino acids and a C-terminal region, which are homologous to that of E6-AP (Metzger, Hristova, &

Weissman, 2012). HECT E3-ligases also include a highly conserved active-site, as well as a cysteine residue near the C-terminus. HECT domain E3-ligases facilitate the formation of the thioester intermediates between the Ub moieties and their target substrates (Metzger et al., 2012). Conversely, the N-terminal regions of HECT E3s are highly variable but may be critical to substrate recognition and target specificity (Metzger et al., 2012).

Future development of E3-ligase targeted therapies should focus on targeting the distinct structural domains and binding motifs that characterize the diverse classes of E3-ligases. Each of the different E3-ligases have distinct structural domain and sequence domains that could be targeted specifically in order to regulate a broader range of E3-ligase substrates. Because of the high specificity of the individual E3-ligases, they are potential targets for chemotherapy if specific inhibitors can be designed to target the E3-ligases that are upregulated in cancer (An, 2008; Ardley & Robinson, 2005). Hence, E3-ligases represent potential candidates for the development of future UPS-targeted therapies in cancer because many play important roles in cancer progression, and their specificity can reduce the risk of off-target side effects (Shen, Schmitt, Buac, & Dou, 2013).

The second class comprises the adaptor or N-end rule Ub ligases. The adaptor E3-ligases are further broken down into RING-finger, U-Box, or plant homeodomain (PHD) containing classes (Ardley & Robinson, 2005; Dikic & Robertson, 2012; Hatakeyama & Nakayama, 2003; Metzger, Hristova, & Weissman, 2012). Adaptor E3-ligases target protein substrates that contain specific N-terminal residues known to destabilize protein half-lives and enhance degradation. These residues include: Type I (Arginine (Arg), Histidine (His), and Lysine (Lys)) and Type II (Isoleucine (Ile), Leucine (Leu), Phenylalanine (Phe), Tryptophan (Trp), and Tyrosine (Tyr)) (Trausch-Azar, Abed, Orian, & Schwartz, 2015). Originally it was unknown why proteins containing these “destabilizing residues” in the N-terminus were more readily targeted and

degraded by the UPS (Ardley & Robinson, 2005). However, discovery and classification of the class of E3-ligases explained their shortened half-lives. Further research into their activity and protein stabilities established N-end Rule E3-ligases as critical regulators of multiple short-lived regulatory proteins. N-end rule E3-ligases include Ubiquitin Protein Ligase E3, Component N-Recognin 1 (UBR1), and Ubiquitin Protein Ligase E3 Component N-Recognin 2 (UBR2) which mediate transcriptional silencing through histone ubiquitination in a spatiotemporal specific fashion in dividing cells, thereby regulating meiotic/mitotic spindle formation (Cole, Clifton-Bligh, & Marsh, 2015; Trausch-Azar et al., 2015; Turco, Gallego, Schneider, & Kohler, 2015). The rapid degradation and fast modulation of protein degradation allows for the precise control of cell cycle progression (Dikic & Robertson, 2012).

Finally, the RING family E3-ligases are the most well studied and classified E3-ligases in the context of breast cancer. RING E3-ligases contain a classic C3H2C3 or C3HC4 RING finger domain with 8 characteristic Zn^{2+} - coordinating residues, where X is any amino acid in the sequence motif N-1-X(2)-2-X(9-17)-3-X(1-3)-4-X(2)-6-X (4-48)7-X(2)-8-C (Smith, Berry, & McGlade, 2013). A RING finger domain binds to two Zn^{2+} atoms that serve as the platform for binding of Ub-conjugated E2-Ligases (Jaitovich et al., 2015). The cross-link formed by the first and third pairs of cysteine/histidine residues form the first binding site. The second and fourth pairs of cysteine/histidine residues form the other E3-Ub-ligases, which exist and act as a single peptide [such as murine double minute 2 (Mdm2) and X-linked IAP (XIAP)] or as multiple component complexes [such as Skp1-Cullin-F-box protein (SCF)] (Sun, 2006). Like the other members of the E3-ligases, RING finger E3-ligases act as a molecular scaffold bringing the E2-Ub complex close to the E3-bound substrate for the direct transfer of Ub to the target protein from the E2-ligase (Jaitovich et al., 2015).

The RING finger E3-ubiqutin ligases constitute > 230 of the approximately 600-1000 E3-ligases found in the human genome. RING-E3-ligases exhibit substrate selectivity (An, 2008; Metzger et al., 2012). Therefore, RING finger E3-ubiqutin ligases may serve as ideal candidates for further development of novel cancer chemotherapeutics and potential cancer biomarkers as they display tissue, cellular-compartment, and pathway specificity (Sun, 2006).

1.4.3 Breast cancer associated gene 2 (BCA2)

Breast Cancer Associated Gene 2 (BCA2) is a RING E3-Ub ligase with promising potential as a therapeutic target in breast cancer treatment. BCA2 protein is encoded by the human Ring Finger Protein 115 (RNF115) gene (aka: T3A12/ZNF364/Rabring7) located on chromosome 1 (1q21.2). The BCA2 protein consists of 304 amino acids with two purported (truncated) isoforms: RNF115-X1 (N-Terminal truncated transcript) and RNF115-X2 (C-Terminal truncated transcript) (Burger et al., 2006b; Burger et al., 2005; Burger et al., 2010; Burger et al., 1998; Wang et al., 2013). BCA2 contains nine exons and 1927 bases in the messenger ribonucleic acid (mRNA) (Burger et al., 2005). Little is known about the BCA2 isoforms. However, sequence analysis and significant data have identified the key features of the full length BCA2 protein (Burger et al., 2006b; Burger et al., 2005; Burger et al., 2010; Burger et al., 1998; Wang et al., 2013).

BCA2 contains an N-Terminal Zinc-finger domain (amino acids 18-49), which contains two critical mutagenic sites that are essential for BCA2 to auto-ubiquitinate (Cys-228, -231 and Lys-26, -32), which is characteristic of many RING E3-ligases. In addition, BCA2 contains a C-terminal RING-finger domain (amino acids 227-272), from which it received its original name RNF115 (Figure 1.3) (Wang et al., 2013). Additional features include an evolutionarily conserved N-acetyl-alanine at residue 2 with unknown significance. However, acetylation has been shown to affect endosomal trafficking/localization, as well as protection against degradation (Bacopulos et

al., 2012; Buac, Kona, Seth, & Dou, 2013; Kona et al., 2012; Wang et al., 2013). The significance of BCA2 as an oncogene has been demonstrated most clearly and comprehensively in breast cancer. However, BCA2 may also play similar roles in other types of cancer (Gumaste et al., 2015; Klein, 2012), as well as in viral transmission (Miyakawa et al., 2009).

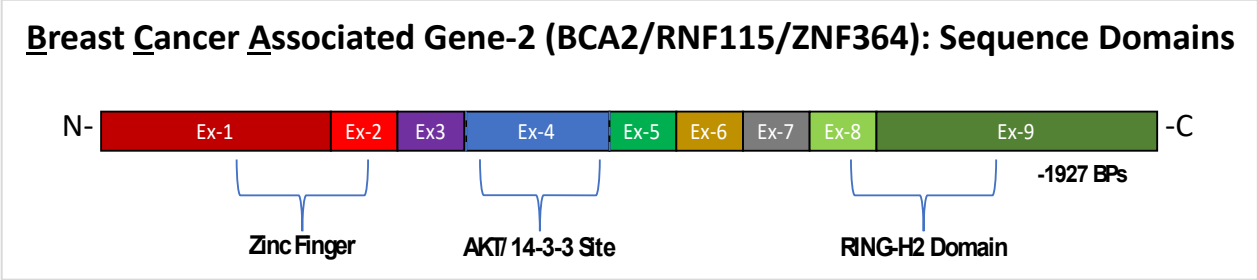

Figure 1.3 Schematic of Breast Cancer Associated gene-2 (BCA2)

The full-length Breast Cancer Associated gene-2 (BCA2) (T3A12/ZNF364/Rabring7 or RNF115) sequence was cloned from TNBC cell line MDA-MB-468 by Dr. Angelika Burger in the lab of Dr. Arun Seth. BCA2 is located on chromosome 1 (1q21.2) and consists of 9 exons. The mRNA is 1927 base pairs long. BCA2 is a RING-H2-type E3 ubiquitin ligase. BCA2 contains an AKT/14-3-3 binding site, a zinc-finger domain near the N-terminus, and a RING-H2-finger domain near the C-terminus. Mutation site studies revealed that lysine residues K26 and K32, located in the N-terminal Zn-finger binding domain, are responsible for its ubiquitination activity.

1.5 The role of BCA2 and AMPK in regulation of cancer cell metabolism

The AMPK energy homeostasis pathway and the Ubiquitin Proteasome System (UPS) play critical and complementary roles in regulating whole cell homeostasis. However, both cellular energy homeostasis (Warburg effect) and aberrant UPS activity have been observed in many different cancers. This suggests that these two pathways may be potential therapeutic targets. AMPK is well known as the master regulator of cellular metabolism, while the UPS is the cells' primary regulator of protein homeostasis and turnover. Some studies have demonstrated that AMPK activation (by using metformin) might have chemo-sensitizing or even anticancer properties. Therefore, it is important to explore the role of the AMPK pathway in breast cancer so

targeted therapies can be developed that specifically target the anticancer activity of AMPK activation in novel chemotherapeutic research.

Preliminary data from the Dou Lab by Dr. Daniella Buac-Ventro demonstrated that ectopic expression of BCA2 inhibited activation of AMPK by metformin. Furthermore, Dr. Buac-Ventro demonstrated that AMPK activation by metformin triggered an inhibitory signaling cascade that resulted in the transcription-independent induction of BCA2, was associated with enhanced AKT signaling activation (Buac et al., 2013). Finally, siRNA -KD of BCA2 and pharmacological inhibition of AKT signaling both inhibited the anticancer properties of metformin in human breast cancer cells, suggesting that metformin in combination with an inhibitor of BCA2 could be used for breast cancer treatment.

Interestingly, it has been shown that low concentrations of metformin (60-80μM) inhibit glucose production and gluconeogenic gene expression in primary hepatocytes through an AMPK-dependent mechanism. This suggests that AMPK may exhibit a negative feedback loop to inhibit its own activity through AMPK's differential role in liver tissues (increase glucose) compared to normal cells where AMPK phosphorylation results in decreased gluconeogenesis and cell growth.

BCA2 has been shown to be highly expressed in 56% of invasive breast cancers (Brahemi et al., 2010). In addition, BCA2 has been integrally implicated in the regulation of multiple critical cellular metabolic processes and pathways including glucose and lipid metabolism (Arkwright et al., 2014). Specifically, expression of BCA2 regulates the activation of adenosine mono-phosphate activated protein kinase (AMPK) and the associated downstream pathways (Buac et al., 2013). AMPK is a highly conserved molecule and an essential sensor of intracellular adenosine nucleotide (ATP, ADP,AMP) levels that are activated with even a modest decrease in ATP production.

AMPK is activated by decreases in the energy status of the cell. This promotes catabolic pathways to generate more energy in the form of ATP.

1.6 BCA2 regulates cancer cell energy homeostasis through modulation of AMPK

AMPK is known as the master regulator of cellular homeostasis (Herzig & Shaw, 2018). AMPK signaling is known to be dysregulated in multiple human cancers, which allows the cancer cells to continue anabolic activities even in the absence of enough metabolites (low ATP/AMP) for normal respiration and cellular proliferation to occur. In cancer cells, anaerobic metabolism persists even in the presence of oxygen; this occurs by the shunting of pyruvate towards the production of lactate and the lactic acid cycle as opposed to aerobic glycolysis that occurs in normal cells in the presence of oxygen. AMPK activation (pAMPK) occurs by an upstream energy sensing kinase LKB1 or the calcium influx sensing CAMKK2. LKB1 phosphorylates AMPK in response to low cellular energy states (high AMP/ATP). However, CAMKK2 activates AMPK in response to calcium. Activated AMPK directly phosphorylates several downstream target substrates, which modulate cellular energy metabolism and proliferation, depending on the energy status of the cell.

A high ratio of AMP/ATP results in the phosphorylation of AMPK (pAMPK) by allosteric regulation of AMPK. AMP displaces ATP in the binding pocket of AMPK and thus increases phosphorylation of AMPK by LKB1 (in response to energy status) or CAMKK2 (Arkwright et al., 2014). The phosphorylation state of AMPK regulates a myriad of metabolic pathways leading to the inhibition of cell growth and the enhancement of cellular respiration, as well as energy generating processes (Koh et al., 2015). Low AMP/ATP results in dephosphorylation of AMPK, allowing a proliferative process to progress under high energy (ATP/AMP) conditions (Arkwright

et al., 2014). However, in cancer cells, the regulation of cellular energy and metabolic homeostasis is dysregulated by a phenomenon known as Warburg Metabolism.

Warburg metabolism is essential to the rapid proliferation of cancer cells (Liberti & Locasale, 2016). Warburg metabolism is characterized by a metabolic shift from aerobic to anaerobic metabolism. By transitioning from aerobic to anaerobic metabolism, the cells can generate energy more rapidly. In addition, anaerobic metabolism generates significantly more biomolecules for anabolic metabolism. The combined effect of the Warburg effect is to facilitate uncontrolled cancer cell growth even under conditions of low glucose, and low oxygen saturation. As a result of Warburg metabolism, cancer cells can create the metabolites and energy necessary to replicate DNA and other cellular components fast enough for rapid cellular proliferation (Liberti & Locasale, 2016). In addition, solid tumors are generally associated with dynamic microenvironments that result in pockets of low oxygen and increased acidity (Estrella et al., 2013). Oxygen is an essential component of aerobic oxidative phosphorylation (Epstein, Xu, Gillies, & Gatenby, 2014). Under normal cellular conditions, low energy status is determined by the increased ratio of AMP relative to ATP (AMP/ATP). Hence, Warburg metabolism drives the cell towards rapid cellular proliferation by directing the cell to increase glucose consumption, while reducing its oxygen dependency and rate of anaerobic metabolism, thereby increasing the accumulation of metabolic intermediates for rapid growth (Liberti & Locasale, 2016).

Regulation of AMPK activation by BCA2 suggests that BCA2 plays a key role in the regulation of cellular metabolism (Arkwright et al., 2014). Endogenous and exogenous BCA2 expression has been shown to play a critical and energy independent role in the activation of AMPK (pAMPK). As a result of the activation of AMPK by phosphorylation, mTOR activation is inhibited, which drives cellular proliferation (Memmott & Dennis, 2009). In addition, AMPK

activation, either via direct AMPK activators like 5-Aminoimidazole-4-carboxamide ribonucleotide (AICAR) or the indirect AMPK activators like metformin, has been shown to induce expression of BCA2. This suggests a potential feedback mechanism that could be AKT-dependent (Arkwright et al., 2014; Buac et al., 2013). BCA2 contains a purported AKT binding site, and AKT is known to play a critical role in the maintenance of cellular energy metabolism (Arkwright et al., 2014; Memmott & Dennis, 2009). Further, inhibition of AKT activation in the presence of AMPK activators has been shown to inhibit increases in BCA2 expression associated with AMPK activation (Arkwright et al., 2014). However, direct interaction between BCA2 and AKT or AMPK has yet to be elucidated (Bacopulos et al., 2012; Buac et al., 2013; Kona et al., 2012) and the exact mechanism by which enhanced BCA2 expression diminishes AMPK activation is unclear.

Experimental evidence also strongly suggests that inhibition of BCA2 by siRNA results in increased AMPK activation, decreased cellular proliferation, and decreased colony forming ability (Arkwright et al., 2014). In addition, cells with diminished BCA2 expression have been shown to exhibit increased sensitivity to the anti-proliferative and anti-cancer effects of metformin (Buac et al., 2013). Therefore, BCA2 may be an ideal candidate for further development of UPS targeted therapies, alone or in combination with other types of chemotherapeutics. Further, BCA2 exhibits a unique and specific expression profile with enhanced expression in metastatic breast cancer cells and low expression in normal tissues. There is evidence that BCA2 also plays a critical role in aberrant cellular metabolism in cancer progression (Warburg effect) and cancer metastasis (Koh et al., 2015).

Experimental evidence suggests that BCA2 can modulate key variables in energy homeostasis, thereby ensuring cancer proliferation and survival even in harsh microenvironments

(Buac et al., 2013; Burger et al., 2005). Based on these findings, the relationship of BCA2 with other catalytic proteins was assessed to determine potential target proteins by phospho-proteomic mass spectrum (MS) analysis (Buac et al., 2013). Dr. Buac-Ventro first conducted the transfection of siBCA2 knockdown (KD) and siNon-targeting (NT) controls in the TNBC cell line MDA-MB-231 and subsequently evaluated the KD of BCA2 protein expression by western blot analysis. Samples were then provided to Dr. Paul Stemmer who conducted the MS technical analysis at the Wayne State University Proteomics core facility. Phosphoproteins were enriched from both conditions in triplicate using titanium dioxide (TiO_2), then the expression profiles of both conditions were analyzed to determine phosphoproteins regulated by BCA2 expression. It was expected that the changes in cellular energy metabolism associated with BCA2 expression was the result of phosphorylation of AMPK via some intermediary between BCA2 and AMPK, possibly targeted for degradation by the proteasome after Ub-targeting by BCA2. Alternatively, AMPK may have been phosphorylating a specific messenger protein downstream of AMPK that was affecting the cells' metabolism (Buac et al., 2013).

The data generated in the MDA-MB-231-siBCA2 model system revealed 36 phospho-proteins of interest (Figure 1.4) specifically upregulated in the siBCA2-KD condition (Buac et al., 2013). Nicotinamide Mononucleotide Adenylyl-Transferase-1 (NMNAT1) was one of those 36 proteins found to be correlated with BCA2-KD. NMNATs are the key enzyme in Nicotinamide Adenine Dinucleotide (NAD) synthesis, and there are three known isoforms (NMNAT1-3), which are localized in different cellular compartments, suggesting differential roles in regulation of NAD metabolism. NMNAT1 localizes to the nucleus (Zhang et al., 2009) and is suggested to suppress tumors and is associated with better patient outcomes (Greenwald et al., 2016; Sultani et al., 2018).

Preliminary research findings warranted further investigation into the association between BCA2 and NMNAT1. BCA2 is suggested to play a role in the inhibition of AMPK activation and downstream pathways (Burger et al., 2010). Prior research findings suggest that BCA2 can inhibit the activation of AMPK in the presence of the AMPK activators, such as Metformin (Buac, Kona, Seth, & Dou, 2013). Metformin is suggested to play a role in the activation of cellular energy homeostasis and the utilization of glucose levels in the cell. Glucose concentration plays a critical role in the regulation of AMPK activation and cancer cell aggressiveness (increased proliferation) even in a cellular state of low energy as determined by the ratio of AMP/ATP (Buac et al., 2013; Ohta & Fukuda, 2004; Shen et al., 2013). A high AMP/ATP ratio suggests that a cell is in a nutrient deprived state, which generally activates AMPK (phosphorylated AMPK: pAMPK). It was also determined previously by Dr. Daniella Buac-Ventro in Dr. Q. Ping Dou's lab that there was no direct interaction between BCA2 and AMPK phosphorylation (Buac et al., 2013). Therefore, the inhibition of AMPK signaling associated with increased BCA2 expression suggests an association with some intermediate. BCA2 in breast cancer is known to be upregulated in metastatic TNBCs. NMNAT1 is known to play a critical role in the regulation of nuclear NAD^+ levels in the nucleus, which plays a key role in transcription regulation of multiple genes associated with cellular energy homeostasis. As a result of NMANT1s known role in sensing cell energy status in complex with the sirtuins (e.g., SIRT1), it was suspected that NMNAT1 may play a role in the regulation of cellular energy homeostasis in TNBCs. Based on the phospho-proteomic data, the following experiments were performed under the assumption that the amount of phosphorylated NMNAT1 (pNMNAT) would correlate with the total NMNAT1 protein expression, and that BCA2 may regulate cellular energy metabolism through control of NMNAT1 activity. The investigation began

by verifying the relationship between BCA2 and NMNAT1 expression in response to stable shBCA2-KD.

A. Phospho-Peptide Enrichment (MS)

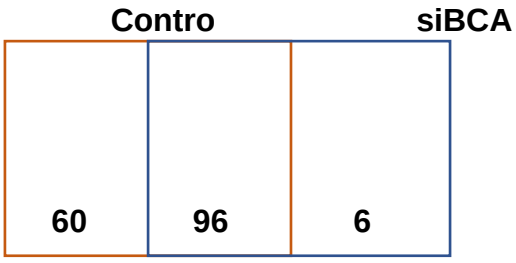

B. Proteins Upregulated after BCA2 siBCA2

NMNA1_HUMAN	Nicotinamide mononucleotide adenyl-transferase 1 OS=Homo sapiens GN=NMNAT1 PE=1 SV=1
NUDC_HUMAN	Nuclear migration protein nudC OS=Homo sapiens GN=NUDC PE=1 SV=1
NU153_HUMAN	Nuclear pore complex protein Nup153 OS=Homo sapiens GN=NUP153 PE=1 SV=1
LARP7_HUMAN	La-related protein 7 OS=Homo sapiens GN=LARP7 PE=1 SV=1
ITPR3_HUMAN	Inositol 1,4,5-triphophate receptor type 3 OS=Homo sapiens GN=ITPR3 PE=1 SV=2

Figure 1.4 Venn Diagram of Phospho-proteomic Analysis of siBCA2-KD Identified pNMAT1 as Inversely Correlated with BCA2 Protein Expression.

Following siBCA2-KD, a phospho-peptide enrichment by TiO_2 pull down of the phosphorylated proteins was performed and an MS analysis of the proteins in the MDA-MB-231-siBCA2 cells was performed by Dr. Buac-Ventro. Analysis of the siBCA2 populations of proteins relative to the siNT control population was performed. The Venn diagram identified 36 proteins which were significantly changed under the siBCA2-KD conditions. B.) Further investigation of the siBCA2-KD population by Dr. Jian Wang identified NMNAT1 as a potential target protein of BCA2.

1.7 Nicotinamide mono-nucleotide adenylyl-transferase (NMNAT1)

NAD^+ is a coenzyme that plays a critical role in cellular energy metabolism, including glycolysis, in which it is used to convert glyceraldehyde-3-phosphate to 1,3-bisphosphoglycerate via glyceraldehyde-3-phophate dehydrogenase, forming reduced nicotinamide adenine dinucleotide (NADH) (Chiarugi et al., 2012). NADH can then be used to convert pyruvate to lactate via lactate dehydrogenase isoform A (LDHA), which forms an abundance of NAD^+ in the cytoplasm. NAD^+ also plays a role in signal transduction. In the nucleus, NAD^+ helps activate enzymes that regulate and protect DNA, as well as transcription factor binding and transcriptional

activity (Brooks, 2010; Chiarugi et al., 2012; Jayaram, Kusumanchi, & Yalowitz, 2011). In a healthy cell, there is a higher ratio of NAD^+ to NADH than in a cancerous cell (Moreira et al., 2016).

NMNAT (Nicotinamide Mononucleotide Adenylyl-Transferase) is the rate limiting enzyme responsible for the biosynthesis of NAD^+ from NMN (Nicotinamide Mononucleotide) and ATP (Chiarugi et al., 2012; Jayaram et al., 2011). Three different isoforms of NMNAT have been identified and found to localize to different compartments of the cell. NMNAT3 is found in the mitochondria and is a homo-tetramer, NMNAT2 is found in the cytoplasm (chromosome 1q25) and is a homodimer, and NMNAT1 is found in the nucleus (chromosome 1 p32-35) and is a homo-hexamer with four exons and 290 base pairs (Jayaram et al., 2011). The NMNAT1 monomeric structure consists of a central six-stranded parallel β-sheet surrounded by several helices and a pyridine-binding site, which might play a role in the substrate recognition.

NMNAT1 appears to play a key role in regulating transcription, as NAD is critical to transcriptional activity (NCBI, 2019; Werner et al., 2002). The biosynthetic action of NMNAT1 increases signaling of the PARP1 [Poly (ADP Ribose) Polymerase] enzyme within the nucleus. This enzyme is thought to account for the bulk of NAD^+ degradation. Therefore, it is plausible that an increase in NMNAT1 could result in a greater reduction of NAD^+ via PARP1. PARP1 and SIRT1 (NAD-dependent deacetylase sirtuin-1) activation slow the rate of glycolysis and reduce the amount of NADH produced. In addition to NMNAT1's biosynthetic and regulatory actions on NAD^+, it also plays a crucial role in DNA-damage repair. NMNAT1 coupled with poly ADP-Ribose and SIRT1 results in the relaxation of chromatin, allowing for enhanced interactions between chromatin regulatory elements and transcriptional factors (Schreiber, Dantzer, Ame, &

de Murcia, 2006). Enhanced NMNAT1 activity may play a role in the regulation of the transcription of glucose metabolic enzymes, overall cellular metabolism, and proliferation.

1.8 The Warburg effect

In the early 20th century, a German physiologist by the name of Otto Heinrich Warburg determined that cancer cells exhibit increased rates of glycolysis even in the presence of normal oxygen (Warburg, Wind, & Negelein, 1927). This phenomenon was termed the Warburg effect and closely resembles aerobic glycolysis (Figure 1.5). It is well known today that the Warburg effect is a hallmark characteristic of cancer cells (Arora et al., 2015; Liberti & Locasale, 2016; San-Millan & Brooks, 2017). It consists of a major metabolic shift where cellular energy metabolism is reprogrammed to primarily anaerobic metabolism. Regulation of cellular energy metabolism is a critical aspect of cancer metabolism in order to produce the metabolites necessary for rapid proliferation, as well as the excess energy needed to duplicate the DNA and other cellular components (Burns & Manda, 2017; Liberti & Locasale, 2016).

The Warburg effect is a well-known phenomenon by which cancer cells revert toward the less efficient yet rapid anaerobic glycolytic glucose metabolism in lieu of oxidative phosphorylation, even in the presence of oxygen (Liberti & Locasale, 2016). The Warburg-like effect is characterized by an increase in glucose consumption, decreased oxygen consumption, and increased lactate production through the enhanced activity of lactate dehydrogenase (LDH). LDH consists of a high activity state (LDHA) and a lower activity state (LDHB). When LDHA predominates, the cells trend towards the production of lactate and anaerobic metabolism, while LDHB trends towards oxidative phosphorylation and the TCA Cycle (Burns & Manda, 2017). The result of this shift in energy metabolism thereby results in increased lactate production, and an increase in glycolytic intermediates, providing the energy and necessary metabolites for rapid

cancer-cell proliferation (San-Millan & Brooks, 2017). Aerobic glycolysis is also characterized by increased acidity in the surrounding tissues or media, which is primarily caused by the increase in lactate production. Thus, the primary characteristics of the Warburg effect are increased glucose uptake, decreased oxygen consumption, increases in the ratio of LDHA/LDHB, increased lactate production, and decreased pH of the media or cellular microenvironment (Burns & Manda, 2017).

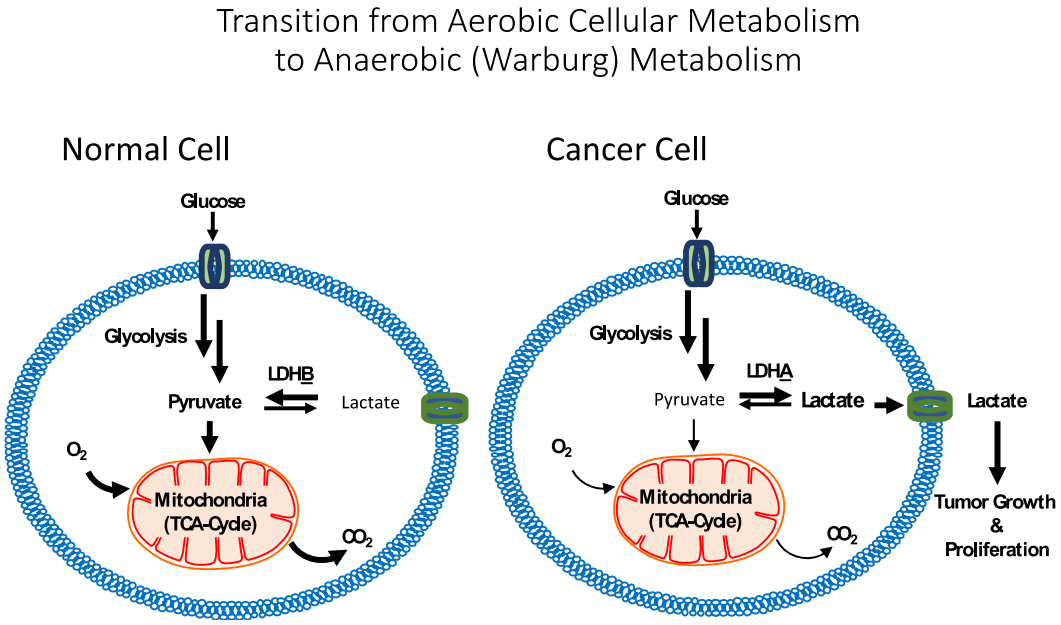

Figure 1.5: Transition from Aerobic Cellular Metabolism to Anaerobic (Warburg) Metabolism

A fundamental change that occurs in metastatic transformation is the transition from normal (aerobic) oxidative phosphorylation (normal glucose metabolism) to anaerobic metabolism (lactate pathway). This transition is known as the Warburg effect. The Warburg effect is characterized by significant increases in glucose consumption, decreased utilization of oxygen, and increased production of lactate and increased accumulation of metabolic intermediates for enhanced cancer cell proliferation and tumor growth. Under normal conditions, cells preferentially utilize aerobic oxidative phosphorylation, which processes glucose into pyruvate, which then enters the mitochondria and the TCA-Cycle to produce ATP. However, cancer cells preferentially undergo anaerobic metabolism even in the presence of oxygen. Anaerobic metabolism is characterized by the rapid consumption of glucose and the processing of glucose by LDHA into lactate. This process provides both the energy and metabolic intermediates necessary for rapid cellular proliferation of cancer cells. Lactate metabolism (anaerobic) is far less efficient at converting glucose into energy (ATP), so the cells consume significantly more glucose. The increased lactate production also increases the acidity of the surrounding microenvironment, further changing the behavior of the tumor cells, thereby facilitating invasion and metastasis.

In normal cells, energy is primarily derived from within the mitochondria by oxidative phosphorylation via the TCA cycle that generates 36 mols of ATP per mol of glucose. The oxygen-dependent process of oxidative phosphorylation is more efficient in producing energy in the form of ATP from glucose. However, cancer cells "modify" their metabolism to use the less efficient but more rapid energy-producing pathway (anaerobic glycolysis), which rapidly processes glucose and results in the formation of critical metabolites for cellular proliferation. Cancer cells upregulate their intake of glucose in order to accommodate enough cellular metabolism to produce the energy and glycolytic metabolites for rapid anabolic growth. In a normal cell, glucose enters the cell and is converted primarily into pyruvate and a small fraction into lactate. In the presence of oxygen, pyruvate enters the mitochondria for oxidative phosphorylation. In the absence of oxygen, pyruvate is converted to lactate, which produces an excess of primary metabolites, which results in a quicker production of energy to be stored in reservoirs of the cell (Burns & Manda, 2017).

In cancer cells, even when oxygen is prevalent, 85% of pyruvate is converted to lactate, and only 5% undergo oxidative phosphorylation (Vander Heiden, Cantley, & Thompson, 2009). The glycolytic pathway is further supported by the production of NAD^+ as a result of pyruvate being converted to lactate. Aerobic glycolysis is also found in normal rapidly proliferating cell types in addition to cancer cells and under conditions of low oxygen, such as exercise. However, normal cells that exhibit aerobic glycolysis only use this type of metabolism for a definitive amount of time, and the mitochondria are not damaged (Burns & Manda, 2017). As in embryonic cells, once the cell has completed rapid growth, it converts to oxidative phosphorylation. Hence, aerobic glycolysis is a property of rapidly proliferating cells, not just cancer cells (Krisher & Prather, 2012). It is theorized that cancer cells use anaerobic metabolism over oxidative phosphorylation because it is faster at the production of ATP in order to meet the energy needs of the cell (Burns

& Manda, 2017; Zdralevic et al., 2018). In addition, anaerobic metabolism produces more biosynthetic metabolites for the prolific needs of the cells (Burns & Manda, 2017).

Specifically, rapidly proliferating cells require a build-up of both glycolytic intermediates and metabolites for the creation of new cells [For example, lipids, fatty acids, proteins, DNA, and R5P (ribose-5-phosphate)) are required (Krisher & Prather, 2012)]. A probable explanation of how aerobic glycolysis is activated is via overexpression of HIF1 (Hypoxia Inducible Factor 1). HIF1 is a master transcriptional regulator (transcription factor) of cellular and developmental responses to hypoxia (Koh et al., 2015). In cancer cells, there is an overexpression of HIF, which increases the transcription of multiple genes that encode for proteins that favor cancer proliferation. Cancer favoring proteins will increase glucose consumption and angiogenesis and facilitate apoptosis resistance (Koh et al., 2015; San-Millan & Brooks, 2017).

In 1966, Otto Warburg stated that "cancer, above all other diseases, has countless secondary causes. But, even for cancer, there is only one prime cause. Summarized in a few words, the primary cause of cancer is the replacement of the respiration of oxygen in normal body cells by a "fermentation of sugar" (Brand, 2010, p. 2). Hence, the consumption of glucose is an essential step in cancer cell proliferation. It is only through the increase in glucose consumption that cancer cells can meet the biosynthetic needs for rapid cell proliferation (Burns & Manda, 2017).

HIF1 increases glucose consumption by upregulating glucose transporter 1 (GLUT1) on the surface of the cell, allowing more glucose to enter the cell more rapidly (Baumann, Zamudio, & Illsley, 2007; Koh et al., 2015). In addition, this upregulation of GLUT1 increases the consumption of glucose. HIF1 also increases glucose phosphorylation through the induction of the glycolytic enzyme hexokinase (HK), thereby converting glucose to glucose-6-phosphate. An increase in HIF1 modulates an increase in glycolytic flux, causes a reduction in ATP production

via oxidative phosphorylation, and decreases oxidation of pyruvate by inducing pyruvate dehydrogenase kinase. All of this induces aerobic glycolysis (Baumann et al., 2007). Although the glycolytic pathway is not as efficient in producing ATP as oxidative phosphorylation, if the amount of glucose is high within the cell, the ATP production rate is sufficient for rapid cell proliferation (Burns & Manda, 2017).

The importance of lactate is more than just a byproduct of anaerobic metabolism and an increased energy source in cancer cells. Lactate has a significant role in normal physiology, as well as in the treatment of injuries and illnesses (Burns & Manda, 2017). The importance of lactate and anaerobic metabolism as an energy source for cancer cells has been extensively studied in recent years (Burns & Manda, 2017; Liberti & Locasale, 2016; Moreira et al., 2016; San-Millan & Brooks, 2017; Vander Heiden et al., 2009; Zdralevic et al., 2018). It also plays a key role in aerobic glycolysis in healthy skeletal muscle, and ultimately influences changes in metabolic gene expression (Bourdeau Julien, Sephton, & Dutchak, 2018; Burns & Manda, 2017).

In cancer cells, lactate promotes carcinogenesis and cancer cell proliferation (tumorigenesis) under nutrient “stressed” conditions due to its acidifying effects. Unfortunately, cancer cells exhibiting an abundance of lactate are associated with increased resistance to both chemotherapy and radiotherapy, increased angiogenesis, increased frequency of metastasis, and immune system evasion (Molina, Morlacchi, Silva, Dennison, & Mills, 2014). Research has concluded that lactate production promotes cancer cell survival rates by facilitating the production of energy in the form of ATP, increasing reduced nicotinamide adenine dinucleotide phosphate (NADPH), glutathione, and the production of an excess of non-essential amino acids required for rapid cellular proliferation. This information suggests that lactate metabolism in cancer cell

biology is a potential target for the development of novel chemotherapeutic compounds (Molina et al., 2014).

1.8.1 Lactate dehydrogenase A/B (LDHA/B)

LDH is the rate limiting enzyme in the conversion of pyruvate to lactate (Jafary, Ganjalikhany, Moradi, Hemati, & Jafari, 2019; Lu, Zhang, Yee, Go, & Lee, 2015; Rani & Kumar, 2019). LDH has two isoforms that regulate the conversion from pyruvate to lactate, utilizing the reducing potential of NADH, which is produced by NMNAT1, the key enzyme in NAD^+ production in the nucleus (Lu et al., 2015). The high activity isoform of the LDH enzyme is LDHA. Therefore, LDHA converts pyruvate to lactate very quickly, thereby depleting the amount of pyruvate that can enter the mitochondria and enter the TCA cycle. It has been demonstrated experimentally that oxamate inhibits the activity and expression of LDHA, resulting in a decrease in glucose consumption and lactate production (Lu et al., 2015). In addition, the same paper showed that the main pharmacologically active compound in green tea, epigallocatechin gallate (EGCG), also decreased the expression of LDHA, increased aerobic oxidative-phosphorylation, and decreased anaerobic lactate metabolism and production. Thus, the inhibition of LDHA results in a dramatic impact on multiple metabolic pathways (Jafary et al., 2019; Lu et al., 2015).

LDHB is another isoform of LDH, which is the less active form of the tetra-hetero-enzyme. LDHB converts pyruvate more slowly, allowing more pyruvate to enter the mitochondria and oxidative phosphorylation via the TCA cycle (Rani & Kumar, 2019). In cancer cells, LDHA is the predominantly expressed isoform in normal tissues. Hence, an increase in LDHA results in increased lactate, which is then shuttled outside of the cell, where it lowers the pH of the microenvironment (Zdralevic et al., 2018). In addition, increased production of lactate also

provides the cancer cell with enough metabolic intermediates and energy for the rapid proliferation and increased tumor growth (Rani & Kumar, 2019).

1.9 Motivation and approach

Exploiting cancer cell metabolism as an anticancer therapeutic strategy has garnered much attention in recent years (Martinez-Outschoorn, Peiris-Pagés, Pestell, Sotgia, & Lisanti, 2016; Weinberg & Chandel, 2014; Zdralevic et al., 2018). As previously discussed, the German scientist Otto Heinrich Warburg observed that cancer cells consistently display an increased rate of glucose consumption, as well as high rates of aerobic glycolysis (Brand, 2010; Warburg et al., 1927) which results in increased lactate production.

The transition from the oxidative phosphorylation (aerobic metabolism) to the anaerobic (lactate) metabolism is known as the Warburg effect (Burns & Manda, 2017; Warburg et al., 1927). This shift in cellular energy metabolism is a fundamental and essential characteristic of metastatic transformation. The composition of the cancer cells biosynthetic (anabolic) metabolic enzymes also change in response to the shifts in the cells catabolic enzyme profile observed during metastatic transformation. The balance of these catabolic and anabolic enzymes is dynamically and tightly regulated in order to continually balance the energy needs of cells catabolic activity of the cancer cells (Burns & Manda, 2017). The complexity of the metabolic pathways makes identifying key regulators or therapeutic targets in cancer a difficult task. However, today, our current understanding of the Warburg effect is that it is mediated by several factors, including overexpression of the insulin-independent glucose transporter GLUT1 and various glycolytic enzymes, including LDHA (Lu et al., 2015; Molina et al., 2014; Rani & Kumar, 2019).

LDHA is the enzyme that catalyzes the reversible conversion of pyruvate and lactate (Rani & Kumar, 2019). During the conversion of pyruvate to lactate, the energy released facilitates the

oxidization of NADH to NAD^+ (Chiarugi et al., 2012). The lactate produced in this reaction is largely excreted into the tumor's microenvironment, where it acidifies surrounding tissues and helps the tumor evade destruction by immune cells (Estrella et al., 2013). The oxidation of NADH to NAD^+ allows for continued ATP production through glycolysis (Brooks, 2010; Epstein et al., 2014). Cell culture and *in-vivo* studies targeting LDHA utilizing RNA interference demonstrated a substantial decrease in cell and tumor cell growth and proliferation. These findings support the hypothesis that LDHA could be a viable anticancer target (Feng et al., 2018; Lu et al., 2015; Rani & Kumar, 2019).

BCA2 is a Zn-H2-RING-Finger E3 ubiquitin ligase (Burger, Amemiya, Kitching, & Seth, 2006a). Previous studies have shown that there is an inverse correlation between BCA2 protein expression and the activation of AMPK (Arkwright et al., 2014; Buac et al., 2013). BCA2 was shown to inhibit the activation of AMPK (phosphorylation), which activates catabolic metabolism in order to generate more energy under low energy states. Activation of AMPK occurs in response to low levels of ATP and high levels of AMP (Low ATP/AMP Ratio) (Arkwright et al., 2014; Mihaylova & Shaw, 2011). Dr. Buac-Ventro demonstrated that enhanced expression of BCA2 protein inhibited AMPK activation. In order to better understand the relationship between BCA2 and AMPK activation, siRNA targeting BCA2 was used to inhibit BCA2 protein expression in MDA-MB-231 cells, and a phospho-peptide mass spectral analysis was performed to identify proteins with enriched phosphorylation. This study revealed an inverse correlation between BCA2 and pNMNAT1 in response to siBCA2-KD and suggests that BCA2 may play a role in the regulation of other metabolic processes (Buac et al., 2013).

The motivation for the current investigation was based on the identification of the inverse correlation between BCA2 and NMNAT1 by Dr. Daniela Buac-Ventro (Buac et al., 2013). Dr.

Buac-Ventro's performed the siRNA-KD of BCA2 and the mass spectra analysis, and Dr. Dou and Dr. Jian Wang identified the inverse correlation between BCA2 and NMNAT1.

After establishing that BCA2 and NMNAT1 were inversely correlated in the pilot studies (mass-spec and in-silico analysis of transcript expression), the study began to define the experimental parameters of the future studies. AMPK activation is known to be regulated by glucose concentration (Salt et al., 1998). The preliminary experiments were designed to establish the ideal glucose concentration for the remaining of the study. In order to study the effects of glucose on the model system, increasing concentrations of glucose were applied to MDA-MB-468 and MDA-MB-231 TNBCCs. The study revealed that BCA2 protein expression was induced by increasing glucose concentration, and BCA2 expression decreased in response to glucose deprivation. These findings revealed an inverse correlation between BCA2 and glucose concentration, which was associated with a concurrent change in NMNAT1 protein expression (Buac et al., 2013).

These preliminary findings support the hypothesis that BCA2 protein expression may be regulating the expression of NMNAT1 protein expression. Further, the preliminary data also suggests that BCA2 might have a role in the regulation of cellular energy metabolism in cancer cells because of the established role of glucose concentration on Warburg metabolism and metastatic transformation. In order to investigate these hypotheses, a systematic evaluation of the role of BCA2 in the regelation of NMNAT1 was performed utilizing stable shRNAs targeting BCA2, NMNAT1, and BCA2/NMNAT1 combined. The model system was then used to examine the effects of RNA inhibition on NMNAT1 protein, transcript, and promoter activity. In addition, the model system was utilized to elucidate the effects of RNAi on Warburg-like metabolism, as

defined by the expression of key markers of Warburg-like metabolism (LDHA/LDHB), Glucose consumption, lactate production, and cellular proliferation.

shRNAi technology was utilized to stably and selectively knockdown the expression of BCA2, or NMNAT1, or BCA2/NMNAT1 together. By comparing the effects of these types of knockdown cell lines, it was possible to determine the specific and individual effects of BCA2 and NMNAT1 expression on glycolytic metabolism, as well as the consequences on glucose consumption and lactate production. By analyzing the different protein expression profiles in a panel of glycolytic enzymes, as well as observing both glucose consumption and lactate production in the three disparate shRNAi cell-lines (shBCA2-KD, shNMNAT1-KD, shBCA2/NMNAT1-double knockdown (dKD), it was possible to discriminate the key glycolytic enzymes that were associated with specific glucose metabolic activities and pathways. The proposed model system for the effects of BCA2 on Warburg-like lactate metabolism is illustrated in Figure 1.6.

1.10 Propose model system for investigating the role of BCA2 and NMNAT1 in regulation of Warburg-like metabolism and tumor progression.

BCA2 is known to inhibit AMPK activation. In addition, the literature suggests that increased glucose concentrations can inhibit AMPK activation, which could be a potential mechanism by which glucose modulates BCA2 expression and modulates aerobic versus anaerobic metabolism in cancer cells. BCA2 protein expression is increased when AMPK is activated pharmacologically. This suggests that BCA2 may be regulated by cellular energy status or may regulate cellular energy homeostasis. The preliminary data already identified an inverse correlation between BCA2 and NMANT1 in TNBCs by both the phospho-peptide enrichment mass spec data, and by an analysis of published relative transcript levels provided by the Broad Institute CCLE database.

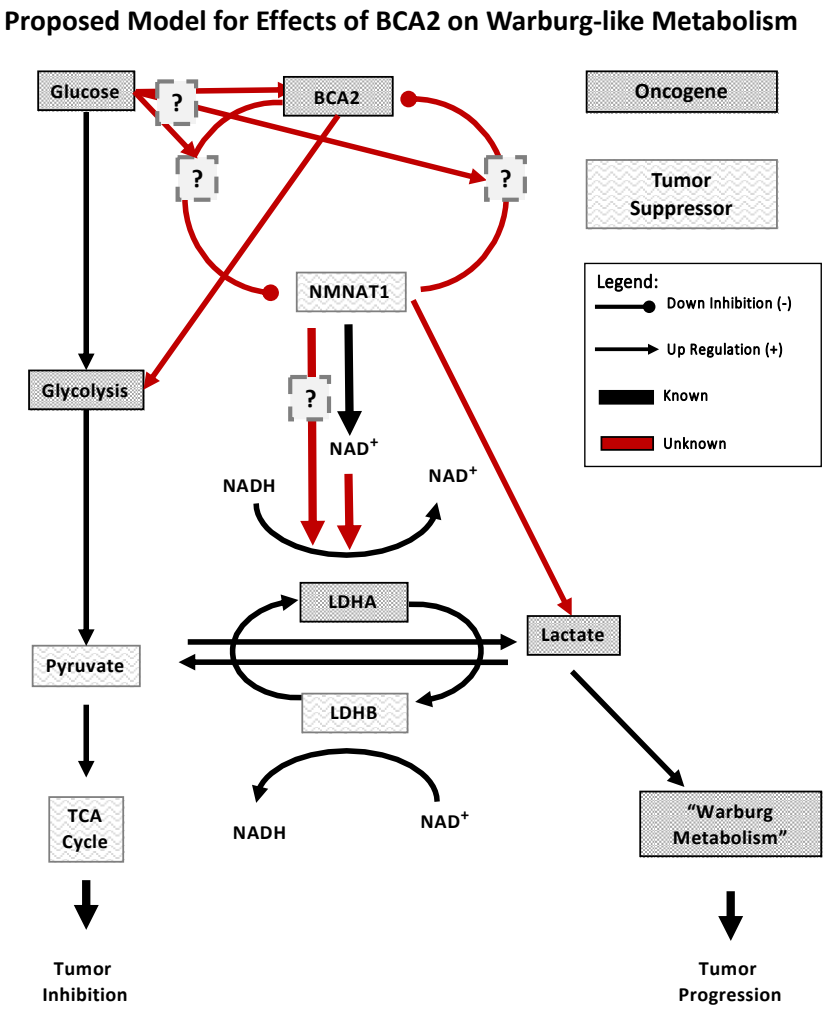

Figure 1.6: Proposed model for effects of BCA2 on Warburg-like metabolism.
The preliminary data supports an indirect role for BCA2 in the regulation of AMPK, the master regulator of cellular energy homeostasis. BCA2 inhibits AMPK phosphorylation either indirectly through modulating the cells energy (ATP/AMP) or by regulating the degradation, activation, or localization of some intermediary protein or transcription factors that shift the cell's energy homeostasis towards anaerobic metabolism and tumor progression. This model proposes that inhibition of BCA2 will increase NMNAT1 expression, which increases cellular NAD^+, driving the cell towards aerobic metabolism through the entry of pyruvate into the TCA cycle and resulting in tumor inhibition. Conversely, if NMNAT1 is inhibited, the model proposes that the effect would be to enhance the Warburg-like metabolism.

Based on the above data, the proposed model system will be used to investigate the relationship between BCA2 and NMANT1 expression at the levels of protein (Western Blot), transcript (rtPCR and qPCR), and promoter activity (Promega dual firefly luciferase assay). shRNA technology will be used to selectively knockdown expression of BCA2, NMNAT1, and

BCA2/NMNAT1, respectively. We will characterize the effects of stable shRNAi-KD of the targets on key markers of Warburg-like metabolism (LDHA/LDHB), as well as evaluating the downstream functional consequences on functional activities of the cancer cells, such as glucose consumption, lactate production and relative proliferation rates.

The proposed model system suggests that BCA2 inhibits expression of NMNAT1 and vice versa. Hence, decreased expression of the oncogene BCA2 would remove the constraints that the tumor suppressor NMNAT1 would be exerting to repress Warburg-like metabolism and decrease cellular proliferation rates. If the effects of shBCA2-KD on tumor progression and Warburg-like metabolism are dependent on NMNAT1, then subsequent inhibition of NMNAT1 by shNMNAT1-KD would reverse the effects observed in the shBCA2-KD clones alone.

This model proposes that the effects associated with BCA2 expression would be decreased NMNT1, increased LDHA/LDHB, increased glucose consumption, increased lactate production, and increased cell proliferation. If the Warburg-like effects associated with BCA2 are being exerted through NMNAT1 or are dependent on an NMNAT1 dependent intermediate, then knocking down NMNAT1 in the shBCA2 clonal populations should rescue the original aggressive Warburg-like metabolic state. BCA2 is highly expressed in breast cancer cells and is relatively low in normal tissues. In addition, Warburg metabolism is a fundamental and essential hallmark of cancer. If it could be inhibited selectively in cancer cells by targeting BCA2, this would offer a promising therapeutic target.

CHAPTER 2: EXPERIMENTAL DESIGN, AND STATISTICAL ANALYSIS

2.1 Experimental design and controls

In order to investigate the role of BCA2 and NMNAT1 in the regulation of Warburg-like metabolism and tumor cell proliferation, shRNAi stable knockdowns of the target transcripts were used to modulate the expression of these two genes within the context of TNBC cell lines. TNBC cell lines were used as the model system because the preliminary investigations were performed in these cell lines, providing the foundation for an investigation into the correlation between BCA2 and NMNAT1. In addition, estrogen is known to play a regulatory role in BCA2 expression and protein cycling (Kona, 2012). This could complicate the interpretation of the data because of the diverse role that estrogen plays in the regulation of cellular metabolic activities.

Dr. Jian Wang identified NMNAT1 from mass spectrometry analysis data in an experiment performed by Dr. Buac-Ventro in the Dou lab. The data was analyzed and interpreted in collaboration with Dr. Caruthers of the Proteomics Core and revealed experimental evidence linking BCA2 and NMNAT1 expression. In order to support the experimental data, the correlation between BCA2 and NMNAT1 transcripts were analyzed using the Broad Institute's CCLE database, which also revealed that there was an inverse correlation between BCA2 and NMNAT1 transcripts when the breast cancer cell lines were sorted for TNBCs.

The proposed model for the effects of BCA2 and NMNAT1 on Warburg-like metabolism hypothesizes that the mechanism of action is through the influence of NMNAT1 on the ratio of NAD+/NADH in the nucleus. It is further hypothesized that the increase in the ratio of LDHA/LDHB is modulated in response to the shift in NAD+/NADH in the nucleus resulting in transcriptional changes increasing LDHA and decreasing LDHB translation (Figure 1.6). The relationship between BCA2 and NMNAT1 and Warburg-like metabolism was unknown. It was

unclear whether cross regulation between BCA2 and NMNAT1 plays a role in the regulation of Warburg-like metabolism.

To investigate the roles of BCA2 and NMNAT1 in the regulation of Warburg-like metabolism, an shRNAi model system was utilized to target: BCA2, NMNAT1, and BCA2/NMNAT1 combined. In order to generate the dKD, two distinct shRNA-KD plasmid of vectors were utilized. shBCA2-KD plasmid stocks were generated using stock vectors from the pLKO plasmid construct library of TRC validated shBCA2 sequences (Vector control for shBCA2-KD was shNon-Targeting-1 shNT1). shNMNAT1-KD plasmids were generated from stock vectors from the pGIPZ construct library of TRC validated shNMNAT1 sequences (Vector control for shNMNAT1-KD was shNon-Targeting-2 shNT2).

The protocols for the generation of a stable knockdown clonal population required multiple transductions approaches. In the preliminary experiments, Sigma's Mission lenti-viral packaging kit was used to generate lentiviral particles with different shBCA2-KD vectors (a minimum of three targeted sequences were used per cell line and gene to generate stable cell lines). This same approach was used for the generation of stable shNMNAT1-KD clonal populations. However, to generate the stable dKD, this lentiviral technique failed, and serial transfections of the shNMNAT1-KD plasmids were necessary to achieve stable shBCA2/NMNAT1-dKD.

To generate dKD clonal populations of TNBCs, serial transfection with the Muris LT1 system every 48 hours for 3 successive treatments with selection in-between each cycle of transfections was performed. This was necessary because the cells already had the pLKO vector in it, so antibiotic selections by puromycin (PUR) alone would not work.

The pGIPZ construct contained the reporter protein GFP, which allowed serial dilution in a 96 well plate for expanding only the clonal populations that had single colonies. Upon expansion

and continued selection, clonal populations still retained GFP expression. At this point, western blots were run, and the clonal populations were identified with stable shBCA2/NMNAT1-dKD relative to the control (shNT2). Stable cell lines were necessary for running the remaining experiments because of the time scale needed to carry out the media analysis and proliferation assays, respectfully.

The controls for the experimental model were required to assess for off-target effects of the shRNAi system. To generate the shBCA2/NMNAT1-dKD, two different plasmid constructs (one for each gene) were used. As important as it was to control for the rigorous selection process, it was equally important to comply with the transfection protocol to obtain stable shBCA2/NMNAT1-dKDs. The dual vector system required the generation and validation of multiple non-targeting control clonal-populations of cells to provide both vector controls (shNT1-pLKO and shNT2-pGIPZ) and the clonal selection needed to generate the dKD. The first step was to identify the system controls and then ensure there were no off-target effects created by their integration. Controls included the parental lines for each cell line (Pr), the shBCA2 control (shNT1), the shNMNAT1 control (shNT2), and the shBCA2/NMNAT1 control (shNT1/2). Experiments were performed with the key controls for each system being investigated and displayed in the corresponding figures below. Additional experiments were performed at the start of each new phase of genetic manipulation to confirm that the control vectors matched the activity and expression profiles of the Pr lines and that the different control vectors all acted the same within the context of the experimental model. These results set the baseline for the remaining experiments to evaluate the effects of shBCA2-KD, shNMANT1-KD, and shBCA2/NMNAT1-dKD in the model system.

2.2 Scientific rigor and statistical analysis

Western blot analysis of the relative protein expression was performed utilizing the ChemiDoc XRS digital imaging platform software analysis. Image J was used to collect relative band intensity values for each western blot. Densitometry and statistical analysis of the experimental model were used to determine the significance of the research findings. In order to ensure the validity of the results, the following practices were used for all experiments (except where noted otherwise). The following preliminary experiments were performed to validate the system before the results were processed and calculated.

Glucose concentration is a well-established modulator of AMPK activation, the preliminary investigation into the project examined the effects of glucose concentration on AMPK activation (Molina et al., 2014). The change in AMPK activation in response to glucose could have been due to either depletion of glucose levels (low cellular energy status) or the result of the buildup of some secondary metabolite, which regulates AMPK through some other pathway. Therefore, it was essential that the experimental conditions, including glucose concentration, cell confluence, and time in media, were carefully controlled.

The following experimental parameters were established for data collection and for statistical analysis of the results: (a) experiments using media containing high glucose media, (b) cells were not allowed to reach confluence (cells were seeded at ~<60%, and harvested within 24 hours of seeding), (c) cells were not left in the same media for longer than 36 hours. Exceeding these parameters resulted in changes in cell morphology, loss of cell adhesion, changes in marker metabolism (protein and transcript), changes in functional measures of metabolism (glucose consumption and lactate production), and cell behavior (proliferation).

A minimum of three independent experiments were performed for each series of experiments (glucose, shBCA2, shNMNAT1, and shBCA2/NMNAT1), and representative western blots were displayed. Replicate images from a minimum of three independent experiments were analyzed by Image-J, and densitometry was performed. The densitometry data were normalized to the housekeeping gene (β-actin) and then normalized to the corresponding vector control. Results were displayed in bar graphs as (% Arbitrary Units (AUs) (normalized to β-actin)). As previously mentioned, corresponding control vectors were used for each targeting vector. These controls were previously validated against each other to evaluate any off-target effects of the controls in the model system.

Error bars were calculated by mean ± SEM (Standard Error Mean +/-) in the experiments, with triplicate experiments performed on separate days. Statistical analysis used a two-tailed student t-test with a *p*-value tolerance of ≤ 0.05. Asterisks (*) were used to indicate data that were statistically significant based on the stated criteria. All analyses were performed in Microsoft Excel and were reviewed by Dr. Seongho Kim of Wayne State University.

2.3 Materials and methods

2.3.1 Reagents

Multiple primary and secondary antibodies were used in this study. Anti-BCA2 antibody (anti-ZNF364 antibody [EPR14539] (ab187642)) and LDHB antibody ([EP1565Y] LDHB rabbit mAb) were obtained from AbCam (Cambridge, MA). LDHA ((C4B5) rabbit mAb (#3582)) antibody came as a component of the glycolysis antibody sampler kit #8337 from Cell Signaling Technologies (Danvers, MA). NMNAT1 antibody ((B-7): sc-271557) was obtained from Santa Cruz Biotechnology Inc. (Dallas, TX.). Finally, anti-β-actin antibody ([AC-15] (ab49900)), horseradish peroxidase (HRP)-conjugated anti-rabbit IgG, and anti-mouse IgG secondary

antibodies were obtained from Sigma-Aldrich Corp (St. Louis, MO). All primary antibodies were stored at -20ºC and secondary antibodies at 4ºC in compliance with the manufacturer's instructions.

2.3.2 shRNA vectors and constructs

Short hairpin RNA (*sh*RNA) sequences were purchased from Sigma-Aldrich Corp (St. Louis, MO). Three BCA2 targeted shRNA pLKO constructs included the clone IDs and their corresponding sequences: sh21: TRCN0000433273; sh22: TRCN0000416451; and sh23: TRCN0000004393. The shRNA clones targeted the following locations (sh21(3'UTR), sh22(CDS), and sh23(CDS). Additional shRNA clones targeted to NMNAT1 were purchased from Invitrogen in the pGIPZ constructs with the following clone IDs, sh73 V3LHS_315167, sh74: V2LHS_98547, and sh75: V2LHS_98548.

The shRNA constructs were provided in 5hα-*E.coli* stabs. *E. coli* stocks were expanded in selection media, and frozen aliquots were stored in -80º C. The *E.coli* stocks were clonally selected and expanded in luria broth from Invitrogen, (Carlsbad, CA), then the plasmids containing the shRNA constructs were isolated with a Qiagen (Valencia, CA) mini prep kit. Purified plasmids were measured with a Nano-drop (Thermo Scientific). Stocks were stored at -20ºC in TE (Tris and EDTA) buffer before transfection into breast cancer cell lines for validation of the knockdown efficiency of the specific shRNA sequences. Non-silencing control shRNA (shNT:sh61) was used as a negative control as this was a non-specific scrambled sequence, designed not to target any mRNA sequences. Validation of the individual shRNA's knockdown efficiencies was assessed by western blots and PCR analysis. Subsequent western blots were run to determine if there were any off-target effects of the shRNAs. After the sequences were validated, the purified plasmids were packaged into lentiviral particles using Sigma's Mission lentiviral packaging kit (Sigma, Cat #:

SHP002), following their protocol for packaging and titration. Following lentiviral transductions, clonal populations were obtained by serial dilution in 96-well plates. Six clones were selected for each plasmid (sh-NT1, -NT2, -BCA2, & -NMNAT1), expanded and validated as with the transfection system.

dKD clonal populations were obtained by serial transfection of the validated shNMNAT1 plasmids into the shBCA2-KD clonal populations. Transfections were repeated every 48 hours for 8 days (4 treatments), after which transfection selection media was applied and the cells were observed for Green Fluorescent Protein (GFP) expression. The pLKO (shBCA2) plasmid vectors did not contain GFP reporter protein, while the pGIPZ (shNMNAT1) plasmid vectors did contain the GFP reporter protein. Therefore, cells that expressed GFP in the shBCA2 background would be dKD populations (shBCA2/NMNAT1). The dKD cells were observed under the microscope until they reached 80% confluence, at which point they were trypsinized and sorted for GFP expression, expanded and validated for knockdown efficiency and off-target effects as in the previous model systems.

2.3.3 Cell culture

Human breast cancer cell lines (MDA-MB-468 & MDA-MB-231) and embryonic kidney fibroblast (HEK293T) cells were obtained from the American Type Culture Collection (Manassas, VA). MDA-MB-468 and MDA-MB-231 cells were cultured in Dulbecco's Modified Eagle's Medium (DMEM) (Invitrogen, Carlsbad, CA) containing 10% Hyclone Fetal Bovine Serum (FBS) (Fisher Scientific, Pittsburgh, PA), 100 µg/ml streptomycin, and 100 units/ml penicillin (Invitrogen, Carlsbad, CA). Further, HEK293T cells were grown in antibiotic free DMEM containing 10% FBS. Cells were maintained at 37°C and 5% CO_2 and passaged routinely upon

approaching 80% confluence. Glucose was obtained from Invitrogen (Carlsbad, CA) and used to supplement the DMEM as stock according to experimental conditions.

2.3.4 Generation of stable shRNA clones

Exponentially growing MDA-MB-468 and MDA-MB-231 cells were plated at 40-50% confluency in 6-well plates and allowed to adhere overnight. The next day, media containing 1% FBS was added in place of the 10% FBS, prior to transfection with shRNA plasmid constructs. Transfections were performed utilizing Lipofectamine® LTX reagent according to the manufacturer's protocol (Invitrogen, Carlsbad, CA), with shNT non-targeting shRNA vector as a control. Following a 48-hour incubation period, cells were selected via puromycin (PUR) antibiotic selection, according to the empirically derived kill curves for each cell line. Stably transfected cells (2-3 weeks of PUR selection) were subsequently expanded by serial dilution to obtain clonal populations. Expanded samples were harvested and lysed for western blot analysis to determine the clones with the most efficient shBCA2-KD.

Co-transfection experiments were performed by serial transduction of the second shRNA (shNMNAT1) vectors into stably selected shBCA2, and shNT (control) clonal cell lines. The shNMNAT1 vectors contained GFP expression vectors, which allowed for the flow cytometry selection of clonal populations of cells that expressed both shBCA2 and shNMNAT1-KD vectors. The knockdown of NMNAT1 was confirmed by western blot analysis, once populations were sufficiently expanded. Transfections were performed using Mirus TransIT®-LT1 transfection reagent (Cat # MIR 2305A; Madison, WI) following the manufacturer's protocol. MDA-MB-468 and MDA-MB-231 breast cancer cells were plated in 60-mm dishes at 60% confluency and allowed to seed overnight. Fresh media without antibiotics, was applied two hours prior to transfection. Transfection reagent/DNA complex was formed with a ratio of 3 µl per LT1/ 1 µg

plasmid DNA and applied to the cells according the manufacturer's protocol. After 48 hours, cells were treated as indicated, then were expanded for validation, and frozen aliquots were stored after two weeks in selection media. Cells were harvested and lysed for analysis by western blotting to assess their initial knockdown efficiency. The best clones were expanded and selected for stable dKD after serial dilution.

2.3.5 Western blotting

The cell lines were transfected, glucose treated, or stably selected before harvesting. Cell lysates (30-40 µg) were mixed with 3X sodium dodecyl sulfate (SDS) buffer and boiled for 5 minutes. They were then analyzed by SDS-polyacrylamide gel electrophoresis using 12% tris-glycine gels (Invitrogen, Carlsbad, CA). Cells were then transferred to polyvinylidene difluoride (PVDF) membranes (Millipore, Billerica, MA), and blocked in 3% blocking buffer (3% non-fat dry milk) in tris-buffered saline, 0.1% tween ® 20 detergent (TBST) at room temperature for one hour. The primary antibodies were diluted in blocking buffer (1:1000) and incubated overnight at 4°C on a rocker. Membranes were washed in TBST and incubated with species-specific secondary antibodies conjugated to HRP (1:10,000) for two hours at room temperature. Signals were developed with Pierce [Picco or Fempto] super signal chemiluminescent ECL reagent (Thermos scientific, CA.) and then imaged using the BioRad ChemiDoc XRS+ imaging system with Image Lab Software (BioRad, CA.). Densitometry analysis was performed using Image Lab software (LICOR Biosciences) to determine relative intensity calculated as a percentage of the loading control (β-actin).

A minimum of three independent experiments were performed for each series of experiments (glucose, shBCA2, shNMNAT1, and shBCA2/NMNAT1). Representative western blots are displayed. Western blot images were analyzed by Image-J, and densitometry was

performed on a minimum of three independent replicate experiments. The densitometry data were normalized to the housekeeping gene (β-actin) and then normalized to the corresponding control vector. The results were displayed in bar graphs as (%AUs) (normalized to β-actin). As previously mentioned, corresponding control vectors were used for each targeting vector. These controls were previously validated against each other to evaluate any off-target effects of the controls in the model system.

2.3.6 Cell proliferation assays

In order to determine the relative proliferation rates of the dipartite shRNAi-KD clonal cell lines, the Beckman Coulter particle counter (Indianapolis, IN.) was used to assess the number of cells present under each condition over a period of six days. Cells were plated in a six-well plates in equal amounts (10,000 cells/well). After counting the number of cells in each sample condition over a period of six days, Excel (Microsoft) was used to determine the relative proliferation rates relative to the shNT-control.

2.3.7 mRNA transcript analysis by qPCR and rtPCR with DNA-gel

A RNeasy Mini Kit (QIAGEN) was used to extract the total RNAs. RNAs were reverse transcribed into complementary DNAs using iScript a cDNA synthesis kit (New England Biolabs). cDNA amplification primer pairs for BCA2 were as follows: forward, 5′-GGGGTCACCAGACTCACACT-3′; and reverse 3′-CAGGAAAAAGGGTGTGGAGA-5′. For NMNAT1, primers were forward 5’-GAGCGCGGCTACAGCTT-3’; and reverse 3’-TCCTTAATGTCACGCACGATTT-5’. β-actin was amplified (forward 5’-GAGCGCGGCTACAGCTT-3’ and reverse 5’-TCCTTAATGTCACGCACGATTT-3’) and used for normalization. A Qiagen qPCR analysis machine was used to perform the qPCR analysis, and

to expand the cDNA sequences for gel agarose analysis (rtPCR). cDNA fragments amplified for rtPCR analysis were run on a DNA-agarose gel with ethidium bromide and imaged on BioRad ChemiDoc XRS+ Imaging System. The images were then analyzed by Image-J. Relative signal intensity was normalized to the housekeeping gene β-actin, and values were presented as % AU normalized to the control.

2.3.8 NMNAT1 promoter luciferase assay

Cells were plated in 96-well plates and co-transfected with the NMNAT1 promoter–luciferase vector (pLightSwitch_Prom: Product # S705857; Switch Gear Genomics; Carlsbad, CA) and a Renilla vector from Promega (Madison, WI), according to Switch Gear Genomics Light Switch Luciferase Assay System. Stable shBCA2-KD cells were plated in both 96-well plates and six-cm dishes for parallel evaluation of protein expression and confirmation of shBCA2-KD. The effects of shBCA2-KD on NMNAT1 promoter activity were calculated as Relative Luciferase Units (RLU) relative to the control Renilla vector. The experiment was repeated twice under high glucose conditions overnight. The results presented represent two experiments performed in triplicate in high glucose (4.5 g/l) media.

2.3.9 Proteomics

Dr. Carruthers and Dr. Caruso of the Wayne State University Proteomics Core assisted with protein analysis. Protein and base peptides were identified via MS/MS analysis and validated using Scaffold version _4.1.1, Proteome Software Inc. (Portland, OR). Per the Peptide Prophet algorithm, peptides identified at greater than 80% were acknowledged (Keller, Nesvizhskii, Kolker, & Aebersold, 2002) with scaffold delta-mass correction and were accepted if they contained at least one identified peptide. Then, protein probabilities were assigned (Nesvizhskii, Keller, Kolker, & Aebersold, 2003). Proteins that could not be identified during the analysis were

either grouped into clusters based on peptide evidence or grouped using the principle of parsimony. Significant peptides were grouped into clusters (courtesy of Dr. Paul Stemmer & Dr. Daniela Buac-Ventro) and plotted into a venn diagram.

2.3.10 Media analysis

All reagents and procedures for the media analyses were generously provided by and performed by Dr. Jian Wang's lab. Experimental conditions and sample preparation were performed in the Dou lab. For the media analysis, all vectors were carried out in triplicate with two independent time points for sample collections. The experiments were repeated with refined experimental parameters, two additional times for each vector, and each cell line used. Cells were plated at 60% confluence in 60 mm^2 plates the day before treatment and allowed to seed in normal media. At time zero hours, media was replaced with fresh media, and the initial glucose sample was collected. The initial experiments examined the changes in media glucose and lactate levels over periods of 12, 24, and 48 hours. The preliminary experiments revealed no difference in glucose consumption or lactate production at 24 and 48 hours. It was determined that the cells were depleting all the available glucose in the media at earlier time points. In order to assess the effects of shBCA2, shNMANT1, and shBCA2/NMNAT1 earlier time points would need to be evaluated. Subsequent experiments narrowed the optimum time to 12 hours. Preliminary experiments also evaluated whether there were functional differences in glucose consumption or lactate production between the parental (Pr) and the non-targeting controls to determine if there were any off-target effects associated with shRNA insertion or clonal selection. No difference was observed between Pr and non-targeting vectors in proliferation rates or media composition. All graphs and data presented are for 12 hours incubation, with three samples run for each of the conditions, and two independent experiment dates to demonstrate reproducibility. Graphs

represent the statistical average percent change in glucose consumption or lactate production relative to the non-targeting control vector (shNT).

2.3.11 Glucose consumption assay

Glucose consumption in the model system was determined by an enzyme-linked assay that compared the initial concertation of glucose at time zero hour (time zero was defined at the moment media was changed the following day after cells were seeded) in the media, relative to the endpoint concentration of glucose in the media, corrected for the number of cells in the plate. The relative glucose consumption was calculated in % Relative Glucose Consumption Normalized to Control. Relative glucose consumption was assessed relative to the shNT control vector specific to the target construct (shBCA2=shNT1, shNMNAT1=shNT2, and shBCA2/NMNAT1=NT1/NT2: shNT2 in the figures and in the text).

All reagents were obtained from Sigma-Aldrich (Sigma, St. Louis, MO) including: Hexokinase/Glucose-6-Phosphate Dehydrogenase (HK/G6PDH) (Sigma, H8629), ATP (Sigma, A2383), $NADP^+$ (Sigma, N5755), $MgCl_2$ (Sigma, M8233), tris base (Fisher, BP152-5), and glucose (Sigma, G7528). The assays were run in a Costar 96-well plate (Costar, 3635) and read by CLARIOstar microplate reader (BGM LABTECH). Media control and stock glucose concentrations were used to establish a standard curve, and the number of cells per well were counted by Beckman Coulter particle counter (Beckman Coulter, Pasadena, CA) (as described previously in the proliferation assay section).

The glucose consumption assay developed and carried out by Dr. Jian Wang's lab was based on an enzyme coupled reduction assay. The assay works by coupling the phosphorylation of the available glucose in the media by HK with ATP, which yields proportional Glucose-6-Phosphate (G6P) and ADP (equation 1).

$$\text{Glucose} + \text{ATP} \xrightarrow{\text{Hexokinase (HK)}} \text{Glucose-6-phosphate (G6P)} + \text{ADP} \quad (1)$$

G6P is then oxidized by glucose-6-phosphate dehydrogenase in the presence of $NADP^+$ to produce 6-phosphogluconolactone while concomitantly reducing NADP+ to NADPH, which gives off an absorbance at 340 nm. The intensity of the absorbance measured at 340 nm is proportional to the glucose concentration in the sample (equation 2).

$$\text{G6P} + \text{NADP}^+ \xrightarrow{\text{Glucose-6-phosphate Dehydrogenase (G6PDH)}} \text{6-P-Gluconolactone (G6P)} + \text{NADPH} \quad (2)$$

In order to determine the actual concentration of glucose, a standard curve with serial dilutions of glucose with the following concentrations was used: 0, 0.156, 0.3125, 0.625, 1.25, 2.5, and 5 mg/ml. The assay mix was prepared with the following components: 25 mM tris-HCL pH 8.0, 1 mM $MgCl_2$, 1 mM $NADP^+$, 1 mM ATP, and 2 units/ml HK/G6PDH. Two μl of standard or sample were added to each well of the assay plate followed by 100 μl assay mix to each well. The assay plate was then incubated at room temperature for 30 minutes.

After the 30-minute incubation period, absorbance was measured at 340 nm and compared against the reagent blank (sample media at time zero hour) on the CLARIOstar microplate reader. Glucose standards were plotted and used to interpolate the sample glucose concentrations. The end glucose concentration was subtracted from the beginning concentration and corrected for the number of cells in each plate, determined by cell counting using the Beckman Coulter particle counter, as described in the proliferation assays.

2.3.12 Lactate production assay

Lactate production in the model system was determined by an enzyme linked (LDH) assay that compared the initial concertation of lactate at time zero hour in the media, relative to the endpoint concentration of lactate in the media, corrected for the number of cells in the plate. The relative lactate production was calculated in % Relative Lactate production Normalized to Control. Relative lactate production was assessed relative to the shNT control clonal population of cells.

All reagents for the assay were obtained by Dr. Jian Wang's lab from Sigma-Aldrich (Sigma, St. Louis, MO) including: LDH (Sigma, L3916), NAD^+ (Sigma, N0632), Hydrazine (Sigma, 215155), Tris Base (Fisher, BP152-5), Bovine Serum Albumin (BSA) (Sigma, A7906) and lactate (Sigma, L7022). The assays were performed and read in a Costar 96-Well plate (Costar, 3635) and read by a CLARIOstar microplate reader (BGM LABTECH). Media controls and stock glucose concentrations were used to establish a standard curve, and a number of cells per well were counted by Beckman Coulter particle counter (Beckman Coulter, Pasadena, CA), as described previously in the proliferation assay section.

The lactate production assay was developed and carried out by Dr. Jian Wang's lab and is based on the enzyme (LDH) linked coupling of the oxidation of lactate to pyruvate, and the concurrent reduction of NAD^+ to NADH which can be measured the by the intensity of absorbance at 340 nm (equation 3).

$$\text{Lactate} + NAD^+ \xrightarrow[(LDH)]{\text{Lactate Dehydrogenase}} \text{Pyruvate} + NADH \qquad (3)$$

The intensity of this absorbance was proportional to the concentration of lactate in the sample. Hydrazine drives the complete conversion and removal of pyruvate from the reaction, drawing the equilibrium of the combined reactions to consume all the lactate present in the sample

(equation 4). By driving the reaction to use up the lactate in the reaction completely, the absorbance measured at 340 nm is proportional to the concentration of lactate present in the sample.

(4)

Comparing the concentrations of lactate at time zero hour and 12 hour and correcting for the number of cells in the plate allowed for the calculation of the nmoles lactate produced / 10^6 cells. This value was then normalized to the control condition as 100% and the data were interpreted as % lactate production relative to the non-targeted controls.

To determine the amount of lactate produced in each condition, serially diluted lactate reference standards were used to generate a standard curve and convert absorbance at 340 nm to nmoles lactate. The following reference standards were used: 0nM, 30nM, 100nM, 300nM, 1,000 nM of lactate. Once the samples were collected and cell counts were determined, the sample assay mix was prepared with the following components: (a) 320 mM tris-HCL pH 9.0, (b) 320 mM hydrazine, (c) 4 mM NAD^+, (d) 1% BSA, and (e) 16 units/ml LDH. Fifty µl of sample and standards were added to each well of the assay plate, then 50 µl assay mix was added to each well and left to incubate at room temperature for 30 minutes.

Two µls of standard or sample are added to each well of the assay plate followed by 100 µls assay mix to each well. The assay plate was then incubated at room temperature for 30 minutes. After the 30 min incubation period, absorbance was measured at 340nm on the CLARIOstar microplate reader and compared against the reagent blank (sample media at time zero hour).

Lactate standards were plotted and used to interpolate the sample lactate concentrations. The initial lactate concentration was subtracted from the end concentration and corrected for the number of cells in each plate, as determined by cell counting using the Beckman Coulter particle counter.

CHAPTER 3: CORRELATION BETWEEN BCA2 AND NMNAT1

A Kaplan Meyer analysis was conducted in a prior study of BCA2 relative to patient survival. The Kaplan Meyer analysis identified BCA2 as an oncogene (Buac et al., 2013). High BCA2 expression is associated with a lower overall survival probability relative to low BCA2 expression (Burger et al., 2010). Although not statistically significant, the analysis conducted by Dr. Jian Wang provided a *p*-value of 0.061, just over the statistically significant threshold. In addition, NMNAT1 is a known tumor suppressor (Henderson, Miranda, & Emerson, 2017).

3.1 Prior research and preliminary evidence for inverse relationship between BCA2 and NMNAT1

Based on these findings, a transcript analysis was performed to examine the association between BCA2 and NMNAT1 expression in TNBC cell lines. The analysis measured mRNA expression normalized to β-actin and suggested an inverse correlation between BCA2 and NMNAT1 transcript levels (Figure 3.1). Data (mRNA Expression (RNAseq) obtained from the Broad Institute for both BCA2 and NMNAT1 were segregated by TNBC cell lines and plotted on a dot plot, and the spearman correlation determined. The relative BCA2 and NMNAT1 transcripts normalized to β-actin revealed an inverse correlation (Figure 3.1). The calculated spearman's correlation was -0.86. Along with the preliminary phosphoproteomic data from Dr. Buac-Ventro, these results provided additional rationale to investigate the association between BCA2 and NMNAT1 in TNBC.

Figure 3.1 BCA2 and NMNAT1 transcript expression are inversely correlated in triple negative breast cancer cell lines

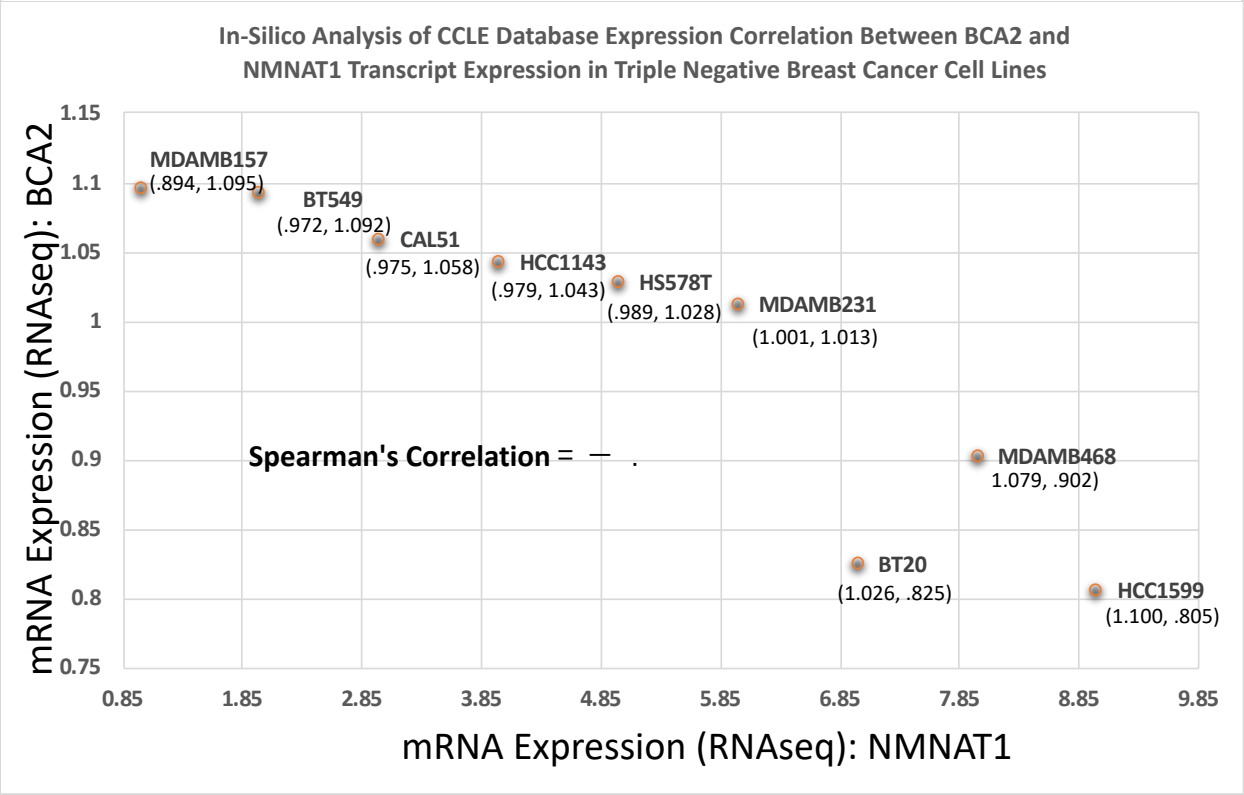

The relative expression of the BCA2 and NMNAT1 transcripts were plotted from data obtained from the Broad Institute's (CCLE) transcript database. The relative transcript expression (mRNA Expression (RNAseq)) normalized to βActin for BCA2 and NMNAT1 in TNBC cell lines was plotted, and statistical analysis performed. The graph revealed an inverse correlation between BCA2 and NMNAT1 in the TNBC cell lines. The spearman's correlation between BCA2 and NMNAT1 in the TNBC cell lines was -0.86. These data provided the rationale to investigate the association between BCA2 and NMNAT1 in TNBC.

3.2 Glucose stimulation increased BCA2 and decreased NMANT1 protein expression

A study was conducted to ascertain the effects of glucose concentration on BCA2 and NMNAT, respectively. Western blots were run where glucose was either added in excess or was deprived in two TNBC cell lines (MDA-MB-468 and MDA-MB-231). Initial glucose deprivation was performed overnight for both TNBC cell lines, resulting in the absence of BCA2 and the presence of NMNAT1 protein expression at zero hour, followed by eight hours of glucose added in excess. Densitometry was performed and results are expressed as % AUs normalized to β-actin

and are reported as mean values for a minimum of two representative blots performed on separate dates. Standard errors were included when triplicate experiments were available. Representative western blots are shown for each graph (Figure 3.2).

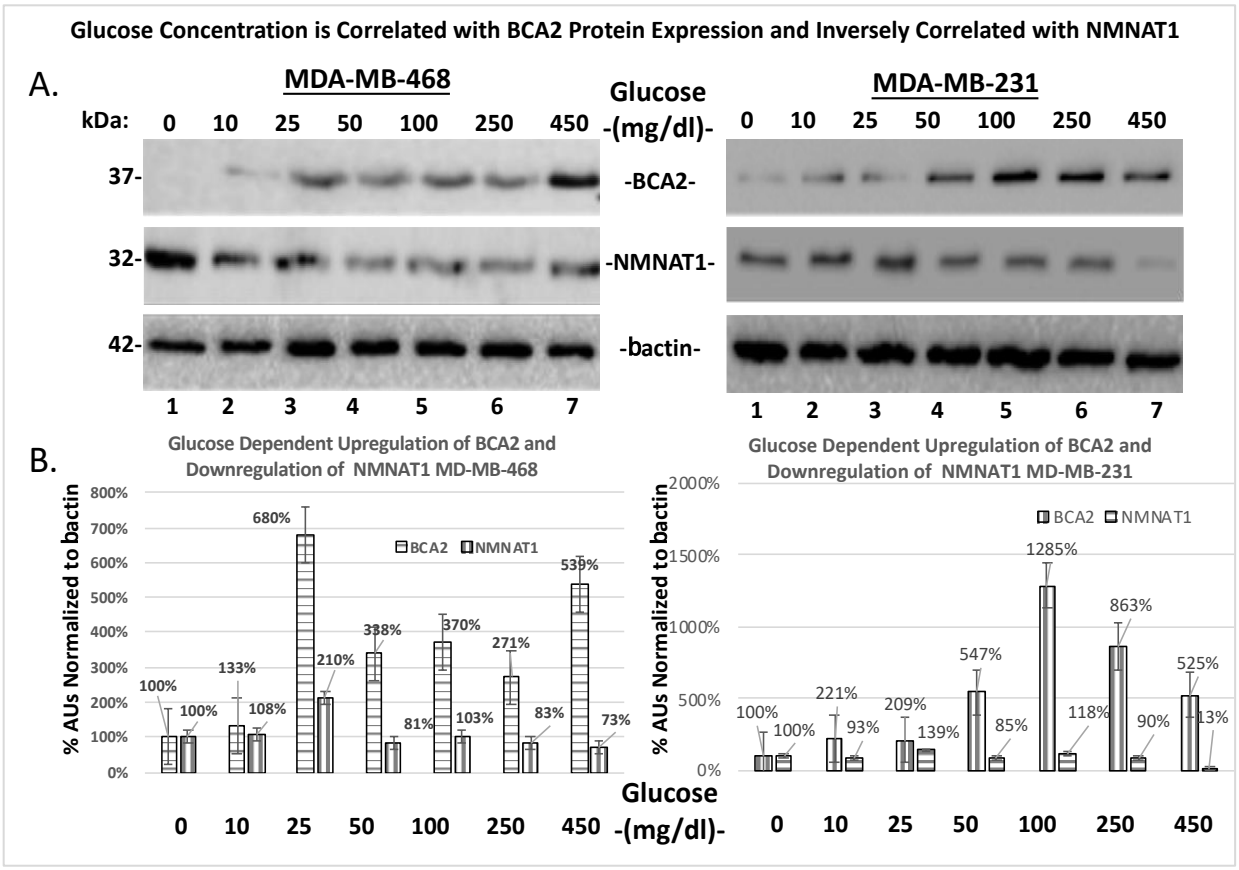

Figure 3.2 Glucose concentration is positively correlated with BCA2 protein expression, and inversely correlated with NMNAT1 protein expression.

BCA2 protein expression is positively correlated with glucose concentration, as demonstrated in the representative western blots of MDA-MB-468 and MDA-MB-231. A. Western blot of TNBCSLs treated with increasing concentrations of glucose (after glucose starvation overnight) for 16 hours. B. Densitometry data showed that glucose stimulated BCA2 in TNBC cell lines increased, with BCA2 protein increased by ~500% at the maximum concentration of glucose in both cell lines. This was accompanied by a decrease in NMNAT1 protein expression in response to glucose stimulation (MDA-468 ~73%; and MDA-231 ~13%). These results show that BCA2 and NMANT1 protein expression is inversely correlated in response to glucose stimulation.

3.3 Glucose deprivation decreased BCA2 and increased NMANT1 protein expression

Figure 3.3 illustrates the effects of glucose deprivation of both TNBC cell lines on BCA2 protein. BCA2 expression was detected at zero hours (lane one) and progressively decreased,

resulting in a complete loss of BCA2 protein expression at 16 hours (lane five). In both breast cancer cell lines, a direct correlation between the presence or absence of glucose with BCA2 was found. There was an inverse relationship between BCA2 and NMNAT1. At eight hours, both cell lines showed an increase in NMNAT1 expression of ~200%, with a corresponding 51-65% decrease in BCA2 protein expression. The glucose stimulation and deprivation experiments were repeated at least three independent times, and representative images from a single experiment are shown along with the corresponding densitometry data that shows the average changes in protein expression in the given conditions.

3.4 Discussion

These data suggest that an inverse relationship between BCA2 and NMNAT1 expression exists in relation to extracellular glucose concentrations. These data in conjunction with prior research findings, substantiate the inverse correlation previously reported between BCA2 and NMNAT1 (Buac et al., 2013). These data show that the effects of glucose concentration on BCA2 and NMNAT1 protein expression support the hypothesis that NMNAT1 may be a potential target protein of BCA2 either directly or indirectly. Further, these data support the CCLE in-silico analysis and the MS/MS data. Finally, these data signify a need for further investigation into the relationships between BCA2 and NMNAT1 expression in TNBC cell lines, as well as a need to explore further the mechanism by which glucose levels affect the expression of both proteins.

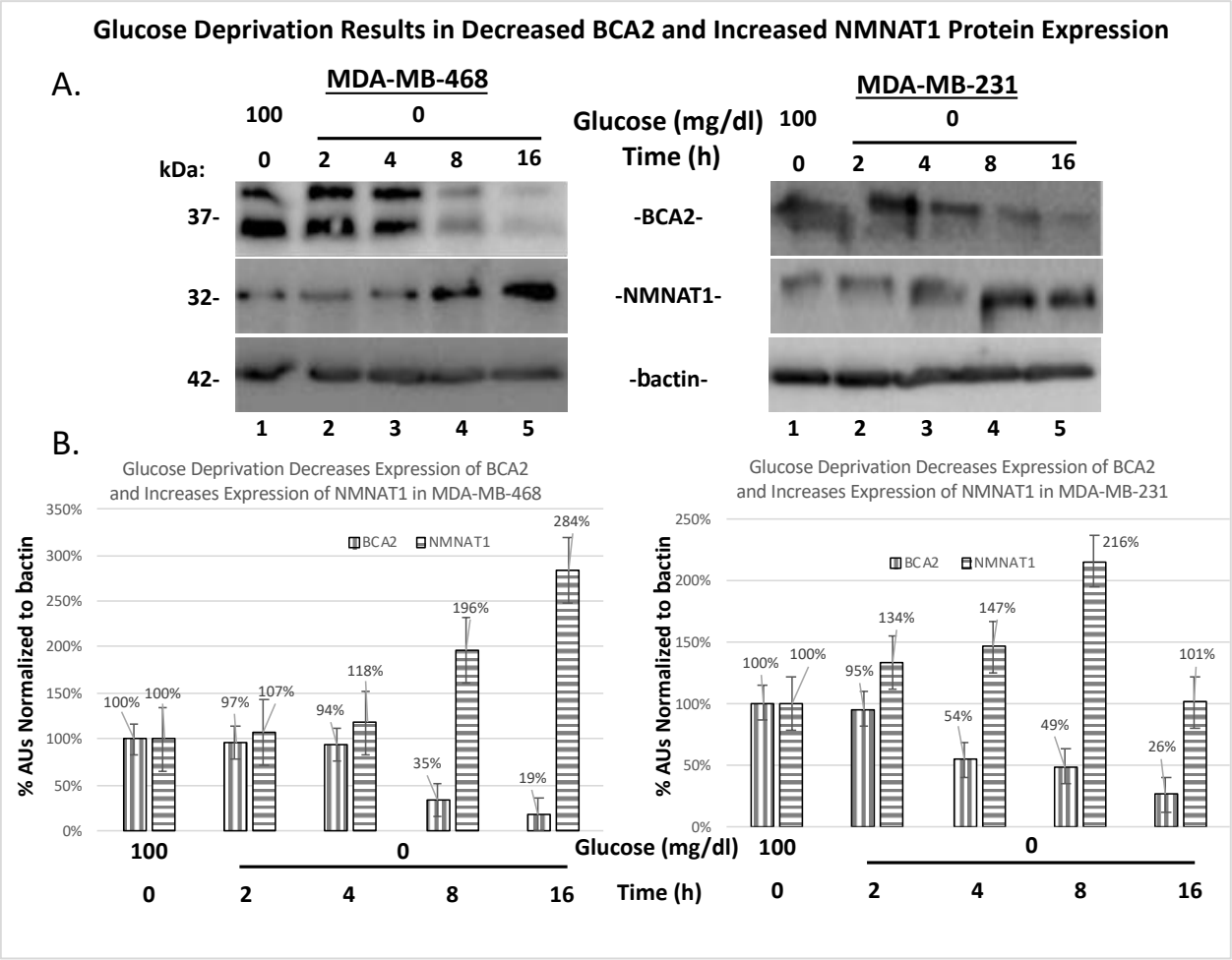

Figure 3.3 Glucose deprivation is associated with decreased BCA2 protein expression, and increased NMNAT1 protein expression

To determine if the inverse association between BCA2/NMNAT1 occurs in response to glucose, a glucose deprivation assay was performed. Cells were plated in normal media and allowed to sit overnight. A. Results are shown that illustrate the effects of glucose deprivation in both TNBC cell lines (MDA-MB-468 and MDA-MB-231) from 0 to 16 hours. B. The graphs show the densitometry for the relative protein expression normalized to βActin. The results indicate that glucose deprivation results in a time-dependent decrease in BCA2 protein expression. In addition, there is an inverse correlation between NMNAT1 protein expression relative to glucose concentration concurrent with the changes in BCA2 protein expression. A minimum of 3 blots were imaged from different passages and averaged for densitometry data; representative blots of the results are shown. These results suggest an inducible inverse correlation between BCA2 and NMNAT1, consistent with the preliminary Mass-Spec and in-silico analyses of BCA2 and NMNAT1 in TNBC cell lines.

CHAPTER 4: shBCA2-KD REGULATES NMNAT1 PROTEIN, TRANSCRIPT, AND PROMOTER ACTIVITY

shRNAi technology was utilized to knockdown the expression of BCA2 through the lentiviral transduction of multiple shBCA2 constructs into the TNBCs, MDA-MB-468 and MDA-MB-231, following manufacturer's protocol as described in the materials and methods section. A minimum of three targeted shRNA sequences for BCA2 were transfected into each cell line. Serial dilutions of the pooled populations of stably expressing shRNA vectors were used to generate clonal populations of shBCA2-KD and were validated by western blot and PCR.

4.1 shBCA2-KD resulted in a significant decrease in BCA2 protein and resulted in a corresponding increase in NMNAT1 expression.

shBCA2-KD by shRNA significantly decreased protein and transcript expression of BCA2. Expression of BCA2 and NMNAT1 proteins were assessed via western blot analysis, and densitometry analyses were performed to assess the relative expression of BCA2 and NMNAT1. BCA2 protein expression significantly decreased in both MDA-MB-468 (54% and 49%) and MDA-MB-231 (31% and 19%) (Figure 4.1).

In addition, the expression of NMNAT1 protein was increased MDA-MB-468 (147% and 216%) and MDA-MB-231 (394% and 604%) and inversely correlated with expression of BCA2 protein. Thus, shBCA2 genetic knockdown decreased BCA2 protein expression and resulted in an increase in NMNAT1 protein expression (Figure 4.1)

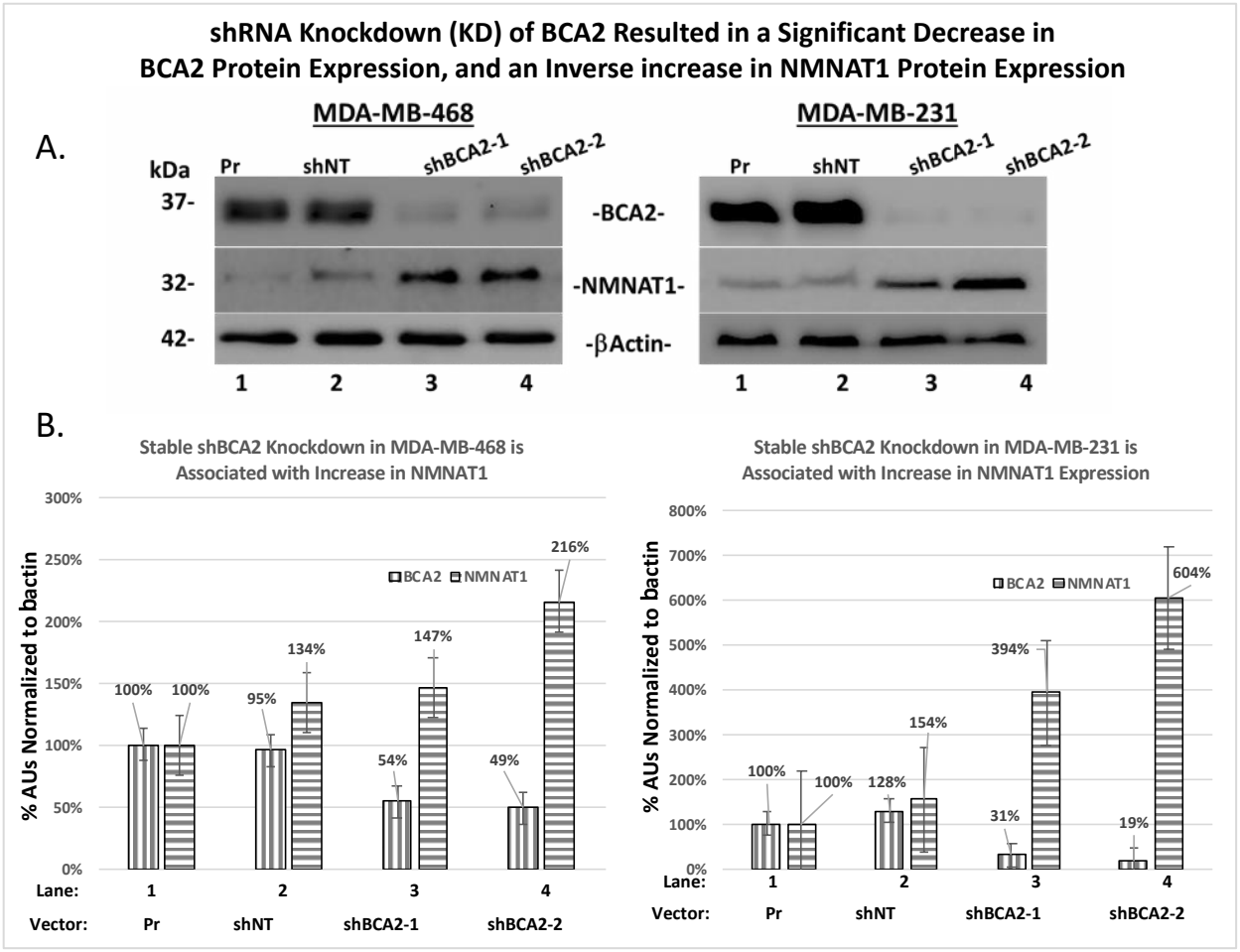

Figure 4.1 shRNA KD of BCA2 in MDA-MB-468 and MDA-MB-231 significantly decreased BCA2 protein expression, associated with a concurrent increase in NMNAT1 protein expression.

Stable clonal populations of shBCA2-KD were achieved through lentiviral transduction of multiple shBCA2 vectors, as well as a sh-Non-Targeting control (shNT), followed by clonal selection, validation, and expansion. A minimum of 3 blots were imaged from different passages and averaged for densitometry data. Representative blots are shown. The shNT control vector had no effect on the expression of BCA2 or NMNAT1 protein expression. However, shBCA2-KD resulted in a stable knockdown of BCA2 in both cell lines (MDA-MB-468: 54% and 49% and MDA-MB-231: 31% and 19%), correlating with a robust increase in NMNAT1 protein expression in both cell lines (MDA-MB-468: 147% and 216% and MDA-MB-231: 394% and 604%).

4.2 shBCA2-KD significantly decreased BCA2 transcript and increased NMNAT1 transcript expression.

The above findings validated the correlation between BCA2 and NMNAT1 at the protein level and showed that this association was both inducible (in response to glucose) and could be

achieved through genetic manipulations (shBCA2-KD). Under both stimuli BCA2 and NMNAT1 were inversely correlated.

In order to determine if shBCA2-KD was modulating NMNAT1 transcript expression rtPCR (DNA-Gel), and qPCR were used to assess the fold change in NMNAT1 transcript. DNA gels were performed in triplicate, and signal intensity was measured using Image-J. Densitometry was normalized to the ß-actin housekeeping gene and the control vector shNT. shBCA2-KD resulted in a significant decrease in BCA2 transcript expression in both cell lines (MDA-MB-468: 12%, MDA-MB-231: 6%). shBCA2-KD was accompanied by an increase in NMNAT1 transcript expression (MDA-MB-468: 315%, MDA-MB-231: 854%) as determined by densitometry of the corresponding western blot DNA-gels.

In order to verify the preliminary transcript data, qPCR analysis was performed in triplicate with a Qiagen q-PCR kit on an Applied Biosystems™ StepOnePlus™ Real-Time PCR System. Results are shown for relative mRNA expression normalized to ß-actin and NT Control (ΔΔCT). shBCA2-KD resulted in significant decreases in BCA2 transcripts (MDA-468, 45%; MDA-231, 31%) and increased NMNAT1 transcripts (MDA-468, 146%; MDA-231, 150%). These data suggest that BCA2 is somehow regulating the expression of NMNAT1 at the transcript level, as well as at the protein level.

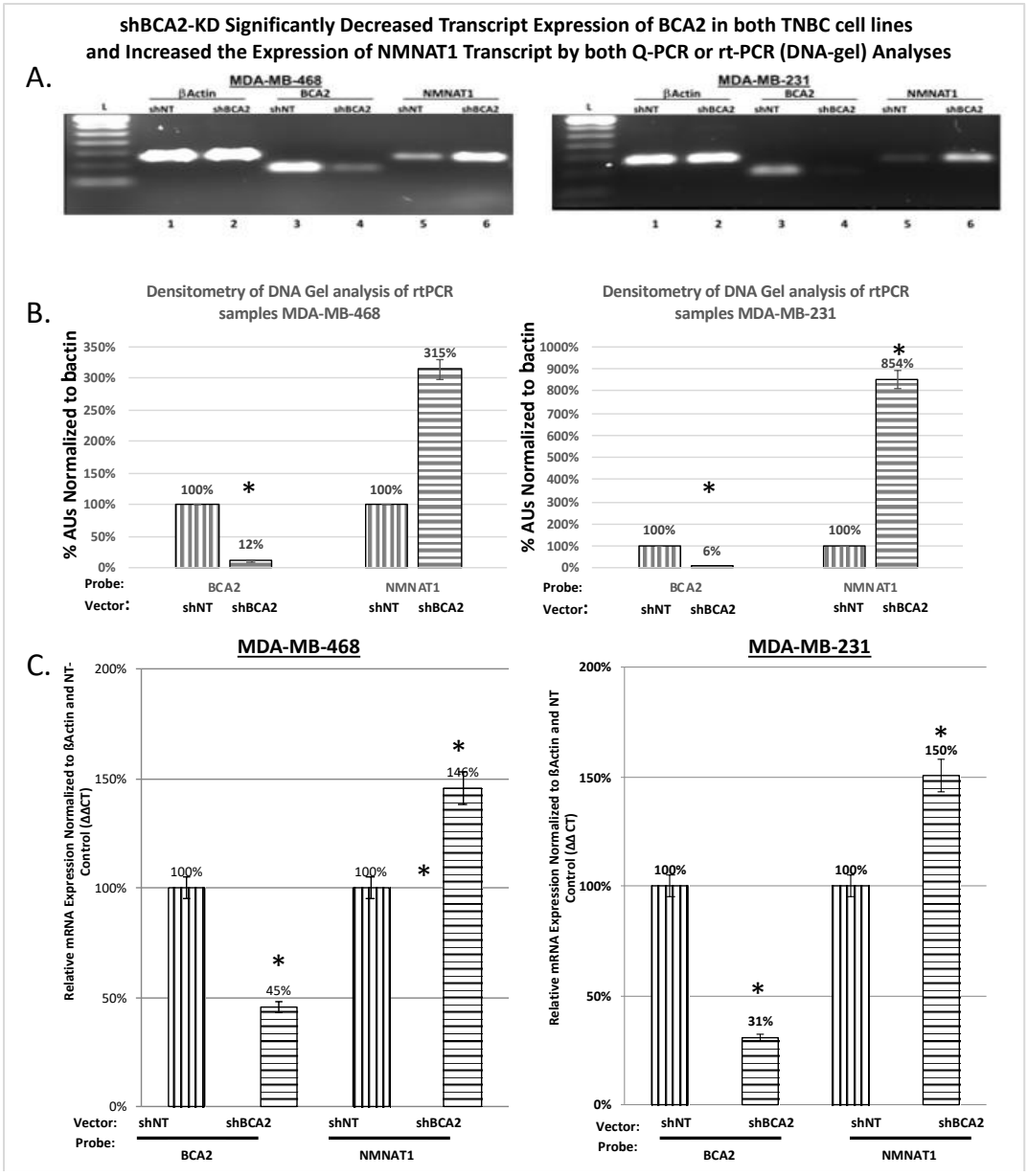

Figure 4.2 shBCA2-KD significantly decreased BCA2 transcripts and increased NMNAT1 transcripts by rt-PCR (DNA-gel) and qPCR analyses in both TNBC cell lines.

shBCA2-KD resulted in decreased BCA2 transcripts and increased NMNAT1 transcripts in both TNBCSLs (shBCA2-MDA-MB-468: 12% BCA2 and 315% NMNAT1 / shBCA2-MDA-MB-231: 6% BCA2 and 854% NMNAT1), as determined by analysis by rt-PCR and staining and densitometry of a DNA gel. Densitometry was normalized to ßActin and the shNT. The densitometry was performed on images from separate experiments done in triplicate. shBCA2 also had similar effects when measured by qPCR analysis. Samples were run in separate experiments in high glucose media and in triplicate. Values represent relative mRNA expression normalized to ß-actin and NT Control (ΔΔCT). Results were as follows: shBCA2-MDA-MB-468: 12% BCA2 and 146% NMNAT1 / shBCA2-MDA-MB-231: 31% BCA2 and 150% NMNAT1. These data suggest that BCA2 is regulating the expression of NMNAT1 at the transcript level as well as at the protein level.

4.3 shBCA2-KD significantly increased NMNAT1 promoter activity

The previous findings demonstrated that shBCA2-KD induces NMNAT1 protein and transcript expression. Switch Gear Genomics Light Switch Luciferase promoter activity assay was used in order to explore whether shBCA2-KD regulated changes in NMNAT1 at the level of NMNAT1's promoter. Cells were plated in 96-well plates and cotransfected with reporter vectors for NMNAT1 promoter–luciferase vector (pLightSwitch_Prom: Product # S705857; Switch Gear Genomics; Carlsbad, CA) and a Renilla vector from Promega (Madison, WI), according to Switch Gear Genomics Light Switch Luciferase Assay Systems protocol. Promoter activity was determined by utilizing Promega's firefly dual luciferase promoter activity assay and a Qiagen plate reader (Section 2.3.13). NMNAT1 promoter activity was assessed relative to the Renilla vector control and then normalized to shNT1. The experiments were performed in high glucose (4.5 g/l) media after overnight seeding with fresh media change as established and performed in the previous experiments.

shBCA2-KD resulted in increased NMNAT1 promoter activity in both cell lines compared to the non-targeted controls (MDA-MB-468: 409% and 459%; MDA-MB-231: 175% and 169%). Interestingly, results for all these experiments were only statistically significant when the experiments were performed under "high" glucose conditions, for time periods not greater than 24 hours after seedings, and a confluence below ~70%. If any of those factors were not controlled, the results became inconsistent and uninterpretable.

The dependence of the inverse correlation between BCA2 and NMNAT1 on glucose concentration in the media, confluence, and seeding time suggests that the metabolic state of the cells is essential to the observed findings. This suggests that the concentration of glucose in the media must be sufficient for shBCA2-KD to induce NMNAT1 expression at the level of the promoter. Therefore, high glucose may be a necessary intermediate metabolite in the mechanism regulating NMNAT1 expression in response to genetic inhibition of BCA2.

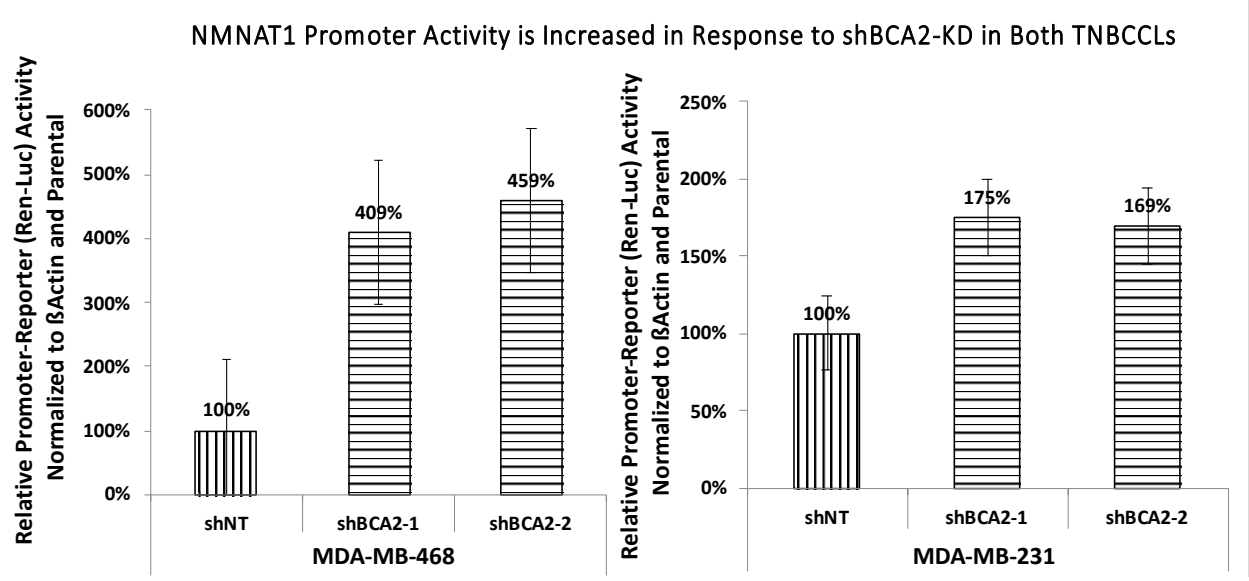

Figure 4.3 shBCA2-KD significantly increased NMNAT1 promoter activity determined by dual renilla luciferase assay in both TNBC cell lines

shBCA2-KD resulted in an increase in NMNAT1 promoter activity. NMNAT1 promoter activity is significantly increased in response to shBCA2-KD in both cell lines as determined by a firefly renilla luciferase dual reporter assay, which normalizes promoter activity to β-actin relative to shNT control. In MDA-MB-468 cell lines, promoter activity increased to 409% and 459% in shBCA2-1 and shBCA2-2 KD clones, respectively. In MDA-MB-231 cells, promoter activity also increased by 175% and 169% in shBCA2-1 and shBCA2-2 KD clones. This, combined with the previous data, suggests that BCA2 is a regulating expression of NMNAT1 protein and transcripts at the level of NMNAT1 transcription.

4.4 Discussion

BCA2 negatively regulates the expression of the NMNAT1 protein and transcripts, as well as at the promoter activity level. The limitations of this study were that they do not delineate a specific mechanism by which BCA2 is modulating NMNAT1 expression. Given that BCA2 is an

E3-ligase, it is likely that BCA2 exhibits its activity through its ubiquitinating activity. In order to further investigate the exact mechanism by which BCA2 is modulating NMNAT1 expression, rescue experiments with wild type (WT) and mutant (MT) variants of BCA2 would help to define the functional domain of BCA2 that the changes in NMNAT1 expression depend on.

If the rescue studies with BCA2-WT reversed the increase in NMNAT1 observed in the previous findings, and one of the mutant variants of BCA2 did not rescue the observations, then the specific region mutated in the BCA2-MT would be identified as a strong candidate for the mechanism of action by which BCA2 regulates NMNAT1 expression. Specifically, if a BCA2-E3 -MT was unable to rescue original findings, this would suggest that the E3 domain of BCA2 is responsible for regulating NMNAT1 directly or through some intermediate. In order to determine potential binding partners of the theoretical BCA2-E3 ligase, a ubiquitin enrichment assay could be used to identify protein ubiquitinated in the BCA2-WT and not ubiquitinated in the BCA2-E3-MT. Any identified proteins in the ubiquitinated population of cells would be a good candidate for an intermediate regulator of NMAT1 by BCA2.

Future studies should focus on elucidating the stability of BCA2 protein in response to glucose deprivation, utilizing cycloheximide to determine how long the protein is stable. The role of BCA2 in regulating whole cell metabolism (metabolomic profile of shNT vector shBCA2) would also be valuable as it could identify potential points in the metabolic pathway, which could be potential chemotherapeutic targets of BCA2. Potential targets could later be verified by immunoprecipitation assays to pull down BCA2 associated proteins, as well as evaluating the ubiquitinated proteins in the presence or absence of BCA2 by shBCA2-KD. Finally, the mechanism by which BCA2 is regulating NMNAT1 expression needs to be further explored to determine.

CHAPTER 5: shBCA2-KD INHIBITS KEY MARKERS OF WARBURG METABOLISM (LDHA/LDHB) AND DECREASED WARBURG-LIKE METABOLISM AND PROLIFERATION

The positive correlation between glucose concentration and expression of BCA2 and the inverse correlation of BCA2 and NMNAT1 is consistent with the hypothesis that BCA2 is a regulator of glucose (Warburg-like) metabolism. In order to investigate this further, shBCA2 clonal populations were evaluated by western blot for key markers of Warburg-like metabolism and the functional consequences on Warburg-like metabolism and cellular proliferation.

5.1 shBCA2-KD is associated with a decrease in Warburg-like metabolism as measured by the observed ratio of LDHA/LDHB

In order to further investigate the finding that shBCA2-KD resulted in decreased Warburg-like metabolism the expression of LDHA and LDHB protein levels were evaluated by western blot analysis in MDA-MB-231 and MDA-MB-468 cells. The findings revealed that a decrease in expression of the oncogene BCA2 was accompanied by a decrease in protein expression for LDHA, and a corresponding increase in LDHB. This decreased ratio of LDHA/LDHB is a known measure of Warburg-like metabolism (Burns & Manda, 2017). The knockdown of BCA2 again was associated with a concurrent upregulation of NMNAT1 protein expression. This was accompanied by a decrease in LDHA expression and an increase in LDHB protein expression (Figure 5.1), which suggested an overall decrease in Warburg-like metabolism.

These research findings verify that BCA2 and NMNAT1 are inversely correlated in both cell lines. The rest of the shBCA2-KD western blots not only recapitulated the previous findings of the inverse correlation between BCA2/NMNAT1, but also validated the proposed hypothesis that BCA2 modulates glycolysis and Warburg-like metabolism. In order to further investigate and

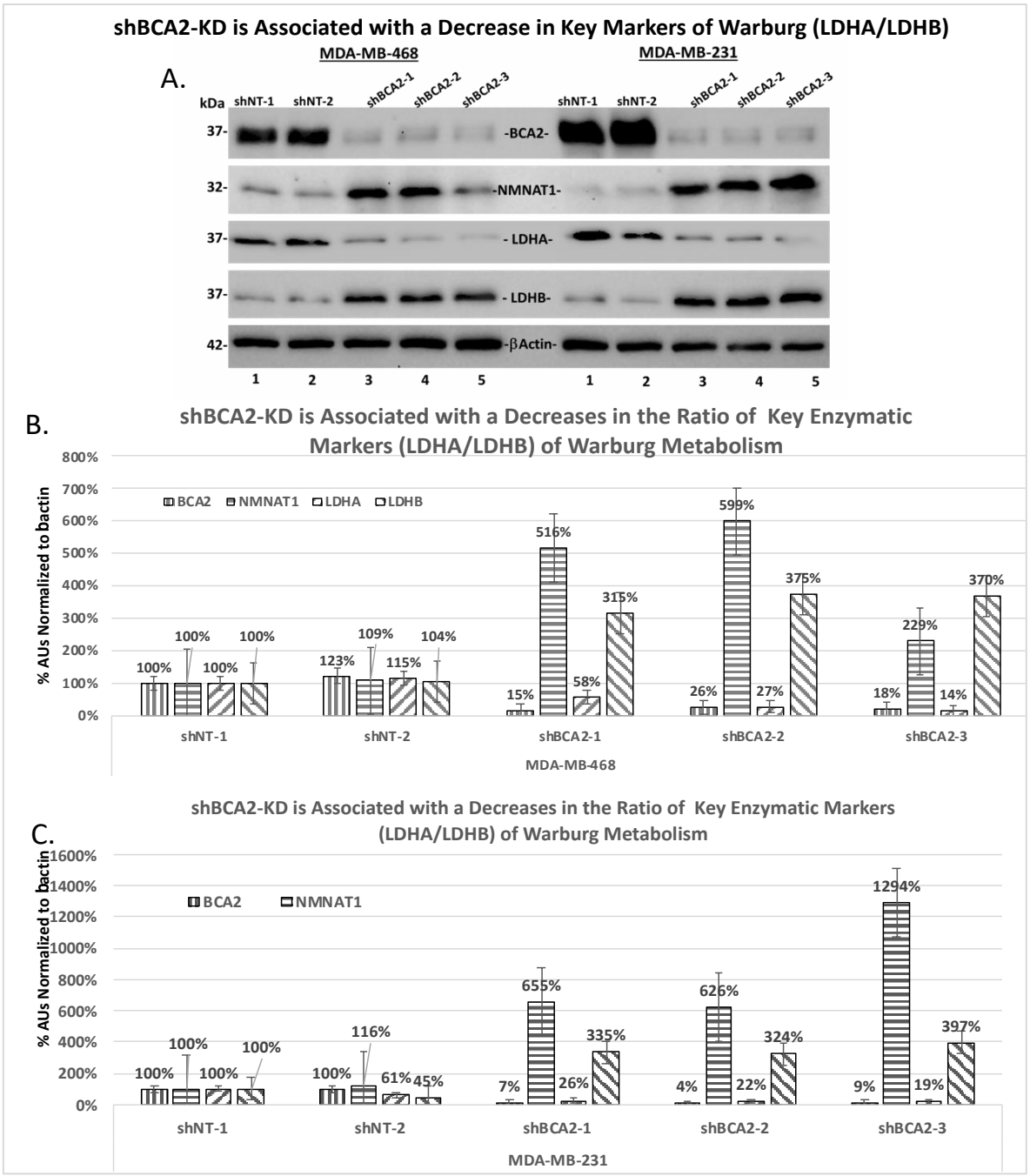

Figure 5.1 shBCA2-KD is Associated with a Decrease in the Ratio of key Enzymatic Markers of Warburg-like metabolismMetabolism (LDHA/LDHB).

shBCA2-KD decreased the ratio of LDHA/LDHB and upregulation of NMNAT1. Increased NMNAT1 (MDA-MB-468: 515%, 599%, and 370%) and (MDA-MB-231: 655%, 626%, and 1294%). Decreased LDHA (MDA-468: 58%, 27%, and 14%) and (MDA-231: 26%, 22%, and 19%), and increased LDHB (MDA-468: 315%, 375%, and 370%) and (MDA-231: 335%, 324%, and 397%). The data show that shBCA2 increases NMNAT1 and decreases LDHA/LDHB, Warburg-like markers. Representative blots are displayed of experiments performed in triplicate, and densitometry was analyzed with Image-J (see section 2.3.5).

validate these findings, it was necessary to measure the consumption of glucose and the production of lactate.

These findings suggest that BCA2 is playing a role in the regulation of the expression of LDHA and LDHB, which are established markers of the relative Warburg-like metabolism in the cell (Burns & Manda, 2017). The results also suggest that these phenomena are at least associated with a change in NMNAT1 expression. However, the exact mechanism and functional consequences are unclear. In order to determine the functional consequences of the effects of shBCA2-KD on LDHA/LDHB, the extent of glucose consumption and lactate production were used as measures of Warburg-like metabolism.

5.2 shBCA2-KD decreased glucose consumption and decreased lactate production

An analysis of the glucose and lactate concentrations was performed in triplicate on the media of the disparate clonal cell lines in order to assess the relative Warburg-like activity of the shBCA2-KD cell lines and the consequences of shBCA2-KD of BCA2 protein expression. This was conducted over time and relative to the shNT control (Figure 5.2). Statistical analysis of the difference in concentrations for shNT-controls (MDA-MB-468 and MDA-MB-231) relative to shBCA2-KD 12 and 24 hours after treatment (at zero hours), revealed a decrease in glucose consumption and lactate production.

Rate analysis of glucose consumption and lactate production using a two-tailed student t-test and three observations, or replicates for each sample, revealed that shBCA21-KD of BCA2 in the TNBC cell lines (MDA-MB-468 and MDA-MB-231) resulted in a decrease in key markers of Warburg-like metabolism. Knockdown of BCA2 expression resulted in an approximate 30% ($t(2)=1.63$, $p=0.24$) and 24% ($t(2)=1.29$, $p=0.32$) decrease in glucose consumption in MDA-MB-468 at 12 hours after treatment. Although reductions in glucose production were observed, the data

was not statistically significant, most likely due to the large variance of the control sample. However, in MDA-MB-231 cells, a significant reduction of 25% ($t(4)=4.37$, $p=0.01$) and 23% ($t(4)=2.88$, $p=0.04$) was recorded 24 hours after treatment (Figure 5.2).

The production of lactate is a significant marker used to assess the extent of Warburg-like activity in cancer cell lines. The key aspect of cellular metabolism, which is modulated when normal cells undergo a metastatic transformation, is that there is an increase in glycolysis (Jang, Kim, & Lee, 2013) followed by an increase in lactate production as the pathway shuts pyruvate away from the TCA-Cycle and toward glycolysis.

The production of lactate is significantly increased in tumor cells. This change increases the acidity of the microenvironment, resulting in increased metastasis and a significant change in the behavior of the cells (Burns & Manda, 2017). In addition to increased acidity, increased lactate "anaerobic" metabolism is associated with increased ATP (energy) production within the cancer cells. However, despite a decrease in energy production efficiency per mole of glucose, cancer cells produce ATP at a greater rate than normal cells. ATP and glycolysis are essential for rapid cellular proliferation. ATP is needed for energy, while glycolysis produces excess biological metabolites necessary for rapid proliferation (Burns & Manda, 2017).

In the shBCA2-KD cells, there was a significant decrease in lactate production in both cell lines (Figure 5.2). At 12 hours after treatment, lactate production was decreased by 31% ($t(4)=6.08$, $p=0.003$) and 28% ($t(4)=6.18$, $p=0.003$) relative to the shNT control in MDA-MB-468 cells. In addition, lactate production was decreased by 47% ($t(4)=34.38$, $p<0.001$) and 55% ($t(4)=34.28$, $p<0.001$) in MDA-MB-231 cells at 12 hours after treatment, and 32% ($t(4)=5.77$, $p=0.004$) and 36% ($t(4)=11.73$, $p<0.001$) at 24 hours after treatment. These data suggest that Warburg-like

metabolism is linked to BCA2 protein expression and that this effect may be mediated through NMNAT1 (See Figure 5.2).

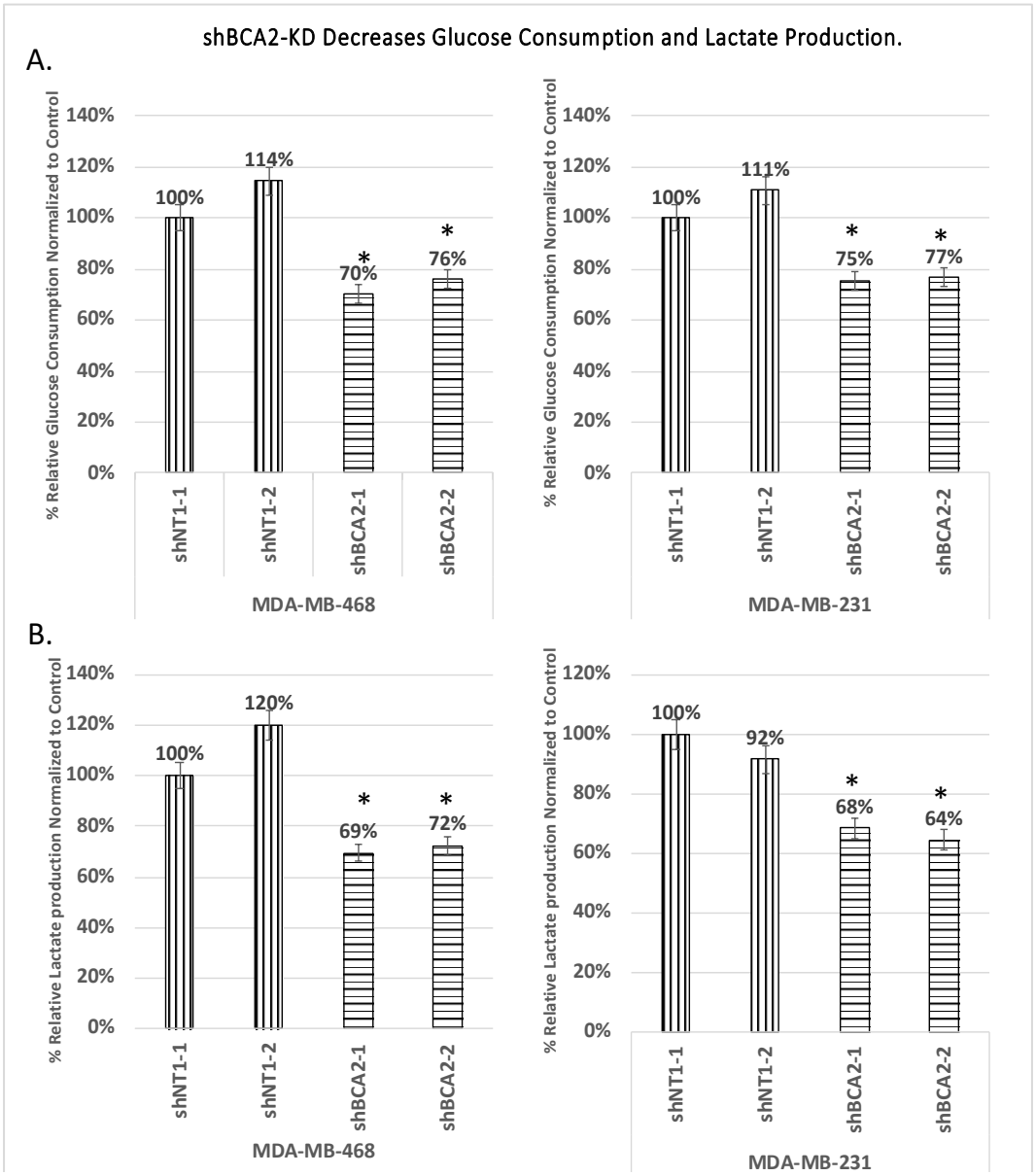

Figure 5.2 shBCA2-KD is Associated with a Decrease in Glucose Consumption and Lactate Production.

The analysis of glucose and lactate concentrations was performed in triplicate on the media of the disparate clonal cell lines. High glucose consumption and lactate production were associated with Warburg-like metabolism. shBCA2-KD significantly (*) decreased lactate production in MDA-MB-468 cells (12 hours) (31% ($t(4)=6.08$, $p=0.003$) and 28% ($t(4)=6.18$, $p=0.003$)) and both glucose consumption (25% ($t(4)=4.37$, $p=0.01$) and 23% ($t(4)=2.88$, $p=0.04$)) and lactate production (32% ($t(4)=5.77$, $p=0.004$) and 36% ($t(4)=11.73$, $p<0.001$)) in MDA-MB-231 cells (24 hours), as indicated by the asterisk in each graph. These data are consistent with a decrease in Warburg-like metabolism, and the change in LDHA/LDHB ratio.

5.3 shBCA2-KD results in significantly decreased rates of cellular proliferation

After evaluation of the effects of shBCA2-KD on protein expression, glucose consumption, and lactate production after 12 and 24 hours, we evaluated the relative proliferation rates of both MDA-MB-468 and MDA-MB-231 TNBC cell lines against the shNT-control group. In previous studies, transient knockdown (siBCA2) resulted in a decrease in relative proliferation rates of MDA-MB-468 and MDA-MB-231 TNBC cell lines (Buac et al., 2013).

In this study, proliferation rates were conducted in triplicate and analyzed using the Beckman Coulter particle counter and corrected for the dilution factor and the total volume of the cell suspension collected. The number of cells per well were calculated by subtracting the total number of cells per well on day zero from the total number on day four. Proliferation rates were then calculated relative to the control group. Three counts were collected for each sample on each day.

shBCA2-KD significantly decreased proliferation in both cell lines. MDA-MB-468 decreased proliferation by 49% ($t(4)=54.07$, $p<0.001$) and 47% ($t(4)=53.61$, $p<0.001$) while in MDA-MB-231 proliferation decreased by 28% ($t(2)=8.29$, $p=0.001$ and 28% $t(2)=26.80$, $p<0.001$) relative to the shNT targeting control. These results are consistent with shBCA2-KD decreasing tumor cell proliferation as previously reported.

5.4 Discussion

The inhibition of BCA2 results in an increase in NMNAT1 protein expression, as well as a decrease in expression of LDHA and an increase in LDHB. The decrease in the ratio of LDHA/LDHB protein expression is indicative of a decrease in Warburg-like metabolism and is characterized by decreased glucose consumption and decreased lactate production. These results indicate that BCA2 plays a significant role in the regulation of Warburg-like metabolism.

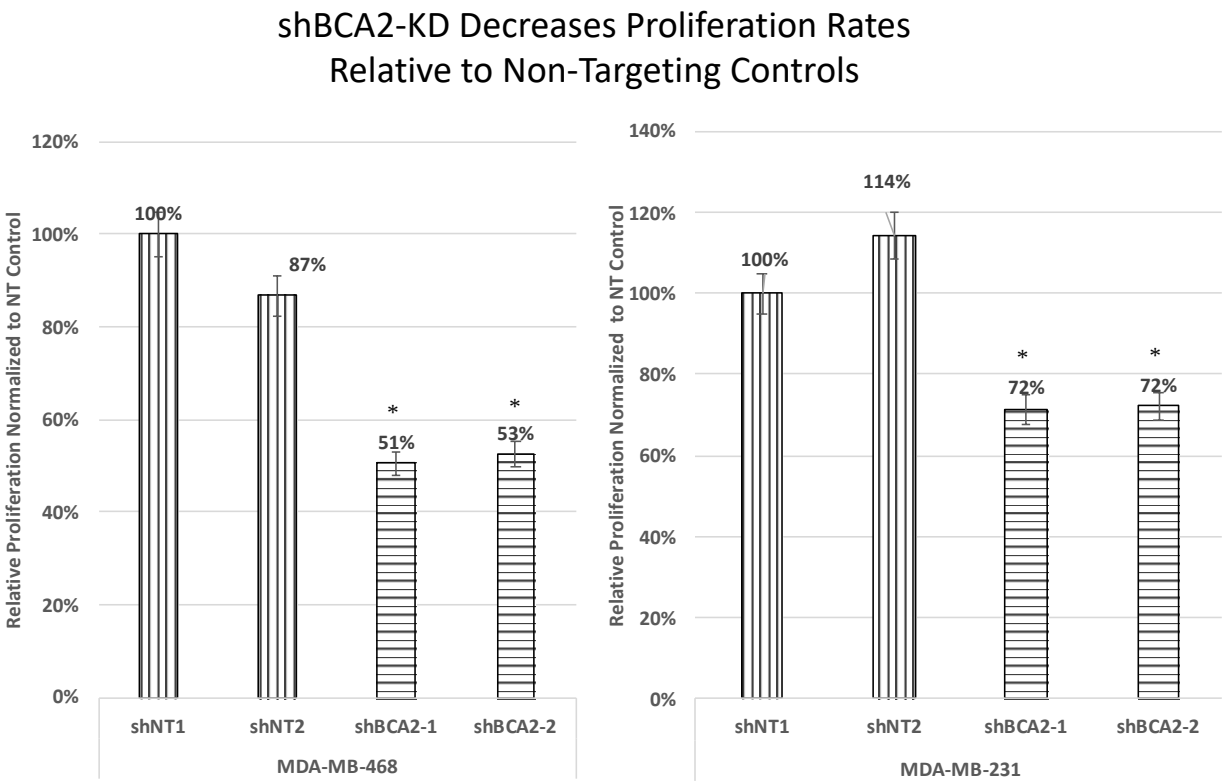

Figure 5.3 shBCA2-KD Decreases Proliferation Rates Relative to Non-Targeting Controls
The relative proliferation rates of both MDA-MB-468 and MDA-MB-231 TNBC cell lines with shBCA2-KD were compared against the shNT-control group and were conducted in triplicate. shBCA2-KD significantly (*) decreased the relative proliferation rates of MDA-MB-468 (49% ($t(4)=54.07$, $p<0.001$) and 47% ($t(4)=53.61$, $p<0.001$)) and MDA-MB-231 (28% ($t(2)=8.29$, $p=0.001$ and $t(2)=26.80$, $p<0.001$) TNBC cell lines relative to the shNT targeting control populations (indicated by the asterisks). The number of cells were directly counted by a Beckman Coulter particle (Cell) counter and proliferation rates were run in triplicate.

The proceeding findings demonstrated a change in Warburg-like metabolism in response to shBCA2-KD. However, they did not offer any insights into the mechanism by which BCA2 is regulating Warburg-like metabolism. Future directions should evaluate protein and transcript data for LDHA and LDHB in response to shBCA2-KD and BCA2-WT rescue to determine if the effects of shBCA2-KD are specific to BCA2, and whether the change in LDHA and LDHB expression is observed at the protein or transcript level.

Furthermore, the exact mechanism by which BCA2 regulates NMNAT1 expression could be evaluated by the introduction of mutant constructs of BCA2 into the shBCA2-KD background to

explore which, if any, mutant constructs are able to rescue the knockdown effects. If any specific mutant variant failed to rescue or exclusively rescues expression of NMNAT1 in the shBCA2-KD cells, this would be a strong indicator of the functional group on BCA2 that contributes to the regulation of NMNAT1 expression.

CHAPTER 6: shNMNAT1-KD INDUCED KEY MARKERS OF WARBURG-LIKE METABOLISM (LDHA/LDHB), INCREASED WARBURG-LIKE METABOLIC ACTIVITY AND PROLIFERATION

6.1 shNMNAT1-KD increases expression of BCA2, LDHA/LDHB, Warburg-like metabolic activity and tumor cell proliferation

Knockdown of NMNAT1 by shNMNAT1 significantly decreased the expression of NMNAT1 protein. As predicted in Figure 1.9, knockdown of NMNAT1 was associated with an increase in BCA2 protein expression, suggesting an inverse relationship between BCA2 and NMNAT1 protein expression. However, the relationship between BCA2 and NMNAT1 and their potential roles in the regulation of Warburg-like metabolism may be either dependent or independent of each other's expression.

shNMNAT1-KD resulted in an increase in relative BCA2 protein expression (MDA-MB-468: 7070%, 6286%, and 8427%; MDA-MB-231: 425%, 583%, and 418%) relative to the control. To examine the effects of NMNAT1 on LDHA and LDHB, their relative levels were identified on western blot and quantified by densitometry. shNMNAT1-KD also increased LDHA expression (MDA-MB-468: 256%, 289%, and 346%; MDA-MB-231: 425%, 583%, and 418%) and was associated with a decrease in LDHB (MDA-MB-468: 18%, 21%, and 9%; MDA-MB-231: 11%, 17%, and 35%). Altogether, shNMNAT1-KD was associated with upregulation of BCA2 protein expression and an increase in the observed ratio of LDHA/LDHB, suggesting that Warburg-like activity may also be enhanced (Figure 6.1).

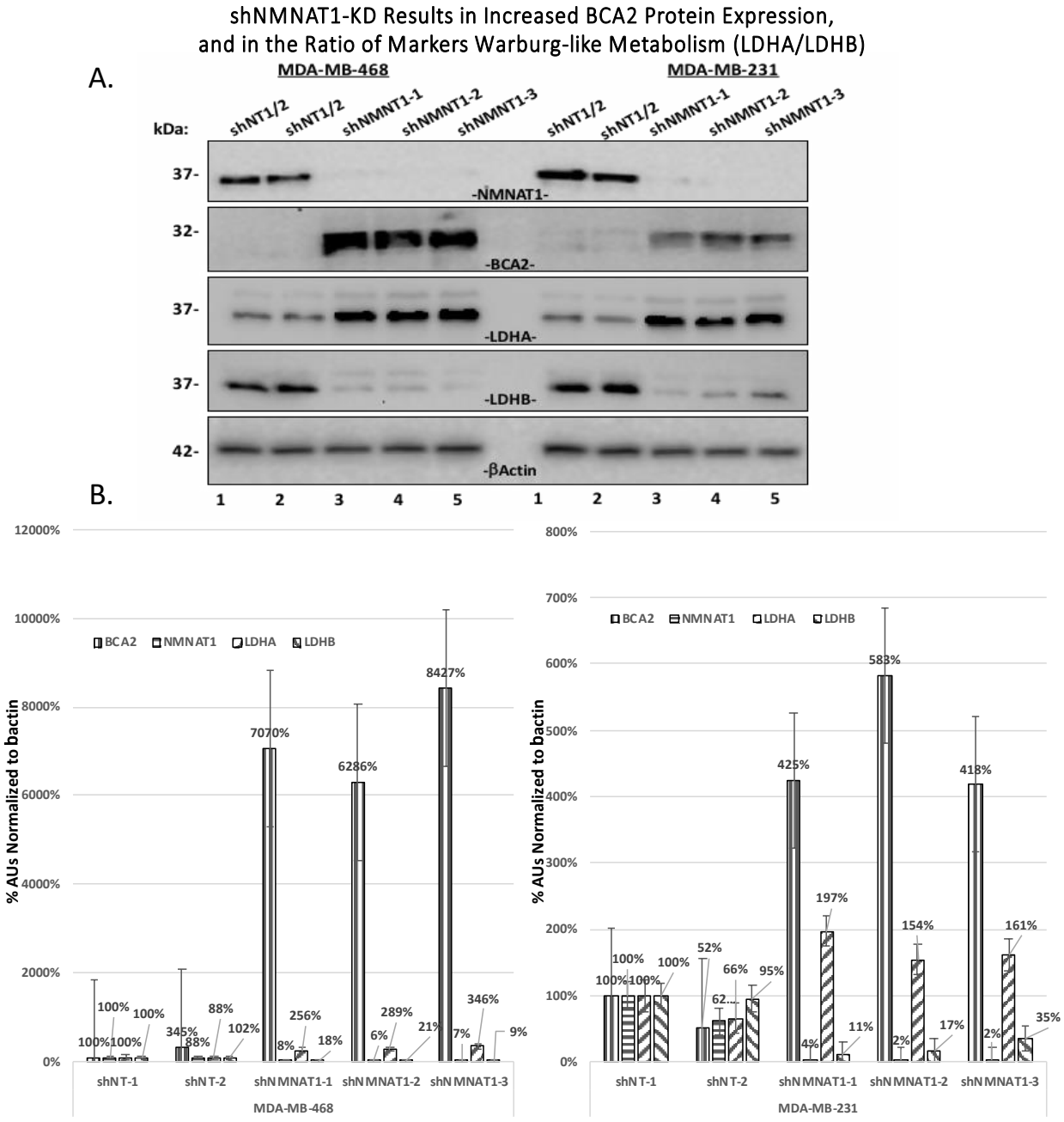

Figure 6.1 shNMNAT1 KD results in an increase of BCA2 expression, and an enhancement of Warburg-like metabolic markers (LDHA/LDHB).

Stable knockdown of NMNAT1 by shNMNAT1 resulted in a significant increase in expression of BCA2 protein, as determined by western blotting. In addition, there was a significant increase in LDHA expression and a concurrent decrease in LDHB protein expression. This increase in the ratio of LDHA/LDHB is indicative of Warburg-like metabolism. LDHA is the more active homo-isoform of LDH, which is a key enzyme in lactate metabolism and, therefore, likely drives cells towards increased lactate production.

6.2 shNMNAT1-KD of NMNAT1 increased glucose consumption and lactate production

An evaluation of the glucose and lactate concentrations in the media was performed in triplicate of the multiple clonal cell lines in order to assess relative Warburg-like activity of the shNMNAT1-KD cell lines and the consequences of shNMNAT1-KD on glucose consumption and lactate production. These experiments were conducted at 12 hours and were normalized relative to the shNT control and the number of cells per plate. Cells were seeded the night before. The media was changed with high glucose media at time zero when the first sample was collected. Subsequent samples were collected for high glucose media at 12 hours. The glucose and lactate levels in the media were analyzed by Dr. Wang's lab using their protocol described in the methods sections. Statistical analysis of the differences in concentrations for the shNT-controls (MDA-MB-468 and MDA-MB-231) relative to shBCA2-KD, revealed an increase in glucose consumption and lactate production (for a detailed explanation of the experimental procedure associated with glucose consumption and lactate, as well as the scientific rigor and statistical analysis used to evaluate the data please see the following sections: 2.1, 2.2, 2.3.6, and 2.3.10-13).

Glucose consumption and lactate production (using a two-tailed student t-test and three replicates for each sample) revealed that shNMNAT1-KD in TNBC cell lines (MDA-MB-468 and MDA-MB-231) resulted in an increase in key markers of Warburg-like metabolism. Evaluation of the effects of NMNAT1-KD after 12 hours on Warburg-like metabolism revealed that NMNAT1-KD was associated with a significant increase in glucose consumption (Figure 6.2) in MDA-MB-468 cells, with samples yielding 349% ($t(4)=-13.87$, $p<0.001$) and 400% ($t(4)=-9.00$, $p<0.001$)) of the glucose consumption compared to the non-targeting control at time zero. NMNAT1-KD in MDA-MB-231 cells also resulted in an increase in glucose consumption, 139% ($t(4)=3.74$, $p=0.02$) and 154% increase ($t(4)=-1.13$, $p=0.32$) (Figure 6.2).

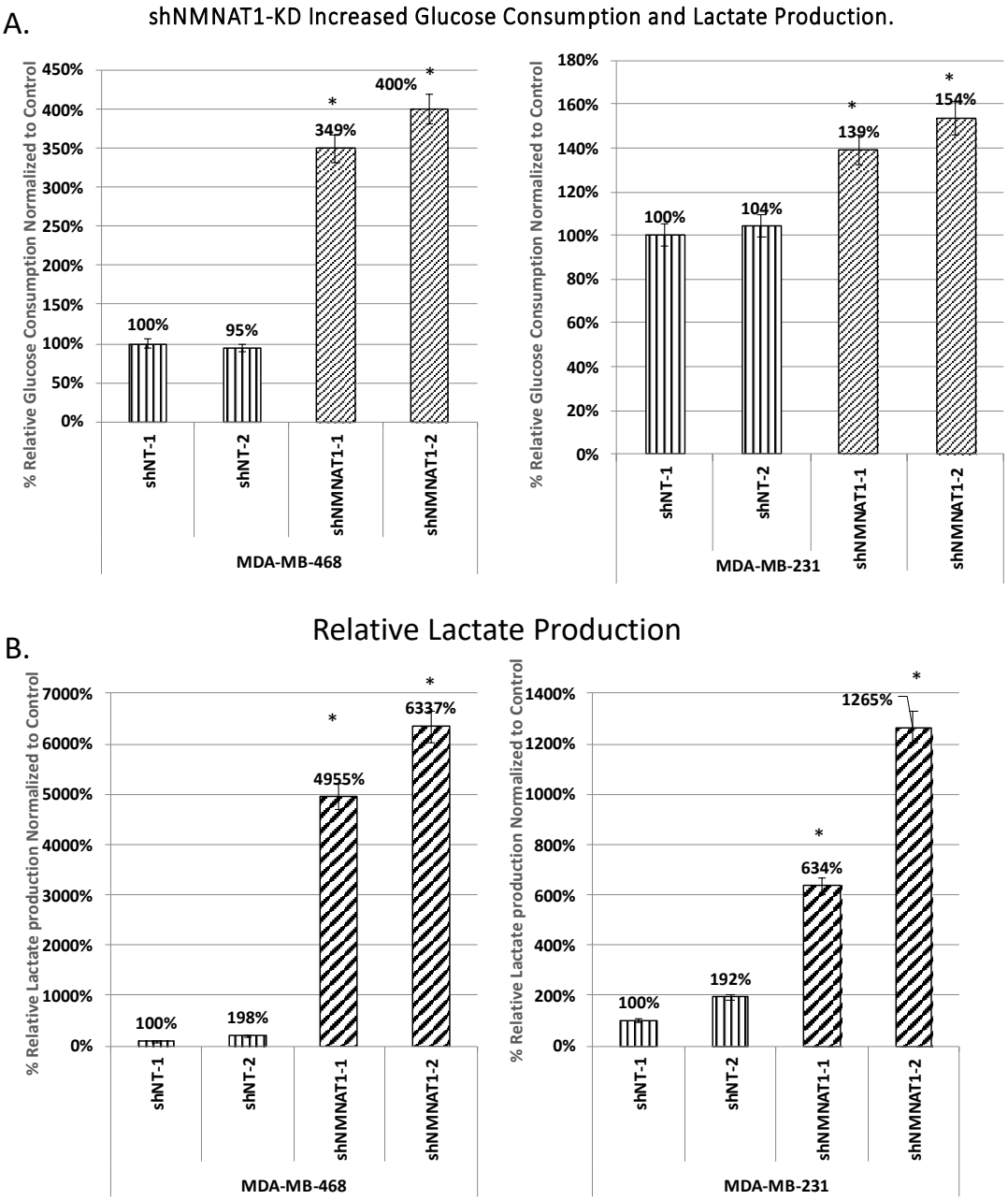

Figure 6.2 shNMNAT1 KD Increased Glucose Consumption and Lactate Production

At 12 hours after treatment, knockdown of NMNAT1 by shNMNAT1 results in a change in glucose consumption with a significant **(*)** increase in glucose consumption in MDA-MB-468 (349% (t(4)=-13.87, p<0.001) and 400% (t(4)=-9.00, p<0.001)), and in MDA-MB-231 (39% Increase (t(4)=3.74, p=0.02) and a 54% increase (t(4)=-1.13, p=0.32). In addition, shNMNAT1 revealed a significant increase in lactate production in both cell lines: MDA-MB-468 (4,955% [t(2)=-4.01, p=0.05] and 6,337% [t(4)=-21.13, p<0.001]) and MDA-MB-231 (634% [t(2)=-23.44, p=0.001] and 1,265% [t(2)=-32.88, p<0.001]). These experiments were performed in triplicate and are suggestive that decreased NMNAT1 plays a significant role in conversion to aerobic metabolism through changes in glucose consumption and a shift towards increased lactate production. These results are consistent with increased Warburg-like effect.

Increased lactate production is consistent with Warburg-like metabolism. Increased lactate production is generally associated with a concurrent increase in glucose consumption as a result of the decreased efficiency of Warburg-like metabolism in ATP production (Burns & Manda, 2017). This factor is a key component to functional MRI studies (Wang et al., 2016). These machines utilize radioactive isotypes of glucose to determine glucose uptake in tissues, thus indicating the potential for tumor formation (Burns & Manda, 2017; Wang et al., 2016). As opposed to a normal cell's aerobic metabolism, cancer cells exhibit anaerobic metabolism, which requires an increase in glucose consumption (Burns & Manda, 2017; Krisher & Prather, 2012; San-Millan & Brooks, 2017; Vander Heiden et al., 2009; Zdralevic et al., 2018).

The results revealed that shNMNAT1-KD resulted in a dramatic and statistically significant increase in lactate production in both MDA-MB-468 (4,955% [$t(2)=-4.01$, $p=0.05$] and 6,337% [$t(4)=-21.13$, $p<0.001$]) and MDA-MB-231 (634% [$t(2)=-23.44$, $p=0.001$] and 1,265% [$t(2)=-32.88$, $p<0.001$]).

These results indicate shNMNAT1-KD increases glucose consumption and lactate production. The results also suggest that it is possible that decreased NMNAT1 expression alters both the mechanism and flux of glucose utilization in both cell lines. shNMNAT1 enhances glucose metabolism and shunts the glucose metabolic pathway towards the anaerobic lactic acid cycle (TCA-Cycle). However, the distinct increase of lactate production is a more prevalent and relevant indicator for anaerobic glycolysis. Therefore, the minimal effects of shNMNAT1 on increased glucose consumption is not as significant as the robust increase in lactate production in both cell lines. These findings are consistent with an enhancement of Warburg-like metabolism.

6.3 shNMNAT1-KD results in a significant increase in cellular proliferation

The relative proliferation rates of MDA-MB-468 and MDA-MB-231 increased in response to shNMNAT1-KD. In this study, proliferation assays (in triplicate) were measured using the Beckman Coulter particle counter according to the manufacturer's instructions and normalized to the nontargeting control (section 2.3.6). The increase in the number of cells per well was calculated by subtracting the total number of cells per well on day zero from the total number on day four. Proliferation rates were then calculated relative to the control group. Three counts were collected for each sample on each day. The proliferation of cells increased significantly in both cell lines. shNMNAT1-KD significantly (*) increased the proliferation rates of MDA-MB-468 (228.4% $p<0.001$ and 278.0% $p<0.001$) and MDA-MB-231 (283.6% $p=0.001$ and 285.5% $p<0.001$) TNBC cell lines relative to the shNT targeting control populations (as indicated by the asterisk in Figure 6.3).

The combined results of the shNMNAT1 data showed that the effects of shBCA2-KD are reversed when NMNAT1 is knocked down. shNMNAT1-KD increased: (a) the expression of BCA2, which is a known oncogene, (b) the ratio of LDHA/LDHB (markers of Warburg-like metabolism), (c) glucose consumption, and (d) lactate production. All these findings, together with the data for shBCA2 suggest that BCA2 may have a role in driving Warburg-like metabolism through the activity of NMNAT1. Conversely, increased NMNAT1 expression is associated with decreases in BCA2 expression as well as a concurrent decrease in Warburg-like metabolism and cellular proliferation rates. Induction of NMNAT1 by shBCA2-KD may occur by removing suppression of the NMNAT1 promoter by BCA2. Promoter suppression of NMNAT1 could be occurring either directly, or indirectly through BCA2's activity.

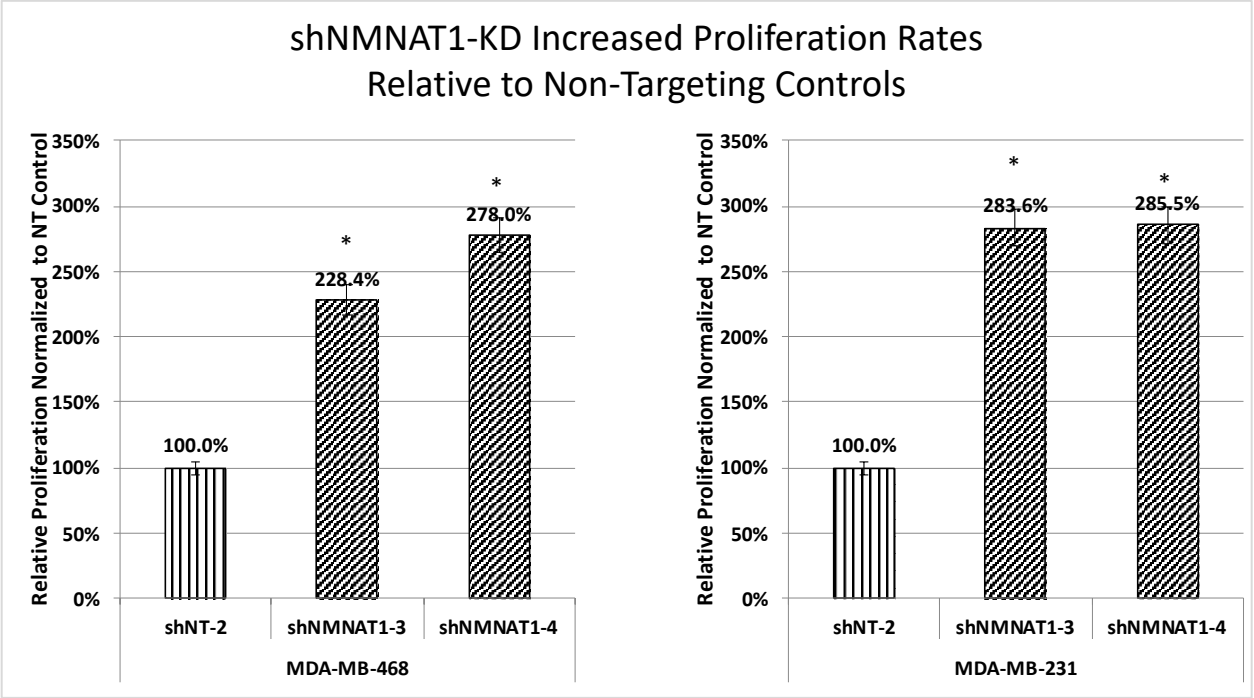

Figure 6.3 shNMNAT1-KD Increased Proliferation Rates Relative to Non-Targeting Controls.

The relative proliferation rates of both MDA-MB-468 and MDA-MB-231 TNBC cell lines with shNMNAT1-KD were compared against the shNT-control group and were conducted in triplicate. shNMNAT1-KD significantly (*) increased the relative proliferation rates of MDA-MB-468 (228.4% $p<0.001$) and (278.0% $p<0.001$) and MDA-MB-231 (283.6% $p=0.001$ and 285.5% $p<0.001$) TNBC cell lines relative to the shNT targeting control populations (as indicated by the asterisk). The number of cells were directly counted by a Beckman Coulter particle (Cell) counter.

These findings suggest that inhibition of NMNAT1 plays a role in the activation of Warburg-like metabolism and is associated with increased BCA2 expression. Therefore, NMNAT1 protein expression inhibits Warburg-like metabolism. However, the precise mechanism by which NMNAT1 regulates Warburg-like metabolism requires further exploration.

6.4 Discussion

In order to further investigate the potential roles of BCA2 and NMNAT1 in the regulation of cellular energy homeostasis, RNAi technology was utilized to inhibit BCA2, NMNAT1, and BCA2/NMNAT1 (Chapter 7) protein expression in the TNBC cell lines MDA-MB-231 and MDA-MB-468. The initial studies with shBCA2-KD demonstrated that loss of BCA2 resulted in: (a)

increased expression of the tumor suppressor NMNAT1, (b) decreased expression of LDHA, (c) increased LDHB, and (d) decreased functional markers of Warburg-like metabolism including decreased glucose consumption, lactate production, and cellular proliferation. These results suggest that BCA2 plays a critical role in the activation of Warburg-like metabolism and that loss of BCA2 (associated with increased NMNAT1 expression) is sufficient to decrease the Warburg-like metabolism in TNBC cells. In addition, measurements of key Warburg-like metabolism markers (LDHA/LDHB) revealed that shBCA2-KD not only resulted in an increase of NMANT1 protein expression, but an increase in the ratio of LDHA/LDHB, an established marker of Warburg-like metabolism (Lu et al., 2015; Rani & Kumar, 2019).

Warburg-like metabolism is characterized by an increase in glucose consumption, lactate production, and relative proliferation rates (Brand, 2010; Burns & Manda, 2017; Zdralevic et al., 2018). In order to determine the role of NMNAT1 in BCA2 dependent modulation of Warburg-like metabolism stable shNMNAT1-KD clonal populations were generated as described previously (Molina et al., 2014), and key markers of Warburg-like metabolism (LDHA and LDHB) were assessed by western blot. In addition, functional assays for glucose consumption, lactate production and cellular proliferation rates were performed to assess the consequences of shNMNAT1-KD on the relative Warburg-like activity of the resulting shNMNMAT1-KD in TNBC cells.

shNMNAT1-KD resulted in increased expression of BCA2 protein as determined by western blot analysis. shNMNAT1-KD increased expression of LDHA a key marker of enhanced Warburg-like metabolism, and decreased expression of LDHB, a marker known to be associated with diminished Warburg-like metabolism. In addition, shNMNAT1-KD modulated functional markers of Warburg-like metabolism resulting in increased glucose consumption, increased lactate

production, and increased cellular proliferation. These results suggest that NMNAT1 suppresses Warburg-like metabolism through some unknown mechanism and that inhibition of NMNAT1 is sufficient to increase Warburg-like metabolism in the presence of BCA2 in TNBC cells MDA-MB-468 and MDA-MB-231. The combined data from the shBCA2-KD and the shNMNAT1-KD experiments suggests that BCA2 and NMNAT1 play dynamic and pivotal roles in the regulation of Warburg-like metabolism. Hence, an exploration of the effects of a double knockdown was warranted.

CHAPTER 7: shBCA2/NMNAT1-KD RESCUED THE EFFECTS OF SHBCA2-KD ON KEY MARKERS FOR WARBURG-LIKE METABOLISM (LDHA/LDHB) AND PROLIFERATION

In order to further assess the association between BCA2 and NMNAT1, pGIPZ shRNA plasmids specific to NMNAT1 (shNMNAT1) were serially transfected into the existing model systems in both cell lines as shown here: (shNT2 = $shNT1_{plko}$ + $shNT_{pGIPZ}$), (shNMNAT1-1-3 =shNT1 + shNMNAT1-(1-3) and shBCA2/NMNAT1 =shBCA2+shNMNAT1-(1-3)). Transfection was performed according to Mirus T1 transfection protocol every 48 hours for three successive transfections with antibiotic selection media applied between transfections. After the final transfection, the cells were selected in media containing high dose antibiotics for two weeks, which was determined empirically by a kill curve. Cells were then allowed to recover in an antibiotic-free media before being passaged into 96 well plates to perform a serial dilution of the stable populations of cells to provide clonal populations for each plasmid. Clonal populations were expanded, preserved, and then characterized by western blot, media analysis (glucose and lactate), and proliferation rates.

Once the stable shBCA2/NMNAT1-dKD cell lines (shBCA2/NMNAT1-dKD) were generated and stabilized, they were characterized by western blot to assess BCA2, NMNAT1, and LDHA/LDHB, the key enzymes involved in the transition to Warburg-like metabolism. Experiments were performed in triplicate on three different occasions, and parallel experiments were carried out to evaluate protein expression levels through western blot and metabolic function (glucose consumption and lactate production) at the same time. These experiments were performed in parallel in order to ensure that the western blot and transcript data coincided with the media analysis data.

Densitometry was performed on all images, and error bars are shown. Representative western blots are shown that were representative of the densitometry data. These included analysis of LDHA, LDHB, BCA2, and NMNAT1 in the model system: shNT1, shBCA2, shNMNAT1, shNT2, and shBCA2/NMNAT1-dKD cells (Figure 7.1).

7.1 shBCA2/NMNAT1-dKD resulted in a reversal or rescue of the effects of shBCA2-KD on markers of Warburg-like metabolism by western blot

These results confirmed that BCA2 was still significantly reduced in the shBCA2-KD cells and confirmed the decreased protein expression of BCA2 (MDA-MB-468: 33% and 32%, MDA-MB-231: 7% and 5%), increased NMNAT1 (MDA-MB-468: 187% and 173%, MDA-MB-231: 212% and 202%), decreased LDHA (MDA-MB-468: 187% and 173%, MDA-MB-231: 212% and 202%), increased LDHB (MDA-MB-468: 573% and 480%, MDA-MB-231: 703% and 583%), and recapitulated the role of BCA2 in inhibition of NMNAT1, and enhancing Warburg-Like metabolism. This was consistent with previous studies in the literature that have demonstrated the correlation between the ratio of LDHA/LDHB and Warburg-like metabolism (Molina, et al., 2014).

Double knockdown of BCA2 and NMNAT1 (shBCA2/NMNAT1-dKD), relative to the shNT2 control background, resulted in an increase in expression of LDHA, and decreased the expression of LDHB. Relative to the shNT control, shBCA2/NMNAT1-KD decreased protein expression of BCA2 (MDA-MB-468: 20% and 20%, MDA-MB-231: 5% and 1%), decreased NMNAT1 (MDA-MB-468: 36% and 41%, MDA-MB-231: 14% and 23%), increased LDHA (MDA-MB-468: 221% and 246%, MDA-MB-231: 83% and 196%), increased LDHB (MDA-MB-468: 573% and 480%, MDA-MB-231: 703% and 583%), and recapitulated the role of BCA2 in

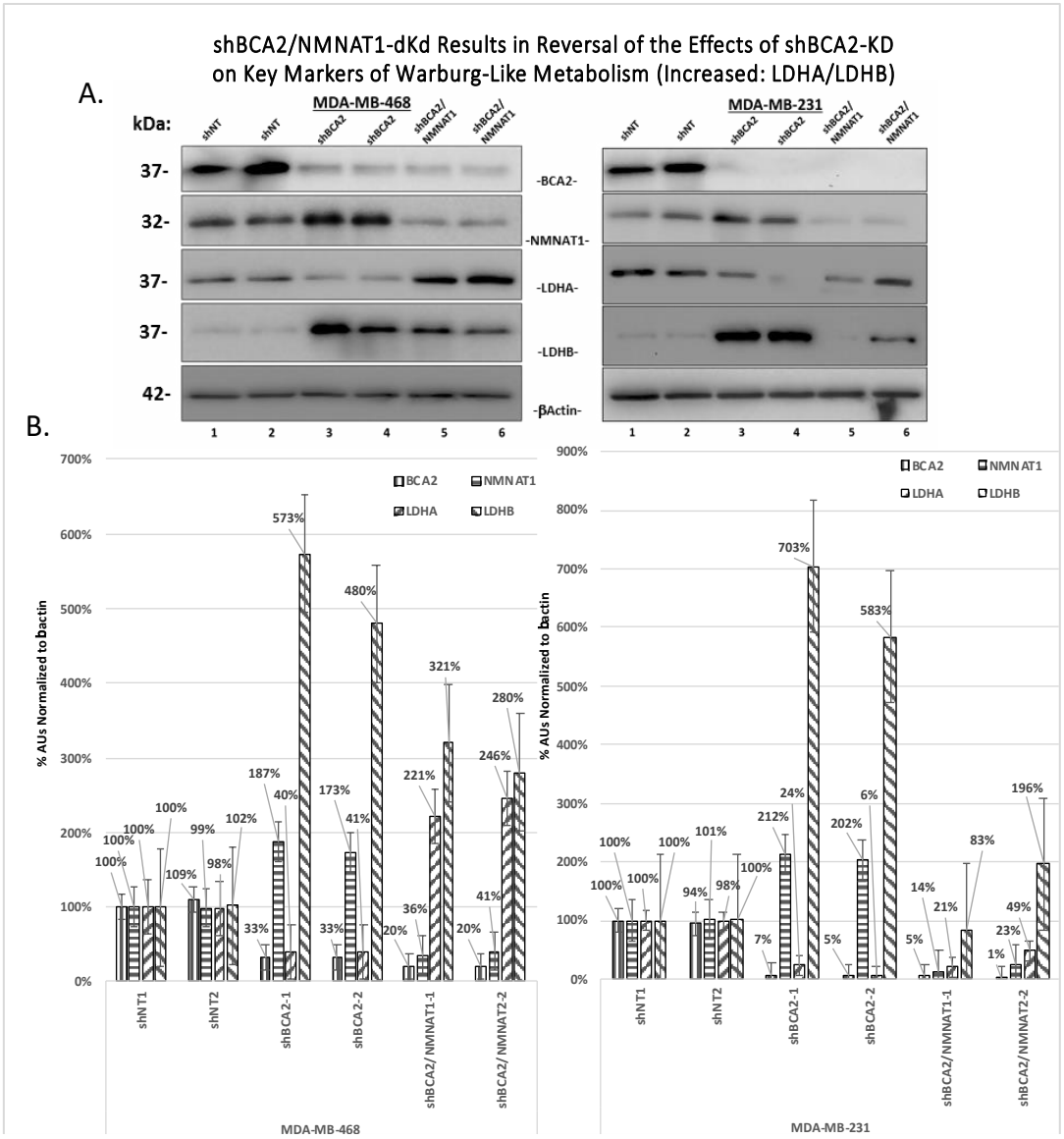

Figure 7.1 shBCA2/NMNAT1-dKD Resulted in Reversal of the Effects of shBCA2-KD on Key Markers of Warburg-Like Metabolism (Increased: LDHA/LDHB).

Western blot analysis, with densitometry, revealed significant changes in the ratio of LDHA/LDHB in response to both shBCA2-KD and shBCA2/NMNAT1-dKD. Both control vectors showed no significant changes. shBCA2-KD resulted in decreased BCA2 (MDA-MB-468: 33% and 33%, and MDA-MB-231: 7% and 5%), increased NMNAT1 (MDA-MB-468: 187% and 173%, and MDA-MB-231: 212% and 202%), decreased LDHA (MDA-MB-468: 40% and 41%, and MDA-MB-231: 24% and 6%) and increased LDHB (MDA-MB-468: 573% and 480%, and MDA-MB-231: 703% and 583%)}. Double knockdown rescued the shNT control's expression of LDHA and LDHB. shBCA2/NMNAT1-dKD resulted in a decrease in BCA2 protein expression (MDA-MB-468: 20% and 20%, and MDA-MB-231: 5% and 1%), Decreased NMNAT1 protein expression (MDA-MB-468: 36% and 41%, and MDA-MB-231: 14% and 23%), Increased LDHA protein expression (MDA-MB-468: 221% and 246%, and MDA-MB-231: 21% and 49%) and increased LDHB protein expression (MDA-MB-468: 321% and 280%, and MDA-MB-231: 83% and 196%) relative to the shNT control vectors. Densitometry data is representative of three separate experiments (standard errors are shown).

inhibition of NMNAT1 and enhancing Warburg-Like metabolism. This constitutes a reversal or rescue of the effects of shBCA2-KD on the TNBC cells.

7.2 shBCA2/NMNAT1-dKD resulted in a reversal or rescue of the decreased glucose consumption and the production of lactate relative to shNT.

After characterizing the shBCA2/NMNAT1-dKD cells by western blot, an analysis of the consumption of glucose and the production of lactate was conducted in these cells in triplicate (Figure 7.2). These results suggest that BCA2 may play a significant role in glucose consumption. At 24 hours after treatment, shBCA2 significantly decreased glucose consumption by 64% ($t(4)=7.98$, $p=0.001$) and 72% ($t(4)=12.15$, $p<0.001$) in MDA-MB-468 cells. However, in MDA-MB-231 cells, mixed results were observed. Namely, one sample generated a significant decrease of 41% ($t(4)=4.87$, $p=0.01$) while the other showed no significant change in glucose consumption (84%, $t(2)=0.005$, $p=0.99$). shBCA2/NMNAT1-dKD did not significantly alter glucose consumption, as compared to the control in the MDA-MB-468 cell line, with relative rates of 100% ($t(4)=-0.05$, $p=0.96$) and 177% ($t(2)=-2.25$, $p=0.15$), but did demonstrate a significant reduction of 62% ($t(4)=9.22$, $p<0.001$) and 67% ($t(2)=13.43$, $p=0.005$) in the MDA-MB-231 cell line. The negative control demonstrated a significant increase in glucose consumption, as compared to the control (196%, $t(4)=-6.87$, $p=0.002$) in MDA-MB-231 cells. However, no significant difference was observed between controls in MDA-MB-468 cells ($t(2)=1.51$, $p=0.27$).

These results demonstrated that shBCA2/NMNAT1-dKD rescued the glucose consumption in the MDA-MB-468 cell line, suggestive of a renewal of Warburg metabolism. This reversal was not observed in the MDA-MB-231 cell line. However, it is unclear whether these results are replicable since the negative control also produced a significantly different rate of

glucose consumption as compared to the control. A possible explanation for this could be attributed to issues during the transduction process resulting in the selection of a subsequent cellular population not originally targeted. The random insertion of genetic material during transduction can disrupt other off-target genes, which could result in this phenomenon. Furthermore, shBCA2/NMNAT1-dKD played a significant role in lactate metabolism in the absence of BCA2 expression. shBCA2 decreased the production of lactate by 35% ($t(4)=2.71$, $p=0.05$) and 19% ($t(4)=1.29$, $p=0.27$) in MDA-MB-468 at 24 hours after treatment, although these reductions were not statistically significant. Larger and statistically significant reductions were observed in MDA-MB-231, where shBCA2 resulted in a 56% ($t(4)=7.04$, $p=0.002$) and 64% ($t(4)=13.31$, $p<0.001$) decrease in lactate production respectfully.

shBCA2/NMNAT1-KD resulted in a significant increase in lactate production, rescuing the effects of shBCA2-KD on decreased lactate production, and elevating the production of lactate above the shNT control levels. Lactate production increased 499% ($t(4)=-26.71$, $p<0.001$) and 496% ($t(4)=-12.53$, $p<0.001$) in MDA-MB-468, and 83% ($t(4)=-12.25$, $p<0.001$) and 81% ($t(2)=-4.40$, $p=0.04$) in MDA-MB-231. The negative control also demonstrated a significant increase in lactate production over the control in the MDA-MB-468 cell line (163%, $t(4)=-5.56$, $p=0.03$). However, no significant difference was observed in the MDA-MB-231 cell line ($t(4)=-2.54$, $p=0.06$). These findings again reiterate the importance of NMNAT1 expression in the modulation of lactate metabolism as the production of lactate is the best indicator of anaerobic metabolism and the dramatic effects that the modulation of NMNAT1 protein expression has on Warburg-like metabolism. However, because of the increase seen in the negative control of the MDA-MB-468 cell line, it cannot be stated with certainty how much of the recovery in lactate production can be

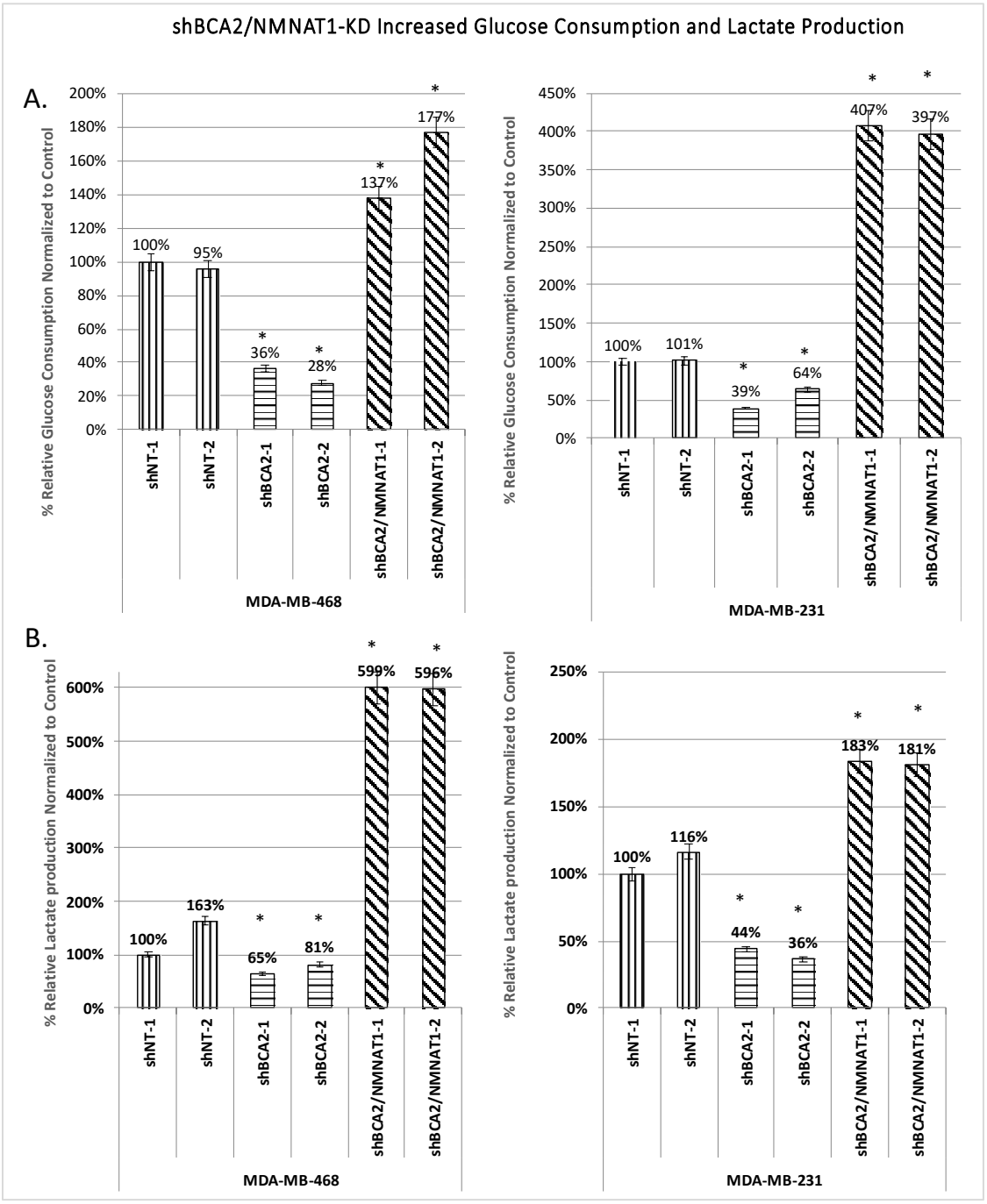

Figure 7.2 shBCA2/NMNAT1-dKD rescued glucose consumption and Lactate production relative to shBCA2-KD and shNT controls

NMNAT1 plays a significant role in both glucose consumption and metabolism, and a significant **(*)** role in lactate metabolism. shBCA2/NMNAT1-dKD rescued glucose consumption relative to shBCA2-KD conditions in the MDA-MB-468 cell line (100% (t(4)=-0.05, p=0.96) and 177% (t(2)=-2.25, p=0.15)) but had a mixed effect in the MDA-MB-231 cell line **(**41% (t(4)=4.87, p=0.01) and (84%, t(2)=0.005, p=0.99)). shBCA2/NMNAT1-dKD resulted in a significant recovery of lactate production relative to both shBCA2-KD populations in the MDA-MB-231 cell line (83% (t(4)=-12.25, p<0.001) and 81% (t(2)=-4.40, p=0.04)). The analysis was done in triplicate.

attributed to shBCA2/NMNAT1-KD, particularly when considering the initial decrease after introducing shBCA2-KD was not significant.

7.3 shBCA2/NMNAT1-KD increased proliferation rates relative to non-targeting controls, and rescued the decrease in proliferation associated with shBCA2

The effects of shBCA2/NMNAT1-KD on LDHA/LDHB protein expression, rescuing both glucose consumption and lactate production, are all consistent with increased Warburg-like metabolism both in MDA-MB-468 and MDA-MB-231 TNBC cell lines. To evaluate the functional consequences of the dKD, relative proliferation rates were examined in triplicate and analyzed using the Beckman Coulter particle counter according to the manufacturer's instructions and normalized to the non-targeting control. The increased number of cells per well were calculated by subtracting the total number of cells per well on day zero from the total number on day four. Proliferation rates were then calculated relative to the control group. Three counts were collected for each sample on each day.

The proliferation of cells decreased significantly (*) in both cell lines in response to shBCA2-KD MDA-MB-468 (33% $p<0.001$ and 19% $p<0.001$) and MDA-MB-231 (52% $p=0.001$ and 22% $p<0.001$) cells. When NMNAT1 was knocked down in the shBA2 cells, generating the dKD clones (shBCA2/NMNAT1-KD), this significantly (*) increased the relative proliferation rates of MDA-MB-468 (190% $p<0.001$ and 206% $p<0.001$) and MDA-MB-231 (228% $p=0.001$ and 278% $p<0.001$) relative to the shNT targeting control populations (as indicated by the asterisk in Figure 7.3) .

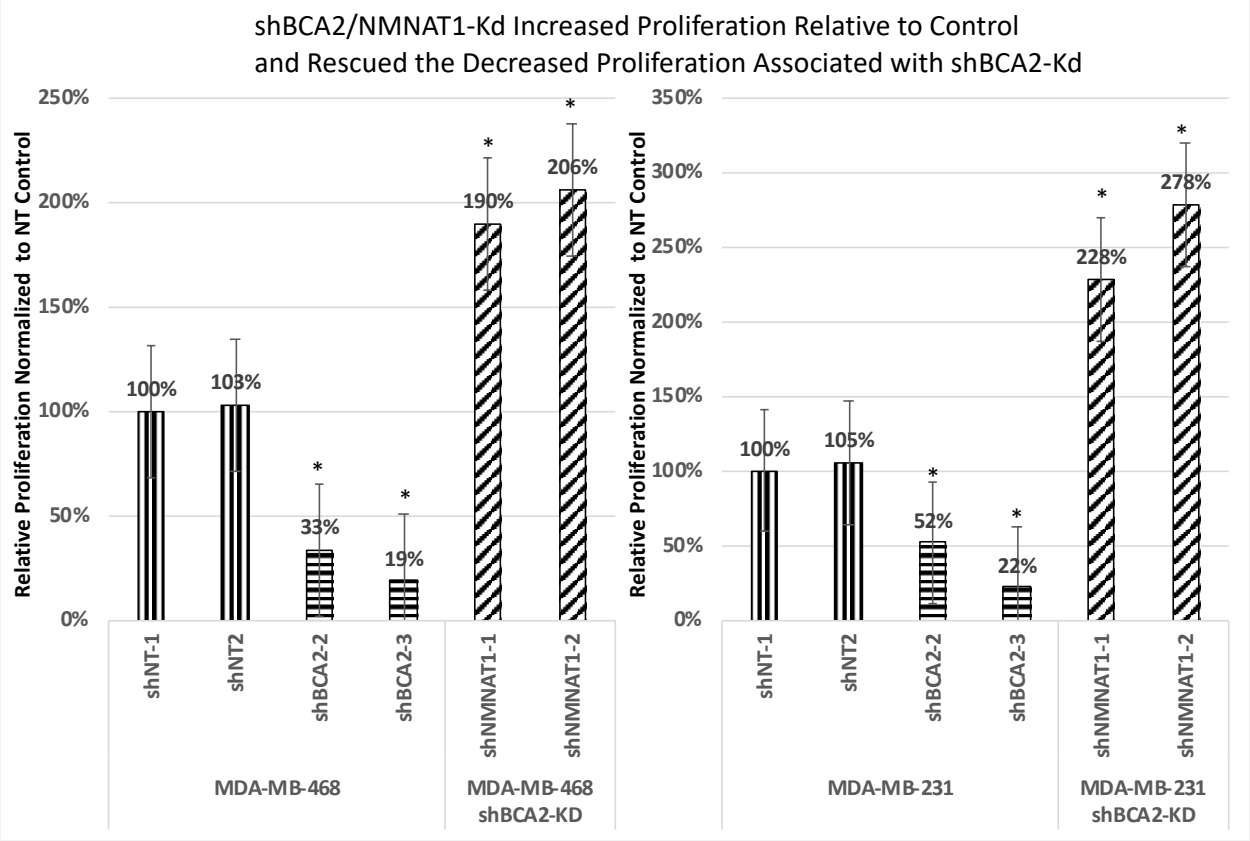

Figure 7.3 shBCA2/NMNAT1-KD Increased Proliferation Rates Relative to Non-Targeting Controls

The relative proliferation rates of both MDA-MB-468 and MDA-MB-231 TNBC cell lines increased in response to dKD relative to the non-targeting controls and rescued the decrease in proliferation associated with shBCA2-KD. Results for KD cells were compared against the shNT-control group and were conducted in triplicate. shBCA2/NMNAT1-KD significantly (*) increased the relative proliferation rates of MDA-MB-468 (190% $p=0.001$ and 206% $p<0.001$) MDA-MB-231 (228.4% $p<0.001$ and 278.0% $p<0.001$) TNBC cell lines relative to the shNT targeted control populations as indicated by the asterisks. shBCA2 decreased proliferation of MDA-MB-468 (33% $p=0.001$ and 19% $p<0.001$), MDA-MB-231 (52% $p<0.001$ and 22.0% $p<0.001$). The increase in proliferation in response to the dKD resulted in a rescue and even enhancement of proliferation greater than the control alone. The number of cells were directly counted by a Beckman Coulter particle (Cell) counter.

7.4 Discussion

These data suggest that both BCA2 and NMANT1 have reciprocal roles in the regulation of Warburg-like metabolism. However, the data is not clear as to whether this change in energy metabolism is dependent on NMNAT1 or independent. To determine if the change in Warburg-

like metabolism was associated with shBCA2-KD, a dKD was used to determine if the BCA2-dependent changes were dependent on NMNAT1.

shBCA2/NMNAT1-dKD rescued the effects associated with shBCA2-KD on markers of Warburg-like metabolism, including increased LDHA expression, decreased expression of LDHB, and increased functional markers of Warburg-like metabolism (increased glucose consumption and lactate production), as well as increased cellular proliferation. These results suggest that inhibition of NMNAT1 plays a necessary role in the changes in Warburg-like metabolism associated with shBCA2-KD of BCA2 protein expression. Hence, these data suggest that BCA2 and NMANT1 are playing reciprocal roles in regulation of Warburg-like metabolism in TNBC cell lines. However, the data does not provide a specific mechanism by which NMNAT1 is regulating the extent of Warburg-Like metabolism in response to modulation of BCA2 in these cells.

The significant implications of these results are the importance of glucose concentration in regulating multiple markers of cancer cell tumorigenicity (oncogenes and tumor suppressors). These investigations dealt specifically with the role of BCA2 in the regulation of cellular glucose metabolism. However, it was interesting to see that glucose concentrations had such significant and rapid effects on the expression of both BCA2 and NMANT1 expression. It would be difficult to determine the exact mechanism by which the BCA2: NMNAT1 axis is regulating glucose metabolism in cancer cells and in response to glucose stimulation because of the diverse effects of glucose on the metabolic state of the cells.

In order to identify the potential mechanisms by which BCA2 and NMNAT1 are regulating Warburg-like metabolism, a few exploratory pilot experiments could be performed including RNA-Seq, ubiquitin enrichment proteomics, or immunoprecipitation, and metabolomics analysis

could be used to identify candidate intermediate proteins or metabolites. These “Omic” studies can provide valuable lists of candidate proteins or metabolites that are modulated in response to genetic manipulation of BCA2 and NMANT1 (shBCA2, shNMNAT1, shBCA2/NMNAT1). Once candidate molecules are identified, traditional molecular chemistry techniques could be used to validate the findings experimentally.

Studies utilizing glucose transporter inhibitors or L-Glucose could also be utilized to determine if the changes in BCA2 and NMNAT1 are dependent on the influx of glucose into the cell, or if some intermediate metabolite of glucose metabolism is involved in the regulation of the system. This information would indicate whether the effects of glucose on BCA2, NMANT1, LDHA, and LDHB expression are dependent on the state of glucose metabolism in the cell. If a specific metabolite could be identified, public data on the metabolic sensors detecting that metabolite, or the enzyme responsible for its conversion could provide valuable insights into the potential mechanism by which glucose is regulating BCA2 and NMNAT1 expression.

CHAPTER 8: CONCLUSIONS, LIMITATIONS, AND CLINICAL SIGNIFICANCE

The goal of this dissertation work was to expand on the role of BCA2 in the regulation of cellular energy homeostasis, established previously in the Dou Lab by Dr. Buac-Ventro. The preliminary work demonstrated that BCA2 modulates AMPK through some indirect mechanism. Based on mechanistic studies with mutant BCA2 constructs and a pharmacological investigation of the model system, an AKT dependent mechanism was suggested to be the cause. To identify a potential mechanism or intermediary by which BCA2 was regulating AMPK activation and cellular energy homeostasis, Dr. Buac-Ventro performed an siRNA-KD of BCA2 in MDA-MB-231 cells with a phospho-peptide enrichment. The preliminary investigation did not identify any potential AMPK interacting phosphoproteins. However, upon further investigation and evaluation of the data by Dr. Wang and Dou, pNMNAT1 was identified as enriched in response to BCA2-KD. This association was the basis for the rest of the investigations.

Due to the lack of a targetable receptor in TNBCs, patients suffer poor outcomes, and the available chemotherapeutics have many off-target effects as a result of being cytotoxic drugs (Park, Ahn, & Kim, 2018; Wahba & El-Hadaad, 2015). BCA2 has been identified as a risk factor for invasive TNBCs (Brahemi et al., 2010; Burger et al., 2010). The association between BCA2 and TNBCs suggests that BCA2 may be a potential therapeutic target in the treatment of BCA2 positive TNBCs (Brahemi et al., 2010; Buac et al., 2013; Burger et al., 2010).

BCA2 was previously found to inhibit the activation of AMPK and is believed to do so through an AKT dependent, albeit indirect mechanism (Buac et al., 2013). The extent of AMPK activation is known to be correlated with glucose concentration in previous studies (Arkwright et al., 2014; Salt, Johnson, Ashcroft, & Hardie, 1998). The preliminary findings from the Dou lab performed by Dr. Buac-Ventro defined the association between BCA2 and AMPK with the

regulation of cellular energy homeostasis. The literature described the role of glucose in the regulation of AMPK signaling in response to cellular energy homeostasis, and the current investigation sought to determine the role of BCA2 in glucose metabolism.

The initial phase of the investigation was intended to establish the experimental conditions and baseline cellular metabolic activity in the context of different concentrations of glucose. This was performed because glucose was known to regulate AMPK activation, so ideal glucose conditions needed to be established to investigate the role of BCA2 on cellular energy homeostasis successfully. The preliminary findings revealed a clear positive correlation between glucose concentration and BCA2 protein expression, which was associated with a concurrent and inverse decrease in NMNAT1 protein expression. The reverse was also found to be true, and these findings represented a potential novel molecular mechanism for the regulation of BCA2 and NMNAT1 in response to glucose levels in the cells. A critical aspect of cancer cell energy homeostasis is the transformation of the cells' primary source of energy from aerobic to anaerobic or "Warburg" metabolism (Liberti & Locasale, 2016; San-Millan & Brooks, 2017; Vander Heiden et al., 2009; Zdralevic et al., 2018).

The culmination of these findings, as illustrated in Figure 8.1, strongly suggests a potent role for both BCA2 and NMANT1 in the regulation of Warburg-like metabolism in response to glucose concentration. Glucose concentration is positively associated with Warburg metabolism (Burns & Manda, 2017), and the combined findings strongly suggest a dynamic role for both BCA2 and NMNAT1 in the regulation of Warburg-like metabolism. It was important to determine what the functional consequences of these changes in BCA2 and NMANT1 expression were on cellular energy metabolism and tumor cell proliferation.

shBCA2-KD resulted in increased NMNAT1 protein, transcript, and promoter activity, which is consistent with BCA2 regulating expression of NMNAT1 at the level of the promoter. However, previous studies have shown that BCA2 is a cytoplasmic protein and NMNAT1 is a nuclear protein, so it is likely there is some intermediary effector molecule modulating this mechanism.

The significance of these findings is that BCA2 may present a potent and selective target for the treatment of TNBCs. Because BCA2 is primarily expressed in early development and in metastatic breast cancer cells, it is possible that it could be selectively targeted therapeutically. Because Warburg metabolism is a fundamental and basic survival mechanism of all cancers, targeting Warburg metabolism has therapeutic potential in that it would selectively inhibit tumor cells over normal tissues. By studying Warburg metabolism and the mechanisms that facilitate its transformation, researchers may reveal strategies and targets for the disruption or inhibition of Warburg metabolism, specifically in cancer cells. These research findings potentially represent a significant advancement in the targeted treatment of cancer.

8.1 Limitations

The limitations of this study include an incomplete evaluation of the extent of Warburg metabolism in the respective experimental conditions. A seahorse analysis of the experimental conditions (shNT, shBCA2, shNMNAT1 and shBCA2/NMNAT1) would have provided a more complete picture of the functional consequences of the genetic manipulation of BCA2 and NMNAT1 alone and in combination. Furthermore, a rescue experiment with BCA2-WT would have demonstrated conclusively that the rescue phenomena observed in response to shNMNAT1-KD was the direct result of BCA2 expression.

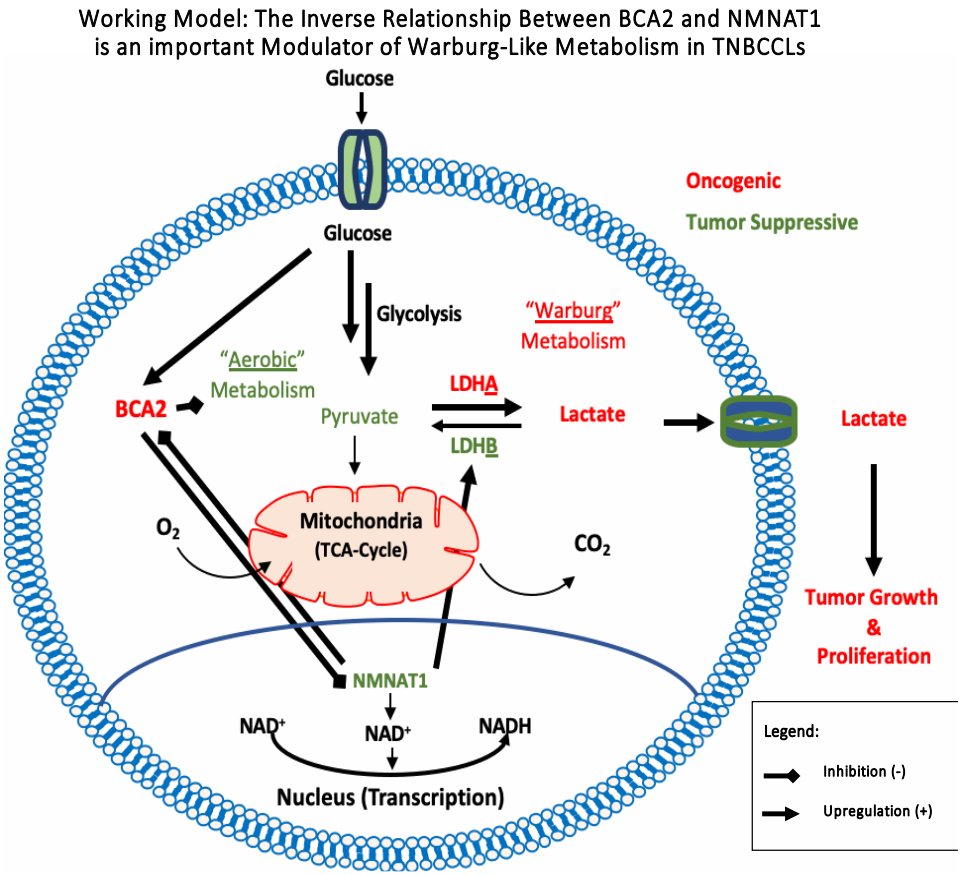

Figure 8.1 Potential Working Model for the Effects of BCA2 and NMNAT1 in regulation of Warburg-like Metabolism.

In summary, BCA2 and NMNAT1 are inversely correlated in response to both glucose concentration (inducible: in excess/deprivation) and genetic modifications by shRNAs. Increased glucose concentration results in an increase in BCA2 protein expression and a decrease in NMNAT1 expression. Findings suggest that BCA2 may inhibit NMNAT1 expression at the protein level. This suggests that there may be an alternative mechanism by which BCA2 and NMNAT1 regulate each other's expression. NMNAT1 is the rate-limiting enzyme in NAD synthesis, and NAD is the key coenzyme in the regulation of oxidation/reduction reactions. NMNAT1 specifically localizes to the nucleus, thus modulating the pool of NAD in the nucleus. NAD modulates DNA's chromatin structure in the nucleus, thereby regulating transcriptional activity through access to DNA by transcription factors. shBCA2-KD is also associated with a decrease in Warburg-like metabolism. This is marked by a decreased ratio of LDHA/LDHB, decreased glucose consumption, and increased lactate production. Conversely, shNMNAT1-KD increases BCA2 protein expression, increases markers of Warburg-like metabolism (increase ratio of LDHA/LDHB), and significantly increases lactate production and significantly affects glucose consumption. shBCA2/NMNAT1-dKD increases the ratio of LDHA/LDHB, and significantly increases the production of lactate, rescuing the decrease in glucose consumption and lactate production resultant from shBCA2-KD. shBCA2/NMNAT1-dKD had no significant effect on glucose consumption. These findings suggest that NMNAT1 plays a significant role in the regulation of lactate metabolism and glucose consumption. These data are suggestive of inhibition of anaerobic metabolism (normal cells) by BCA2, while NMNAT1 appears to inhibit Warburg metabolism and significantly regulates lactate production.

Additional experimentation with site MT (mutant) variants of BCA2 could reveal the functional domain necessary for the role of BCA2 in the regulation of NMNAT1. Reintroducing BCA2-WT and other mutant variants into the shBCA2-KD background would have indicated which functional domain of BCA2 was essential for the change in NMNAT1 protein, transcript, and promoter activity level. Preliminary experiments with transfection of BCA2-WT and MT constructs in the qPCR and promoter assays resulted in significant technical error due to the variance in transfection efficiency and the sensitivity of the cells to the transfections in the first place. When these experiments were carried out transiently, insufficient samples (cell-lysates) were obtained to perform the experiments, and without stable expression of the rescue vectors, their effect on the functional consequences of shBCA2 and shNMNAT1-KDs could not be assessed. For this reason, a need to assess the association between BCA2 and NMNAT1 in the regulation of Warburg-like metabolism was determined.

This was determined because BCA2 and NMNAT1 were found to be reciprocally regulated in response to glucose concentration in the TNBC cells. Increased glucose concentrations are known to induce the Warburg effect and enhance tumor-like characteristics of TNBC cells. In order to determine the role of NMNAT1 in BCA2 dependent regulation of cellular energy, homeostasis shBCA2/NMNAT1-dKDs were used to inhibit the induction of NMNAT1 associated with inhibition of BCA2 protein expression.

8.2 Clinical significance

Interestingly, only under conditions of high glucose were the results associated with shBCA2-KD, shNMNAT1-KD, and shBCA2/NMANT1-KD found to be consistent and yield statistically reproducible data. If glucose levels were not controlled, or the cells were left in culture for too long, the phenomena were not observed. This is presumably due to some mechanism by

which glucose is regulating BCA2 or NMNAT1 either directly or indirectly, but independently of each other. In other words, the increase in BCA2 expression associated with shNMNAT1-KD was not as reproducible under conditions of low glucose as opposed to high glucose. This could be a consequence of a direct feedback mechanism of glucose on BCA2, or through some indirect mechanism. Regardless, the results suggest that regulation is dependent on the presence of glucose.

In addition, it is unclear which function of BCA2 is responsible for its regulation of Warburg-like metabolism. However, the AKT binding domain MT variant presents an interesting potential explanation of the observed phenomena. AMPK and AKT play critical roles in a double negative feedback loop in breast cancer, driving the survival of cells as they detach from the primary site, and helps them survive while detached from the extracellular matrix (ECM) (Saha et al., 2018). AMPK and AKT appear to function as a molecular switch mediating the survival of cancer cells during metastatic transformation. The detachment of cells from the matrix triggers AMPK activity and inhibits AKT activity via upregulation of AKT phosphatase (PHLPP2) (Garcia & Shaw, 2017). The resultant $pAMPK^{high}/pAKT^{low}$ state was found to be critical for cell survival in suspension. Matrix reengagement resulted in an AKT-mediated inactivation of AMPK by PP2C-α-thus restoring the $pAKT^{high}/pAMPK^{low}$ state, which allows the cells to recommence proliferation (Saha et al., 2018).

As previously mentioned, BCA2 has been shown to be upregulated in invasive breast cancers (Burger et al., 2010) and has been shown to be a negative regulator of AMPK activation (Buac et al., 2013). BCA2 is purported to contain an AKT binding domain, suggesting that BCA2 may be regulating the activation of AMPK via an AKT dependent signaling cascade (Buac et al., 2013). In addition, these research findings demonstrated that both BCA2 and NMNAT1 expression is modulated by the concentration of glucose in the media. The decrease in BCA2 expression and

decreased availability of glucose to the cell would cause the activation of AMPK through direct (AMP binding) and indirect (BCA2/AKT dependent) mechanisms (Buac et al., 2013). This presents a possible mechanism by which BCA2 and AMPK/AKT signaling pathways are regulated in metastatic transformation. As the tumor mass continues to grow, the available glucose surrounding the tumor cells decreases, which would decrease the expression of BCA2, and increase the activation of AMPK and decrease AKT ($pAMPK^{high}/pAKT^{low}$ state) which is essential for the survival of cancer cells in suspension. Consequently, upon entry into the interstitial fluid and blood stream, the availability of glucose would once again rise resulting in an increase in BCA2, which inhibits AMPK switching the cells back to a state of ($pAKT^{high}/pAMPK^{low}$) which allows the cells to reattach and recommence proliferation.

A cancer cell's dynamic ability to respond to a changing environment is essential to its survival, as well as the ability of the cell to adapt to the high energy and biomass demands of rapid proliferation (Warburg-like metabolism). The research findings suggest that BCA2 plays a critical role in the coordination of Warburg-Like metabolism, which is dependent on the expression of NMNAT1. The inhibition of NMNAT1 expression that is induced by shBCA2-KD is sufficient to reverse the decrease in Warburg-like metabolism associated with shBCA2-KD.

PUBLICATIONS

Arkwright, R. T., Pham, T. M., Zonder, J. A., & Dou, Q. P. **(2017)**. The preclinical discovery and development of bortezomib for the treatment of mantle cell lymphoma. *Expert Opinion in Drug Discovery, 12*(2), 225-235. doi:10.1080/17460441.2017.1268596

Arkwright, R. T., Hayes, P. M., & Dou, Q. P. (**2015**, March 1). What we don't know: The intersection of nutrition and cancer. *Cultures Magazine*. Retrieved June, 2018, from https://www.asm.org/index.php/archives-cultures/378-international/international-affairs/cultures/cultures-archives/93763-march-2015-exploring-food-security

Farshi, P., Deshmukh, R. R., Nwankwo, J. O., **Arkwright**, R. T., Cvek, B., Liu, J., & Dou, Q. P. **(2015)**. Deubiquitinases (DUBs) and DUB inhibitors: a patent review. *Expert Opinion on Theraputic Patents, 25*(10), 1191-1208. doi:10.1517/13543776.2015.1056737

Arkwright, R. T., Deshmukh, R., Adapa, N., Stevens, R., Zonder, E., Zhang, Z., Farshi, P., Ahmed. R.S., El-Banna, H. A., Chan, T.H., Dou, Q. **(2014)**. Lessons from nature: Sources and strategies for developing AMPK activators for cancer chemotherapeutics. *Anti-Cancer Agents in Medicinal Chemistry, 15*(5), 657-671. doi:10.2174/1871520615666141216145417

Fu, H. L., Valiathan, R. R., **Arkwright**, R. T., Sohail, A., Mihai, C., Kumarasiri, M., Mahasenan, K. V., Mobashery, S., Huang, P., Agarwal, G., Fridman, R. **(2013)**. Discoidin domain receptors: Unique receptor tyrosine kinases in collagen-mediated signaling. *Journal of Biological Chemistry, 288*(11), 7430-7437. doi:10.1074/jbc.r112.444158

REFERENCES

ACS. (2019). About breast cancer. Retrieved from https://www.cancer.org/cancer/breast-cancer/about/how-common-is-breast-cancer.html

An, J. Y. (2008). *The physiological roles of E3 ubiquitin ligases of the N-end rule pathway*. Pharmacy. University of Pittsburgh. Pitssburgh, PA. Retrieved from http://d-scholarship.pitt.edu/9751/1/An_JY_NOV2008.pdf

Ardley, H. C., & Robinson, P. A. (2005). E3 ubiquitin ligases. *Essays in Biochemistry, 41*(1), 15-30. doi:10.1042/eb0410015

Arora, R., Schmitt, D., Karanam, B., Tan, M., Yates, C., & Dean-Colomb, W. (2015). Inhibition of the Warburg effect with a natural compound reveals a novel measurement for determining the metastatic potential of breast cancers. *Oncotarget, 6*(2), 662-678. doi:10.18632/oncotarget.2689

Bacopulos, S., Amemiya, Y., Yang, W., Zubovits, J., Burger, A. M., Yaffe, M., & Seth, A. K. (2012). Effects of partner proteins on BCA2 RING ligase activity. *BMC Cancer, 12*, 63. doi:10.1186/1471-2407-12-63

Baumann, M. U., Zamudio, S., & Illsley, N. P. (2007). Hypoxic upregulation of glucose transporters in BeWo choriocarcinoma cells is mediated by hypoxia-inducible factor-1. *American Journal of Physiology-Cell Physiology, 293*(1), C477-C485. doi:10.1152/ajpcell.00075.2007

Bourdeau Julien, I., Sephton, C. F., & Dutchak, P. A. (2018). Metabolic Networks Influencing Skeletal Muscle Fiber Composition. *Frontiers in cell and developmental biology, 6*, 125-125. doi:10.3389/fcell.2018.00125

Brahemi, G., Kona, F. R., Fiasella, A., Buac, D., Soukupova, J., Brancale, A., Burger, A. M., & Westwell, A. D. (2010). Exploring the structural requirements for inhibition of the ubiquitin E3 ligase breast cancer associated protein 2 (BCA2) as a treatment for breast cancer. *Journal of Medicinal Chemistry, 53*(7), 2757-2765. doi:10.1021/jm901757t

Brand, R. A. (2010). Biographical sketch: Otto Heinrich Warburg, PhD, MD. *Clinical orthopaedics and related research, 468*(11), 2831-2832. doi:10.1007/s11999-010-1533-z

Brooks, G. A. (2010). What does glycolysis make and why is it important? *Journal of Applied Physiology, 108*(6), 1450-1451. doi:10.1152/japplphysiol.00308.2010

Buac, D., Kona, F. R., Seth, A. K., & Dou, Q. P. (2013). Regulation of metformin response by breast cancer associated gene 2. *Neoplasia, 15*(12), 1379-1390.

Burger, A., Amemiya, Y., Kitching, R., & Seth, A. K. (2006a). Novel RING E3 ubiquitin ligases in breast cancer. *Neoplasia (New York, N.Y.), 8*(8), 689-695. doi:10.1593/neo.06469

Burger, A. M., Amemiya, Y., Kitching, R., & Seth, A. K. (2006b). Novel RING E3 ubiquitin ligases in breast cancer. *Neoplasia, 8*(8), 689-695. doi:10.1593/neo.06469

Burger, A. M., Gao, Y., Amemiya, Y., Kahn, H. J., Kitching, R., Yang, Y., Sun, P., Narod, S. A., Hanna, W. M., & Seth, A. K. (2005). A novel RING-type ubiquitin ligase breast cancer-associated gene 2 correlates with outcome in invasive breast cancer. *Cancer Res, 65*(22), 10401-10412. doi:10.1158/0008-5472.can-05-2103

Burger, A. M., Kona, F., Amemiya, Y., Gao, Y., Bacopulos, S., & Seth, A. K. (2010). Role of the BCA2 ubiquitin E3 ligase in hormone responsive breast cancer. *The open cancer journal, 3*(1), 116-123.

Burger, A. M., Li, H., Zhang, X. K., Pienkowska, M., Venanzoni, M., Vournakis, J., Papas, T., & Seth, A. (1998). Breast cancer genome anatomy: Correlation of morphological changes in

breast carcinomas with expression of the novel gene product Di12. *Oncogene, 16*(3), 327-333. doi:10.1038/sj.onc.1201517

Burns, J. S., & Manda, G. (2017). Metabolic Pathways of the Warburg Effect in Health and Disease: Perspectives of Choice, Chain or Chance. *International journal of molecular sciences, 18*(12), 2755. doi:10.3390/ijms18122755

Chen, W. L., Luan, Y. C., Shieh, M. C., Chen, S. T., Kung, H. T., Soong, K. L., Yeh, Y. C., Chou, T. S., Mong, S. H., Wu, J. T., Sun, C. P., Deng, W. P., Wu, M. F., & Shen, M. L. (2006). Effects of cobalt-60 exposure on health of Taiwan residents suggest new approach needed in radiation protection. *Dose Response, 5*(1), 63-75. doi:10.2203/dose-response.06-105.Chen

Chiarugi, A., Dolle, C., Felici, R., & Ziegler, M. (2012). The NAD metabolome--a key determinant of cancer cell biology. *Nature Reviews Cancer, 12*(11), 741-752. doi:10.1038/nrc3340

Chua, J. S., Liew, H. P., Guo, L., & Lane, D. P. (2015). Tumor-specific signaling to p53 is mimicked by Mdm2 inactivation in zebrafish: insights from mdm2 and mdm4 mutant zebrafish. *Oncogene, 34*(48), 5933-5941. doi:10.1038/onc.2015.57

Ciechanover, A., Elias, S., Heller, H., Ferber, S., & Hershko, A. (1980). Characterization of the heat-stable polypeptide of the ATP-dependent proteolytic system from reticulocytes. *The Journal of Biological Chemistry, 255*(16), 7525-7528.

Cole, A. J., Clifton-Bligh, R., & Marsh, D. J. (2015). Histone H2B monoubiquitination: roles to play in human malignancy. *Endocr Relat Cancer, 22*(1), T19-33. doi:10.1530/erc-14-0185

De Duve, C., Pressman, B. C., Gianetto, R., Wattiaux, R., & Appelmans, F. (1955). Tissue fractionation studies. 6. Intracellular distribution patterns of enzymes in rat-liver tissue. *The Biochemical journal, 60*(4), 604-617. doi:10.1042/bj0600604

DeHart, C. J., Perlman, D. H., & Flint, S. J. (2015). Impact of the Adenoviral E4 Orf3 Protein on the Activity and Posttranslational Modification of p53. *Journal of Virology, 89*(6), 3209-3220. doi:10.1128/jvi.03072-14

Deshmukh, R., Adapa, N., Stevens, R., Zonder, E., Zhang, Z., Farshi, P., Ahmed, R., El Banna, H., Chan, T.-H., & Dou, Q. (2014). Lessons from nature: Sources and strategies for developing AMPK activators for cancer chemotherapeutics. *Anti-cancer agents in medicinal chemistry, 15*(5), 16. doi:10.2174/1871520615666141216145417

Dikic, I., & Robertson, M. (2012). Ubiquitin ligases and beyond. *BMC biology, 10*, 22-22. doi:10.1186/1741-7007-10-22

Epstein, T., Xu, L., Gillies, R., & Gatenby, R. (2014). Separation of metabolic supply and demand: Aerobic glycolysis as a normal physiological response to fluctuating energetic demands in the membrane. *Cancer & Metabolism, 2*(7), 10. doi:10.1186/2049-3002-2-7

Estrella, V., Chen, T., Lloyd, M., Wojtkowiak, J., Cornnell, H. H., Ibrahim-Hashim, A., Bailey, K., Balagurunathan, Y., Rothberg, J. M., Sloane, B. F., Johnson, J., Gatenby, R. A., & Gillies, R. J. (2013). Acidity generated by the tumor microenvironment drives local invasion. *Cancer Res, 73*(5), 1524-1535. doi:10.1158/0008-5472.Can-12-2796

Etlinger, J. D., & Goldberg, A. L. (1977). A soluble atp-dependent proteolytic system responsible for the degradation of abnormal proteins in reticulocytes. *Proceedings of the National Academy of Sciences of the United States of America, 74*(1), 54-58.

Feng, Y., Xiong, Y., Qiao, T., Li, X., Jia, L., & Han, Y. (2018). Lactate dehydrogenase A: A key player in carcinogenesis and potential target in cancer therapy. *Cancer medicine, 7*(12), 6124-6136. doi:10.1002/cam4.1820

Garcia, D., & Shaw, R. J. (2017). AMPK: Mechanisms of cellular energy sensing and restoration of metabolic balance. *Molecular cell, 66*(6), 789-800. doi:10.1016/j.molcel.2017.05.032

Greenwald, S. H., Charette, J. R., Staniszewska, M., Shi, L. Y., Brown, S. D. M., Stone, L., Liu, Q., Hicks, W. L., Collin, G. B., Bowl, M. R., Krebs, M. P., Nishina, P. M., & Pierce, E. A. (2016). Mouse models of NMNAT1-Leber Congenital Amaurosis (LCA9) recapitulate key features of the human disease. *The American journal of pathology, 186*(7), 1925-1938. doi:10.1016/j.ajpath.2016.03.013

Gumaste, P. V., Penn, L. A., Cymerman, R. M., Kirchhoff, T., Polsky, D., & McLellan, B. (2015). Skin cancer risk in BRCA1/2 mutation carriers. *The British Journal of Dermatology, 172*(6), 1498-1506. doi:10.1111/bjd.13626

Haas, A. L., Warms, J. V., Hershko, A., & Rose, I. A. (1982). Ubiquitin-activating enzyme. Mechanism and role in protein-ubiquitin conjugation. *The Journal of Biological Chemistry, 257*(5), 2543-2548.

Hatakeyama, S., & Nakayama, K. I. (2003). U-box proteins as a new family of ubiquitin ligases. *Biochemical and Biophysical Research Communications, 302*(4), 635-645. doi:10.1016/s0006-291x(03)00245-6

Henderson, D. J. P., Miranda, J. L., & Emerson, B. M. (2017). The β-NAD(+) salvage pathway and PKC-mediated signaling influence localized PARP-1 activity and CTCF Poly(ADP)ribosylation. *Oncotarget, 8*(39), 64698-64713. doi:10.18632/oncotarget.19841

Hershko, A., Ciechanover, A., Heller, H., Haas, A. L., & Rose, I. A. (1980). Proposed role of ATP in protein breakdown: conjugation of protein with multiple chains of the polypeptide of

ATP-dependent proteolysis. *Proceedings of the National Academy of Sciences of the United States of America, 77*(4), 1783-1786. doi:10.1073/pnas.77.4.1783

Hershko, A., Eytan, E., Ciechanover, A., & Haas, A. L. (1982). Immunochemical analysis of the turnover of ubiquitin-protein conjugates in intact cells. Relationship to the breakdown of abnormal proteins. *The Journal of Biological Chemistry*, *257*(23), 13964-13970.

Hershko, A., Heller, H., Elias, S., & Ciechanover, A. (1983). Components of ubiquitin-protein ligase system. Resolution, affinity purification, and role in protein breakdown. *The Journal of Biological Chemistry, 258*(13), 8206-8214.

Herzig, S., & Shaw, R. J. (2018). AMPK: guardian of metabolism and mitochondrial homeostasis. *Nature reviews. Molecular cell biology, 19*(2), 121-135. doi:10.1038/nrm.2017.95

Jafary, F., Ganjalikhany, M. R., Moradi, A., Hemati, M., & Jafari, S. (2019). Novel Peptide inhibitors for lactate dehydrogenase a (LDHA): a survey to inhibit LDHA activity via disruption of protein-protein interaction. *Scientific Reports, 9*(1), 4686. doi:10.1038/s41598-019-38854-7

Jaitovich, A., Angulo, M., Lecuona, E., Dada, L. A., Welch, L. C., Cheng, Y., Gusarova, G., Ceco, E., Liu, C., Shigemura, M., Barreiro, E., Patterson, C., Nader, G. A., & Sznajder, J. I. (2015). High CO2 levels cause skeletal muscle atrophy via AMP-activated kinase (AMPK), FoxO3a protein, and muscle-specific Ring finger protein 1 (MuRF1). *Journal of Biological Chemistry, 290*(14), 9183-9194. doi:10.1074/jbc.M114.625715

Jang, M., Kim, S. S., & Lee, J. (2013). Cancer cell metabolism: Implications for therapeutic targets. *Experimental & molecular medicine, 45*(10), e45-e45. doi:10.1038/emm.2013.85

Jayaram, H. N., Kusumanchi, P., & Yalowitz, J. A. (2011). NMNAT expression and its relation to NAD metabolism. *Curr Med Chem, 18*(13), 1962-1972.

Keller, A., Nesvizhskii, A. I., Kolker, E., & Aebersold, R. (2002). Empirical statistical model to estimate the accuracy of peptide identifications made by MS/MS and database search. *Anal Chem, 74*(20), 5383-5392.

Klein, A. P. (2012). Genetic susceptibility to pancreatic cancer. *Molecular Carcinogenesis, 51*(1), 14-24. doi:10.1002/mc.20855

Koh, M. Y., Nguyen, V., Lemos, R., Jr., Darnay, B. G., Kiriakova, G., Abdelmelek, M., Ho, T. H., Karam, J., Monzon, F. A., Jonasch, E., & Powis, G. (2015). Hypoxia-induced SUMOylation of E3 ligase HAF determines specific activation of HIF2 in clear-cell renal cell carcinoma. *Cancer Res, 75*(2), 316-329. doi:10.1158/0008-5472.can-13-2190

Kona, F. R., Stark, K., Bisoski, L., Buac, D., Cui, Q., & Dou, Q. P. (2012). Transcriptional activation of breast cancer-associated gene 2 by estrogen receptor. *Breast Cancer Res Treat, 135*(2), 495-503. doi:10.1007/s10549-012-2107-4

Krisher, R. L., & Prather, R. S. (2012). A role for the Warburg effect in preimplantation embryo development: metabolic modification to support rapid cell proliferation. *Molecular reproduction and development, 79*(5), 311-320. doi:10.1002/mrd.22037

Lehmann, B. D., Bauer, J. A., Chen, X., Sanders, M. E., Chakravarthy, A. B., Shyr, Y., & Pietenpol, J. A. (2011). Identification of human triple-negative breast cancer subtypes and preclinical models for selection of targeted therapies. *The Journal of Clinical Investigation, 121*(7), 2750-2767. doi:10.1172/JCI45014

Liberti, M. V., & Locasale, J. W. (2016). The warburg effect: how does it benefit cancer cells? *Trends in Biochemical Sciences, 41*(3), 211-218. doi:https://doi.org/10.1016/j.tibs.2015.12.001

Lu, Q.-Y., Zhang, L., Yee, J. K., Go, V.-L. W., & Lee, W.-N. (2015). Metabolic Consequences of LDHA inhibition by Epigallocatechin Gallate and Oxamate in MIA PaCa-2 Pancreatic Cancer Cells. *Metabolomics : Official journal of the Metabolomic Society, 11*(1), 71-80. doi:10.1007/s11306-014-0672-8

Martinez-Outschoorn, U. E., Peiris-Pagés, M., Pestell, R. G., Sotgia, F., & Lisanti, M. P. (2016). Cancer metabolism: a therapeutic perspective. *Nature Reviews Clinical Oncology, 14*, 11. doi:10.1038/nrclinonc.2016.60

Matyskiela, M. E., & Martin, A. (2013). Design principles of a universal protein degradation machine. *Journal of molecular biology, 425*(2), 199-213. doi:10.1016/j.jmb.2012.11.001

McClellan, A. J., Laugesen, S. H., & Ellgaard, L. (2019). Cellular functions and molecular mechanisms of non-lysine ubiquitination. *Open Biology, 9*(9), 190147. doi:doi:10.1098/rsob.190147

Memmott, R. M., & Dennis, P. A. (2009). Akt-dependent and -independent mechanisms of mTOR regulation in cancer. *Cellular Signalling, 21*(5), 656-664. doi:https://doi.org/10.1016/j.cellsig.2009.01.004

Metzger, M. B., Hristova, V. A., & Weissman, A. M. (2012). HECT and RING finger families of E3 ubiquitin ligases at a glance. *J Cell Sci, 125*(Pt 3), 531-537. doi:10.1242/jcs.091777

Mihaylova, M. M., & Shaw, R. J. (2011). The AMPK signalling pathway coordinates cell growth, autophagy and metabolism. *Nature cell biology, 13*(9), 1016-1023. doi:10.1038/ncb2329

Miyakawa, K., Ryo, A., Murakami, T., Ohba, K., Yamaoka, S., Fukuda, M., Guatelli, J., & Yamamoto, N. (2009). BCA2/rabring7 promotes tetherin-dependent HIV-1 restriction. *PLOS Pathogens, 5*(12), e1000700. doi:10.1371/journal.ppat.1000700

Molina, J., Morlacchi, P., Silva, L., Dennison, J., & Mills, G. (2014). Extracellular lactate cooperates with limited glucose and glutamine to sustain breast cancer cell survival by providing ATP, NADPH, amino acids, and glutathione. *Cancer & Metabolism, 2*(Suppl 1), P49-P49. doi:10.1186/2049-3002-2-S1-P49

Moreira, J. d. V., Hamraz, M., Abolhassani, M., Bigan, E., Pérès, S., Paulevé, L., Nogueira, M. L., Steyaert, J.-M., & Schwartz, L. (2016). The redox status of cancer cells supports mechanisms behind the warburg effect. *Metabolites, 6*(4), 33. doi:10.3390/metabo6040033

Morreale, F. E., & Walden, H. (2016). Types of Ubiquitin Ligases. *Cell, 165*(1), 248-248.e241. doi:10.1016/j.cell.2016.03.003

NCBI. (2019). Structure summary MMDB: 1GZU crystal structure of human nicotinamide mononucleotide adenylyltransferase in complex with NMN. Retrieved from https://www.ncbi.nlm.nih.gov/Structure/pdb/1GZU

Nesvizhskii, A. I., Keller, A., Kolker, E., & Aebersold, R. (2003). A statistical model for identifying proteins by tandem mass spectrometry. *Anal Chem, 75*(17), 4646-4658. doi:10.1021/ac0341261

Nounou, M. I., ElAmrawy, F., Ahmed, N., Abdelraouf, K., Goda, S., & Syed-Sha-Qhattal, H. (2015). Breast cancer: Conventional diagnosis and treatment modalities and recent patents and technologies. *Breast cancer: Basic and clinical research, 9*(S2), 17-34.

Ohta, T., & Fukuda, M. (2004). Ubiquitin and breast cancer. *Oncogene, 23*(11), 2079-2088. doi:10.1038/sj.onc.1207371

Ooga, M., Suzuki, M. G., & Aoki, F. (2015). Involvement of histone H2B monoubiquitination in the regulation of mouse preimplantation development. *J Reprod Dev, 61*(3), 179-184. doi:10.1262/jrd.2014-137

Park, J. H., Ahn, J.-H., & Kim, S.-B. (2018). How shall we treat early triple-negative breast cancer (TNBC): From the current standard to upcoming immuno-molecular strategies. *BMJ Journals, 3*(Suppl 1), e000357. doi:10.1136/esmoopen-2018-000357

Paul, S. (2008). Dysfunction of the ubiquitin-proteasome system in multiple disease conditions: therapeutic approaches. *Bioessays, 30*(11-12), 1172-1184. doi:10.1002/bies.20852

Rabinovitz, M., & Fisher, J. M. (1964). Characteristics of the inhibition of hemoglobin synthesis in rabbit reticulocytes by threo-α-amino-β-chlorobutyric acid. *Biochimica et Biophysica Acta, 91*(2), 313-322. doi:https://doi.org/10.1016/0926-6550(64)90255-5

Rani, R., & Kumar, V. (2019). *Lactate dehydrogenase (ldh): biochemistry, function and clinical significance*. India: Nova Science Publishers.

Saha, M., Kumar, S., Bukhari, S., Balaji, S. A., Kumar, P., Hindupur, S. K., & Rangarajan, A. (2018). AMPK-Akt double-negative feedback loop in breast cancer cells regulates their adaptation to matrix deprivation. *Cancer Res, 78*(6), 1497-1510. doi:10.1158/0008-5472.Can-17-2090

Salt, I. P., Johnson, G., Ashcroft, S. J., & Hardie, D. G. (1998). AMP-activated protein kinase is activated by low glucose in cell lines derived from pancreatic beta cells, and may regulate insulin release. *The Biochemical journal, 335 (Pt 3)*(Pt 3), 533-539. doi:10.1042/bj3350533

San-Millan, I., & Brooks, G. A. (2017). Reexamining cancer metabolism: lactate production for carcinogenesis could be the purpose and explanation of the Warburg Effect. *Carcinogenesis, 38*(2), 119-133. doi:10.1093/carcin/bgw127

Schreiber, V., Dantzer, F., Ame, J.-C., & de Murcia, G. (2006). Poly(ADP-ribose): novel functions for an old molecule. *Nature Reviews Molecular Cell Biology, 7*(7), 517-528. doi:10.1038/nrm1963

Schuster, S., Penke, M., Gorski, T., Gebhardt, R., Weiss, T. S., Kiess, W., & Garten, A. (2015). FK866-induced NAMPT inhibition activates AMPK and downregulates mTOR signaling in hepatocarcinoma cells. *Biochemical and Biophysical Research Communications, 458*(2), 334-340. doi:https://doi.org/10.1016/j.bbrc.2015.01.111

Shen, M., Schmitt, S., Buac, D., & Dou, Q. P. (2013). Targeting the ubiquitin-proteasome system for cancer therapy. *Expert opinion on therapeutic targets, 17*(9), 1091-1108. doi:10.1517/14728222.2013.815728

Smith, C. J., Berry, D. M., & McGlade, C. J. (2013). The E3 ubiquitin ligases RNF126 and Rabring7 regulate endosomal sorting of the epidermal growth factor receptor. *J Cell Sci, 126*(Pt 6), 1366-1380. doi:10.1242/jcs.116129

Sultani, G., Bentley, N., Osborne, B., Joshi, S., Araki, T., Montgomery, M., Polly, P., Byrne, F., Wu, L., & Turner, N. (2018). PO-011 Impact of compartment-specific changes in NAD biosynthesis on diethylnitrosamine-induced liver cancer. *ESMO Open, 3*(Suppl 2), A25. doi:10.1136/esmoopen-2018-EACR25.56

Sun, Y. (2006). E3 ubiquitin ligases as cancer targets and biomarkers. *Neoplasia, 8*(8), 645-654. doi:10.1593/neo.06376

Tanaka, K. (2009). The proteasome: overview of structure and functions. *Proceedings of the Japan Academy. Series B, Physical and biological sciences, 85*(1), 12-36. doi:10.2183/pjab.85.12

Trausch-Azar, J. S., Abed, M., Orian, A., & Schwartz, A. L. (2015). Isoform-specific SCF(Fbw7) ubiquitination mediates differential regulation of PGC-1alpha. *Journal of Cellular Physiology, 230*(4), 842-852. doi:10.1002/jcp.24812

Turco, E., Gallego, L. D., Schneider, M., & Kohler, A. (2015). Monoubiquitination of histone H2B is intrinsic to the Bre1 RING domain-Rad6 interaction and augmented by a second Rad6-binding site on Bre1. *The Journal of Biological Chemistry, 290*(9), 5298-5310. doi:10.1074/jbc.M114.626788

Vander Heiden, M. G., Cantley, L. C., & Thompson, C. B. (2009). Understanding the Warburg effect: the metabolic requirements of cell proliferation. *Science, 324*(5930), 1029-1033. doi:10.1126/science.1160809

Wahba, H. A., & El-Hadaad, H. A. (2015). Current approaches in treatment of triple-negative breast cancer. *Cancer biology & medicine, 12*(2), 106-116. doi:10.7497/j.issn.2095-3941.2015.0030

Wang, J., Weygand, J., Hwang, K.-P., Mohamed, A. S. R., Ding, Y., Fuller, C. D., Lai, S. Y., Frank, S. J., & Zhou, J. (2016). Magnetic resonance imaging of glucose uptake and metabolism in patients with head and neck cancer. *Scientific Reports, 6*, 30618-30618. doi:10.1038/srep30618

Wang, Z., Nie, Z., Chen, W., Zhou, Z., Kong, Q., Seth, A. K., Liu, R., & Chen, C. (2013). RNF115/BCA2 E3 ubiquitin ligase promotes breast cancer cell proliferation through targeting p21Waf1/Cip1 for ubiquitin-mediated degradation*Neoplasia, 15*(9), 1028-1035.

Warburg, O., & Burk, D. (1967). *The Prime cause and prevention of cancer : with two prefaces on prevention*. Wurzburg, Germany: Konrad Triltsch.

Warburg, O., Wind, F., & Negelein, E. (1927). The metabolism of tumors in the body. *The Journal of general physiology, 8*(6), 519-530.

Weinberg, S. E., & Chandel, N. S. (2014). Targeting mitochondria metabolism for cancer therapy. *Nature Chemical Biology, 11*, 9. doi:10.1038/nchembio.1712

Werner, E., Ziegler, M., Lerner, F., Schweiger, M., & Heinemann, U. (2002). Crystal structure of human nicotinamide mononucleotide adenylyltransferase in complex with NMN. *FEBS Letters, 516*(1-3), 239-244. doi:10.1016/s0014-5793(02)02556-5

Zdralevic, M., Brand, A., Di Ianni, L., Dettmer, K., Reinders, J., Singer, K., Peter, K., Schnell, A., Bruss, C., Decking, S. M., Koehl, G., Felipe-Abrio, B., Durivault, J., Bayer, P., Evangelista, M., O'Brien, T., Oefner, P. J., Renner, K., Pouyssegur, J., & Kreutz, M. (2018). Double genetic disruption of lactate dehydrogenases A and B is required to ablate the "Warburg effect" restricting tumor growth to oxidative metabolism. *The Journal of Biological Chemistry, 293*(41), 15947-15961. doi:10.1074/jbc.RA118.004180

Zhang, T., Berrocal, J. G., Frizzell, K. M., Gamble, M. J., DuMond, M. E., Krishnakumar, R., Yang, T., Sauve, A. A., & Kraus, W. L. (2009). Enzymes in the NAD^+ salvage pathway regulate SIRT1 activity at target gene promoters. *J Biol Chem, 284*(30), 20408-20417. doi:10.1074/jbc.M109.016469

ABSTRACT

THE ROLE OF BCA2 IN REGULATION OF WARBURG-LIKE GLUCOSE AND LACTATE METABOLISM IN BREAST CANCER CELL LINES

by

RICHARD T. ARKWRIGHT III

May 2020

Advisor: Dr. Q. Ping Dou

Major: Cancer Biology

Degree: Doctor of Philosophy

Modified metabolism is a hallmark of cancer cell biology known as "The Warburg Effect," characterized by increased glucose-consumption and lactate-production, providing the metabolites and energy necessary for rapid proliferation. Breast-cancer-associated-gene-2 (BCA2) is an E3-Ub-ligase known to modulate AMPK, the "master-regulator of energy-homeostasis." BCA2 is an oncogene associated with poor patient-survival and breast cancer invasiveness. Phospho-proteomic analysis of siBCA2-MDA-MB-231 knockdown-(KD) revealed enrichment of Nicotinamide-Nucleotide-Adenylyl-transferase-1 (NMNAT1), an essential enzyme in nuclear NAD-synthesis and a tumor-suppressor.

Initial experiments demonstrated that glucose concentration was positively correlated with BCA2 and inversely with NMNAT1 protein expression. shBCA2-KD in MDA-MB-468/-231 reproduced the inverse correlation between BCA2 and NMNAT1. shBCA2 -KD resulted in a decrease in BCA2 protein (MDA-MB-468: 54% and 49%; MDA-MB-231: 31% and 19%), qPCR-transcript (MDA-MB-468: 45%; MDA-MB-231: 31%) expression.

shBCA2-KD also resulted in an inverse increase In NMNAT1 qPCR-transcript (MDA-MB-468: 146%; MDA-MB-231: 150%) and promoter levels (MDA-MB-468: 409% and 459%; MDA-MB-231: 175% and 169%). shBCA2-KD was also associated with a decrease in the ratio of key enzyme associated with Warburg metabolism (LDHA/LDHB); high LDHA/LDHB is associated with Warburg-like metabolism, and low LDHA/LDHB is associated with decreased Warburg-like metabolism. Consistent with these findings, shBCA2 -KD resulted in decreased glucose consumption (MDA-MB-468: 70% and 76%; MDA-MB-231: 75% and 77%), decreased lactate production (MDA-MB-468: 69% and 72%; MDA-MB-231: 68% and 64%), and decrease cellular proliferation (MDA-MB-468: 54% and 49%; MDA-MB-231: 31% and 19%). All of these data are consistent with a role for BCA2 in maintaining Warburg-like metabolism in breast cancer cell lines, and that inhibition of BCA2 decreases Warburg-like metabolism and tumor cell proliferation.

In order to investigate the reciprocal role of NMNAT1 in triple negative breast cancer cells NMNAT1 was knocked down. The shNMNAT1-KD induced BCA2 protein, indicating a potential reciprocal feedback loop. shNMNAT1 -KD resulted in a decrease in NMNAT1 protein (MDA-MB-468: 7070%, 6286 and 8427%; MDA-MB-231: 212%, 202% and 19%), qPCR-transcript (MDA-MB-468: 45%; MDA-MB-231: 31%) expression.

shBCA2-KD also resulted in an inverse increase in NMNAT1 qPCR-transcript (MDA-MB-468: 146%; MDA-MB-231: 150%) and promoter levels (MDA-MB-468: 409% and 459%; MDA-MB-231: 175% and 169%). shBCA2-KD was also associated with a decrease in the ratio of key enzyme associated with Warburg metabolism (LDHA/LDHB); high LDHA/LDHB is associated with Warburg-like metabolism, and low LDHA/LDHB is associated with decreased Warburg-like metabolism. Consistent with these findings, shBCA2 -KD resulted in decreased

glucose consumption (MDA-MB-468: 70% and 76%; MDA-MB-231: 75% and 77%), decreased lactate production (MDA-MB-468: 69% and 72%; MDA-MB-231: 68% and 64%), and decrease cellular proliferation (MDA-MB-468: 54% and 49%; MDA-MB-231: 31% and 19%). All of these data are consistent with the role of BCA2 in maintaining Warburg-like metabolism in breast cancer cell lines, and that inhibition of BCA2 decreases Warburg-like metabolism and tumor cell proliferation.

In addition, shBCA2/NMNAT1-KD differentially regulates the expression of LDHA/LDHB. The ratio of LDHA/LDHB modulates lactate/pyruvate equilibria and is a recognized marker of the relative level of Warburg metabolism. High LDHA/LDHB is positively correlated with enhanced Warburg activity.

NMNAT1, differentially regulates glucose-consumption and lactate-production. shBCA2-KD diminished LDHA/LDHB-ratio, lactate-production, and glucose-consumption. shNMNAT1-KD increased the LDHA/LDHB-ratio and lactate-production significantly, with and on glucose-consumption. shBCA2/NMNAT1-double-KD reversed the effects of shBCA2-KD, resulting in significant increases in lactate production with an increase of LDHA and LDHB relative to shNT and shBCA2, and increased LDHA/LDHB ratios relative to shBCA2-KD, as well as rescuing the effects of shBCA2 on glucose consumption relative to shNT and shBCA2.

Collectively, these data suggest that BCA2 and NMNAT1 modulate breast-cancer-cell-metabolism. The role of energy status indicated by the role of glucose in the regulation of BCA2/NMNAT1 could provide clues to the significance of these findings and thereby direct future investigations.

AUTOBIOGRAPHICAL STATEMENT

Richard T. Arkwright III was born in Southfield, Michigan. He received his Bachelor of Science degree from Michigan State University with majors in Physiology and Human Biology in 2008. Richard continued his education at Wayne State University School of Medicine in the Basic Medical Sciences Graduate program and matriculated to the Cancer Biology Ph.D. program in the fall of 2011. He began his Ph.D. research in the lab of Dr. Rafael Fridman studying the role of the extracellular matrix in breast cancer cell growth. Specifically, he investigated the role of the Collagen Binding Discoidin Domain receptor (DDR1 & DDR2) in the regulation of cancer metastases. Richard joined Dr. Q. Ping Dou's laboratory in May of 2014 where he began his study of BCA2 and its regulation of glucose metabolism in breast cancer. His work provided the framework for the basis of targeting BCA2 in cancer in order to modulate cancer cell metabolism.